

Wine and NMR (low field)

Philippe R. Bodart, Régis D. Gougeon

Team Physical Chemistry of Food and Wine,

UMR PAM AgroSup Dijon, Université de Bourgogne Franche-Comté

1 esplanade Erasme, Bâtiment EPICURE 21000 Dijon, France





Dyonisos grec god of vine, wine, and its excess
Mosaic dating from the III century AD J.-C
Syria - Shahba Museums
<https://www.theoi.com/Gallery/Z12.16.html>



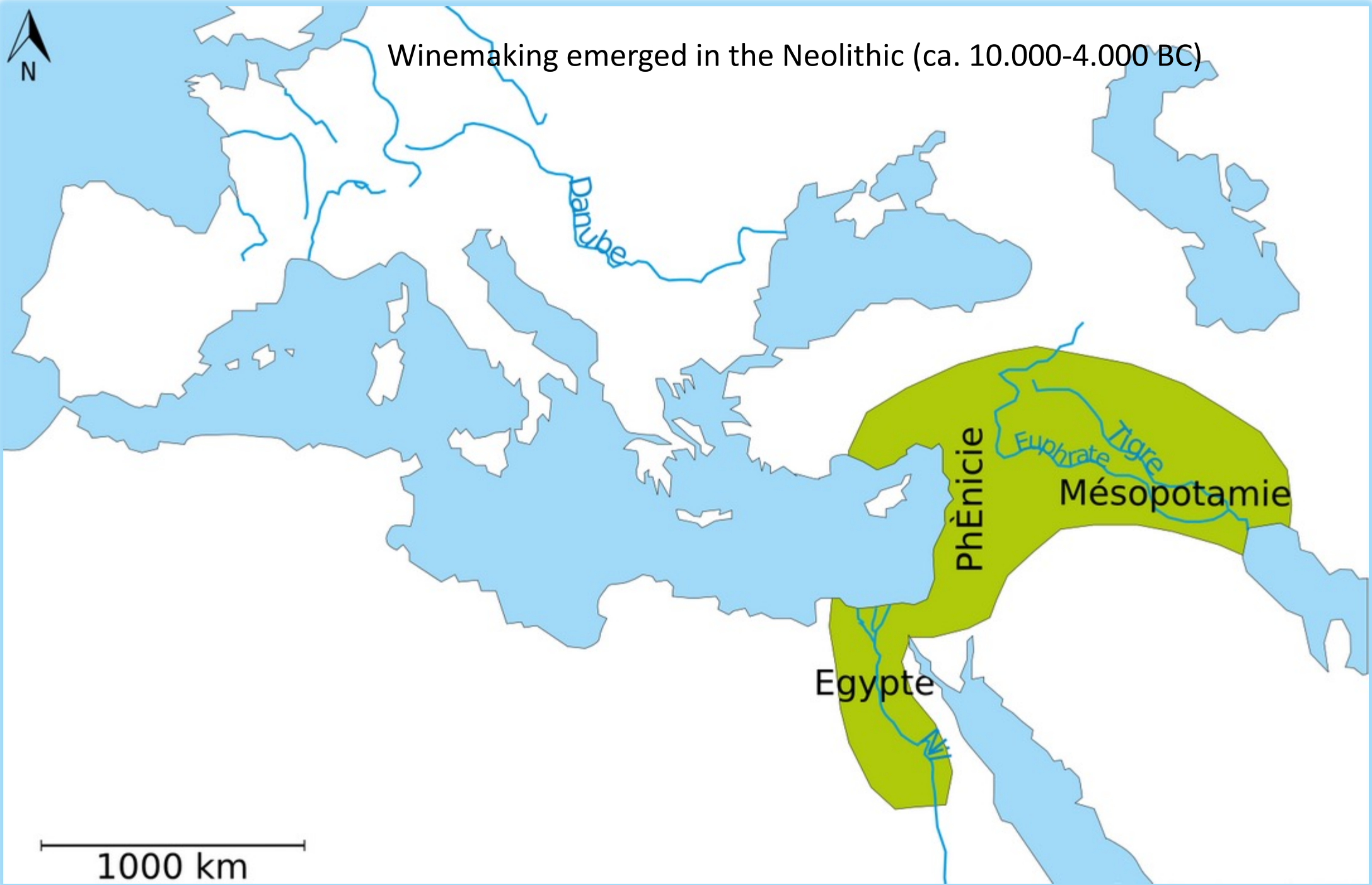
Ash, god of the oasis and the vineyards of the western delta of the Nile.
[https://fr.wikipedia.org/wiki/Ach_\(divinit%C3%A9\)](https://fr.wikipedia.org/wiki/Ach_(divinit%C3%A9))



Sucellus, Celtic god of agriculture and wine
-125BC / 500AD
<https://fr.wikipedia.org/wiki/Sucellos>



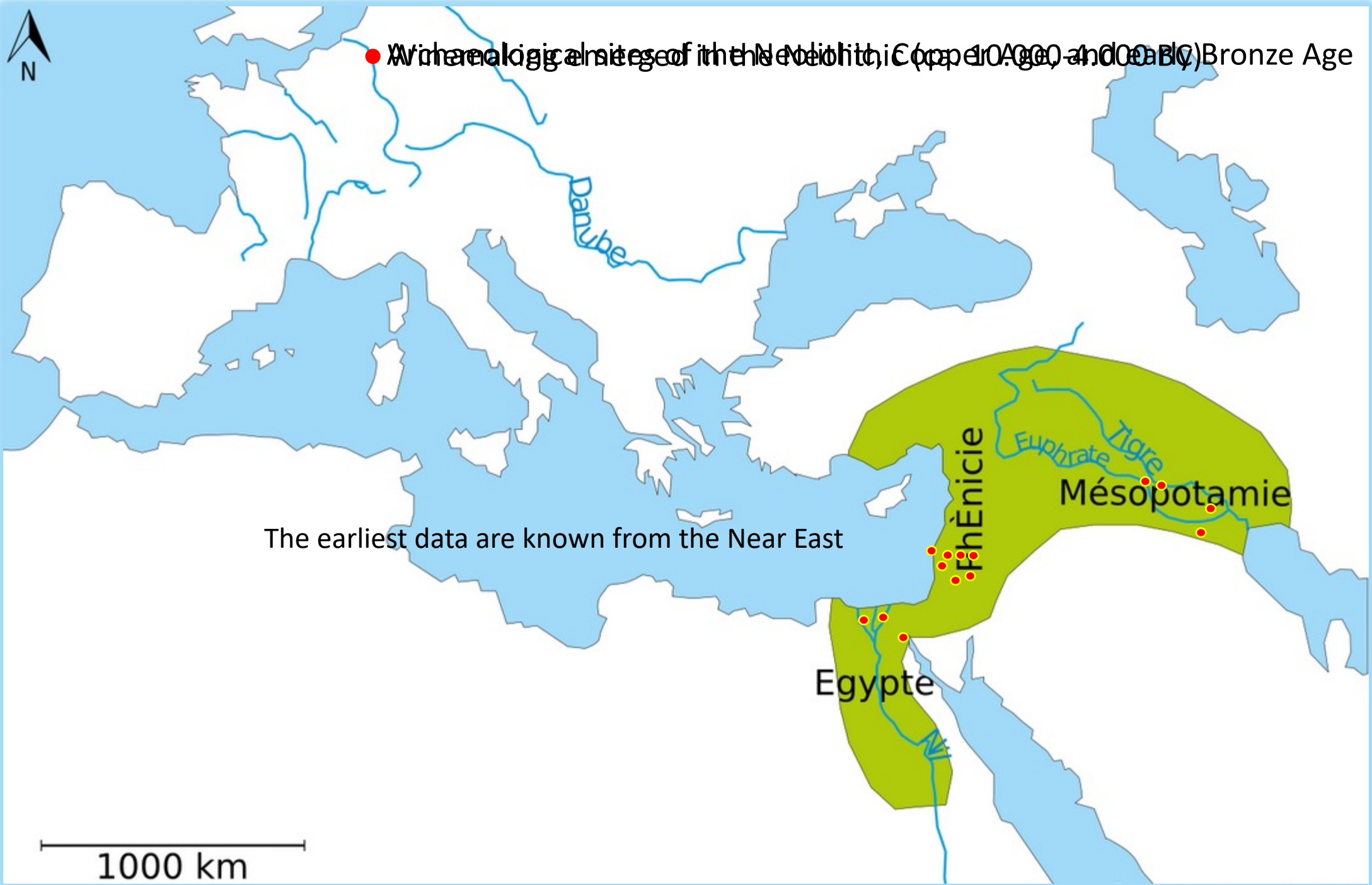
Winemaking emerged in the Neolithic (ca. 10.000-4.000 BC)



1000 km



• With archaeological sites of the Neolithic, Copper Age, and (rarely) Bronze Age

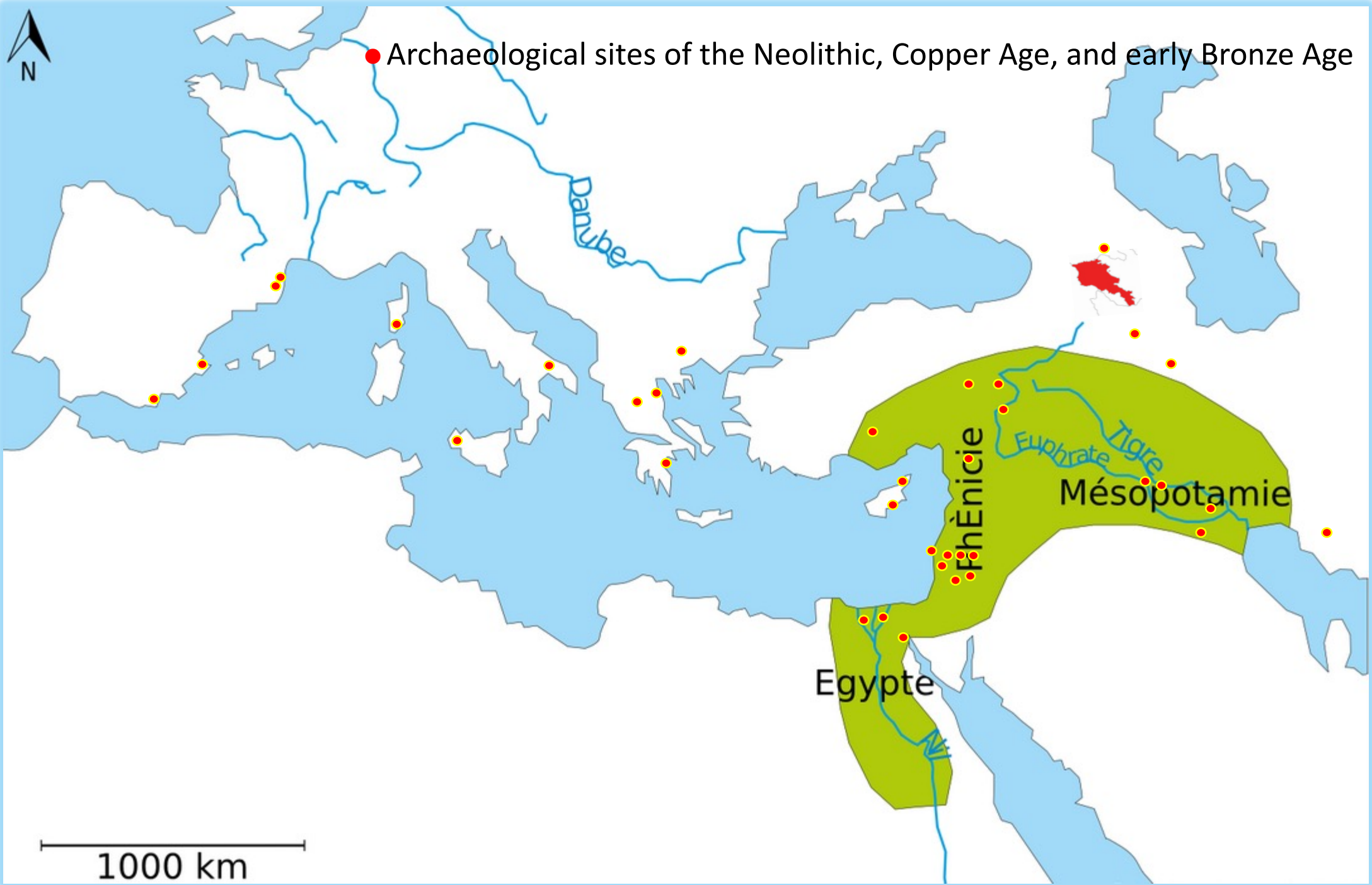


The earliest data are known from the Near East

1000 km



● Archaeological sites of the Neolithic, Copper Age, and early Bronze Age



1000 km

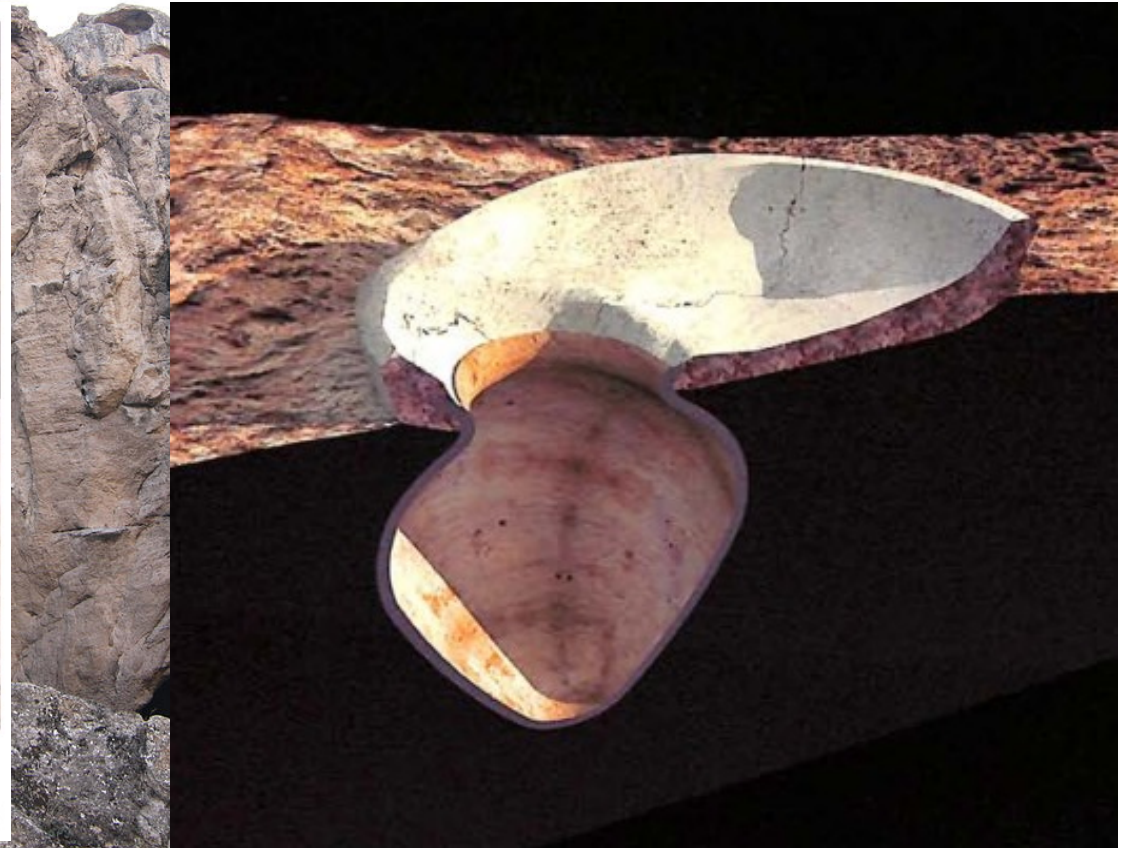
A fragment of a fresco portraying harvesting and winemaking. Tomb belonging to Nakht (1500 BC, Theban, Egypt, New Kingdom period, de Garis Davies, 1930)



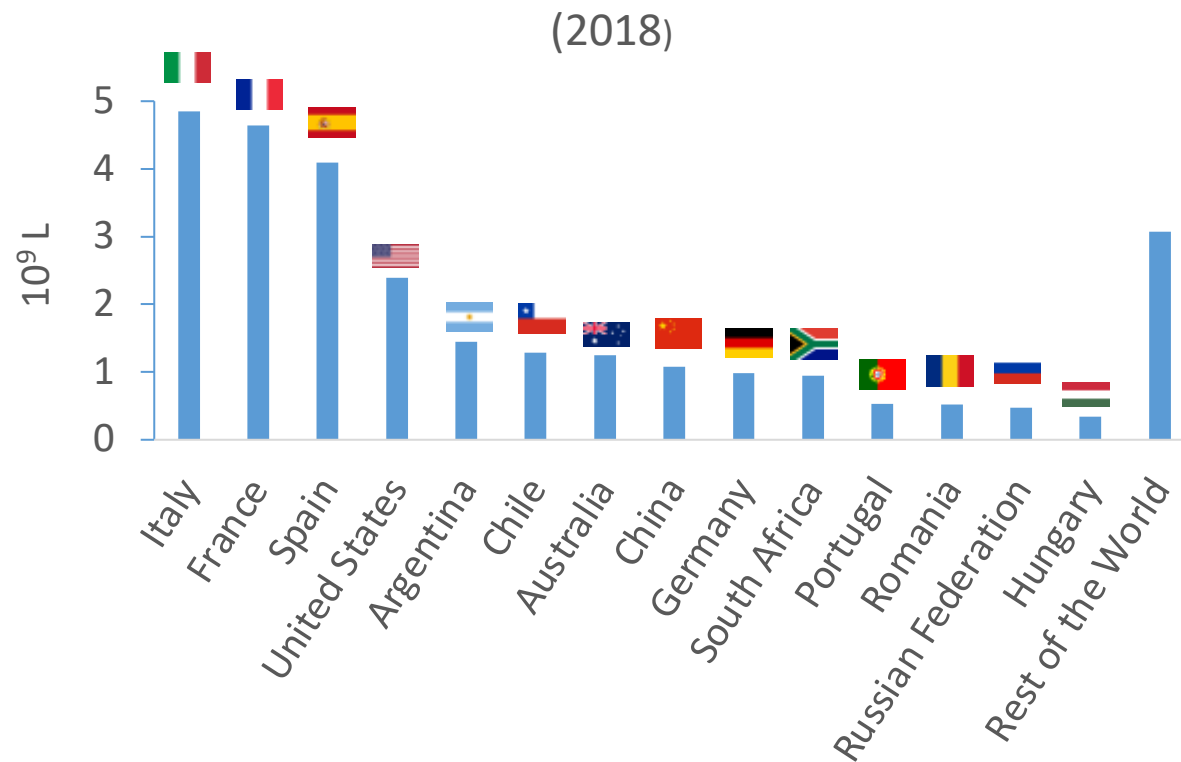
Oldest vinery (Areni, Armenia - 4100 BC)



Fig. 113: Winepress in Areni-1 cave (beginning of the IV Millennium BC)



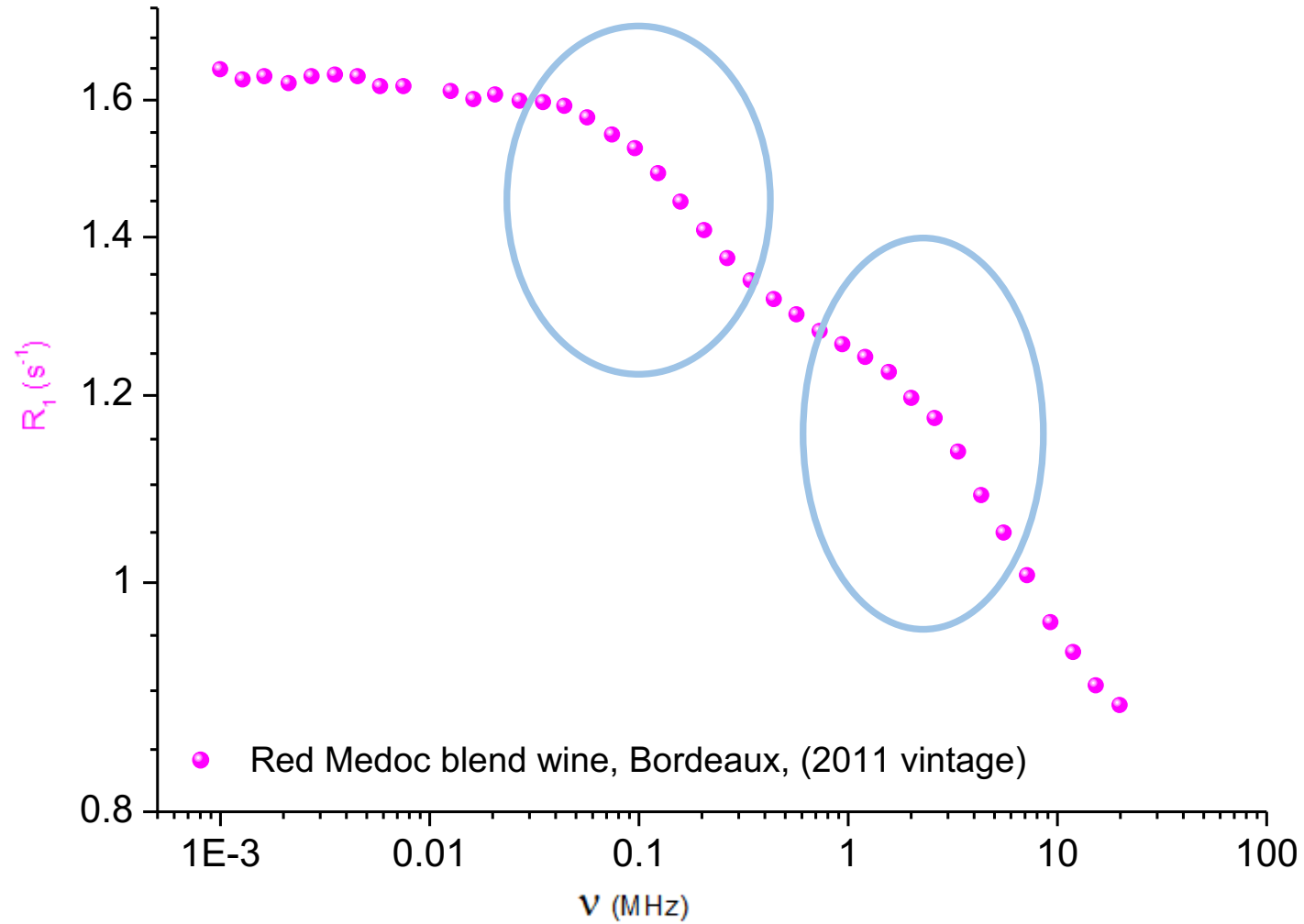
Nowadays wine production



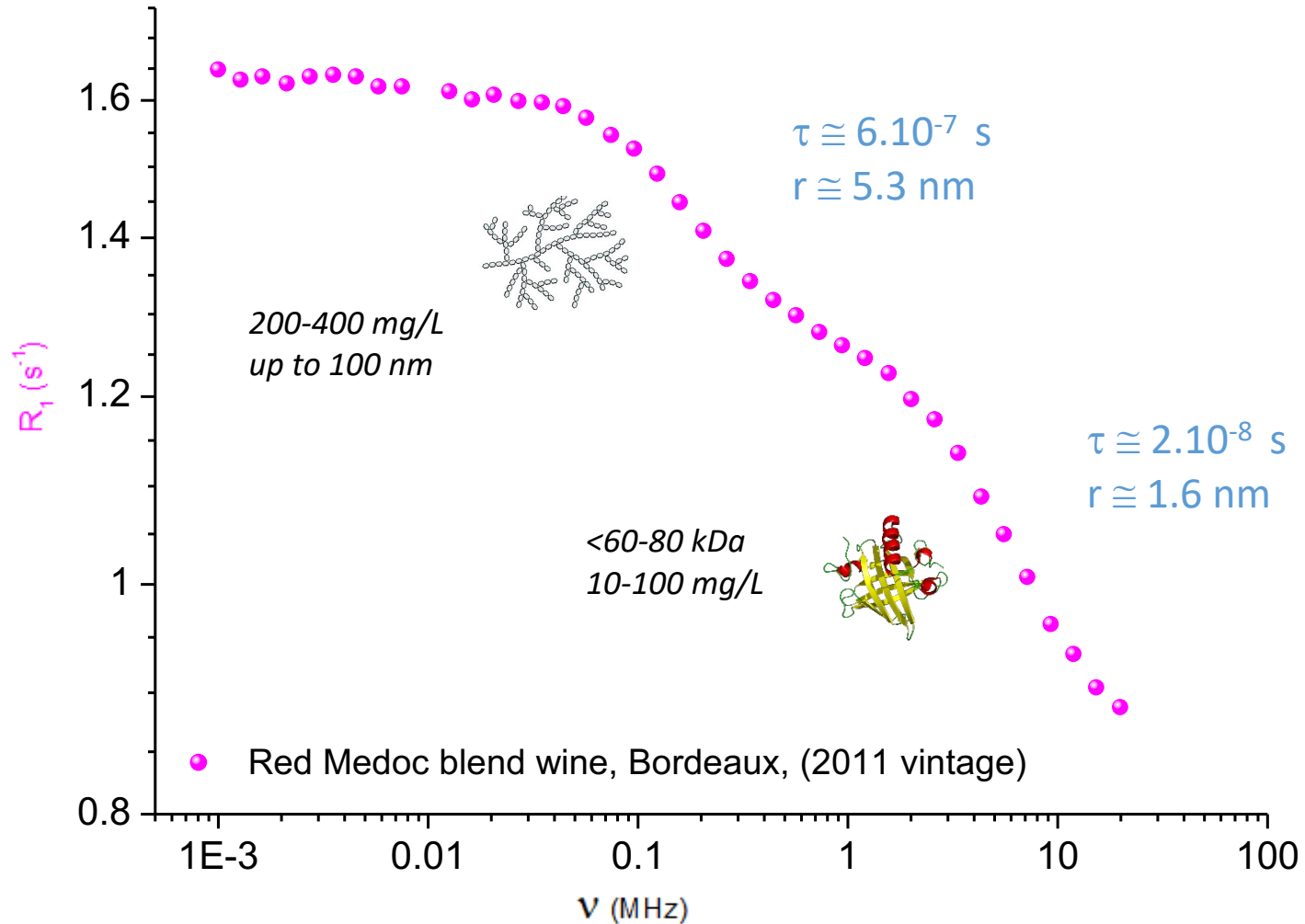
Over the last decade,
World Production ~26 10⁹ L/ year.

World trade in 2018, 31.3 billion euros.

^1H NMRD profile of wine (red Medoc blend)



^1H NMRD profile of wine (red Medoc blend)



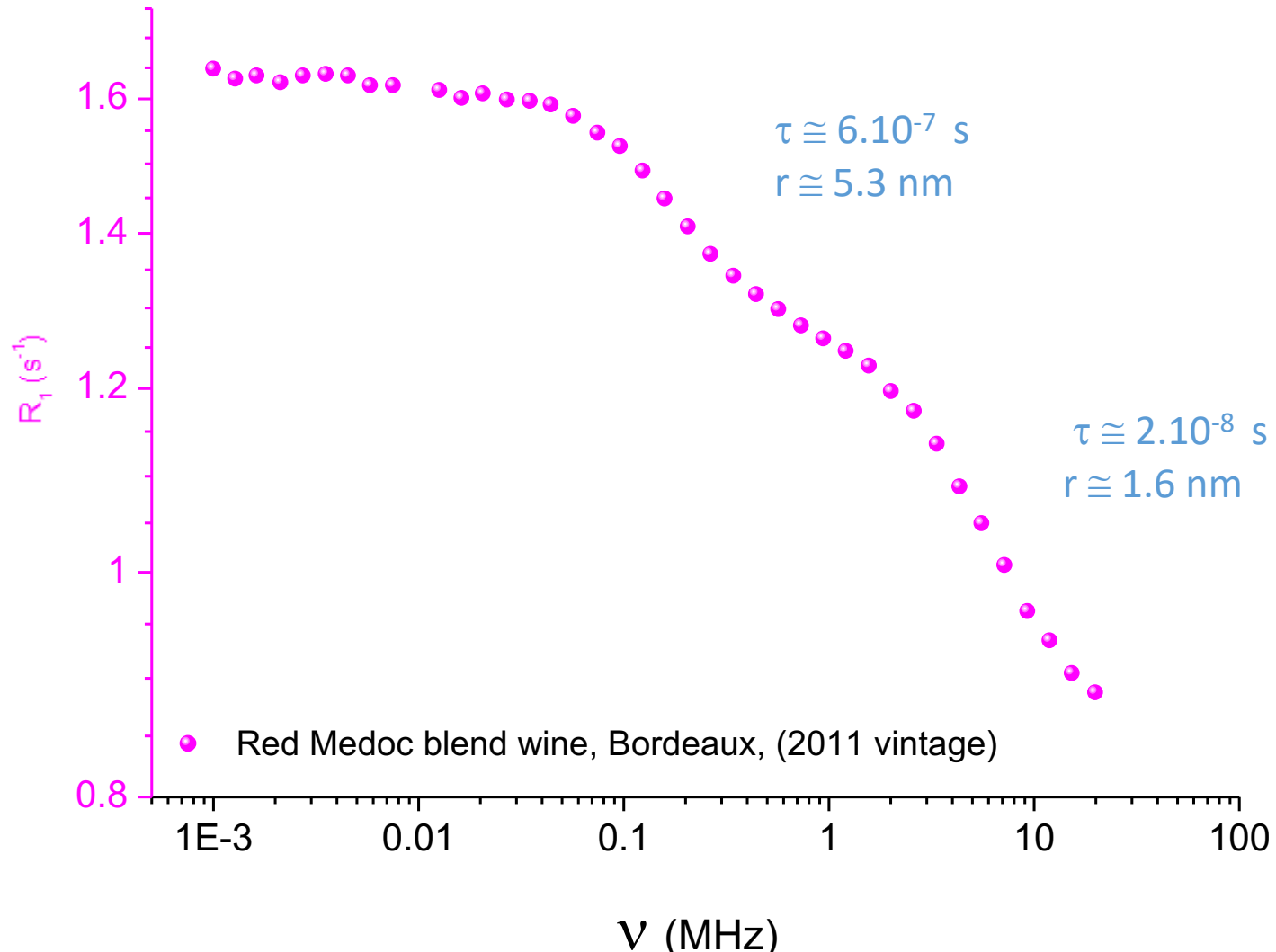
Sometimes some lees, particles in suspension, or crystals may be seen in the wine

Rotational diffusion of big molecules (proteins, polysaccharides) ?

$$\tau_c = \frac{4\pi\eta r^3}{3kT}$$

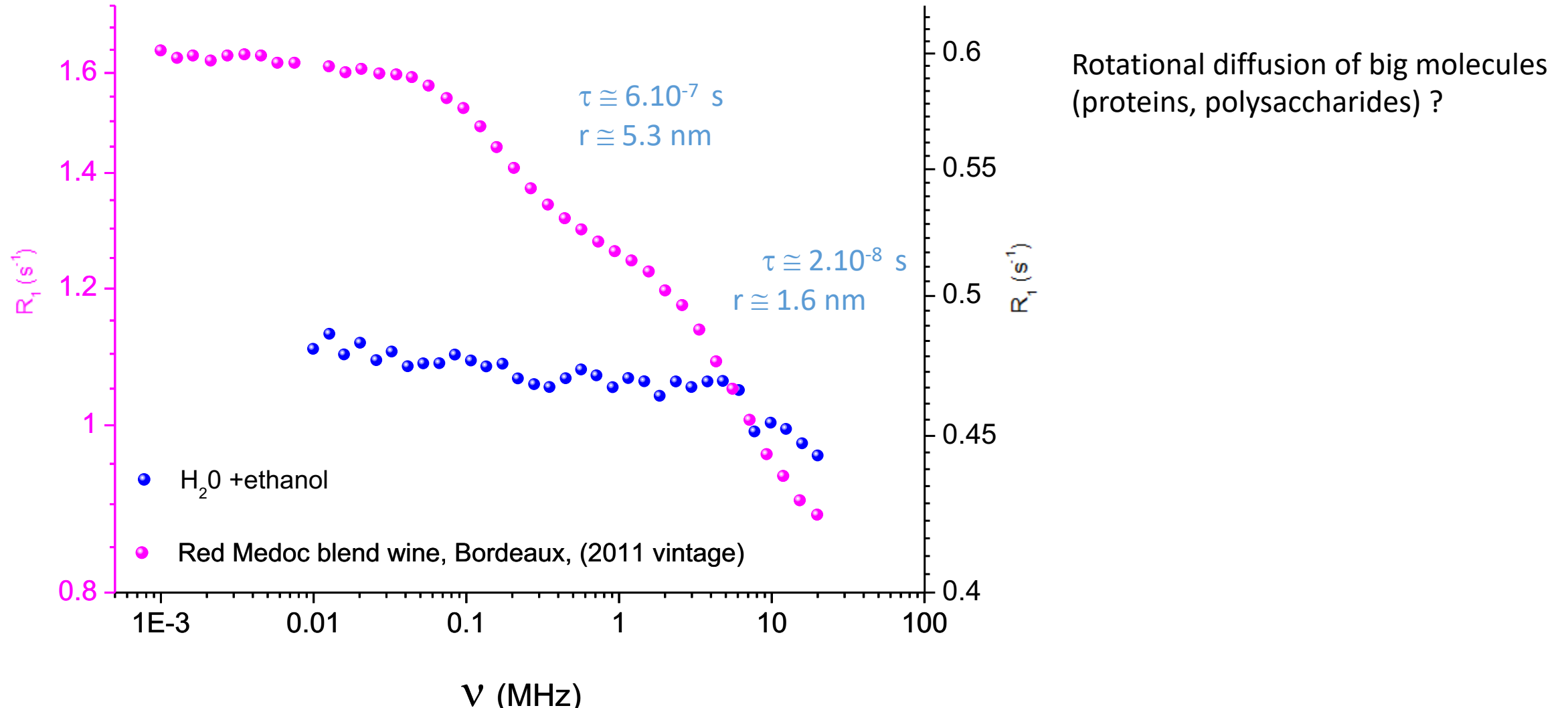
$$\eta \sim 4 \text{ mPa}\cdot\text{s}$$

NMRD profile of wine (red Medoc blend)

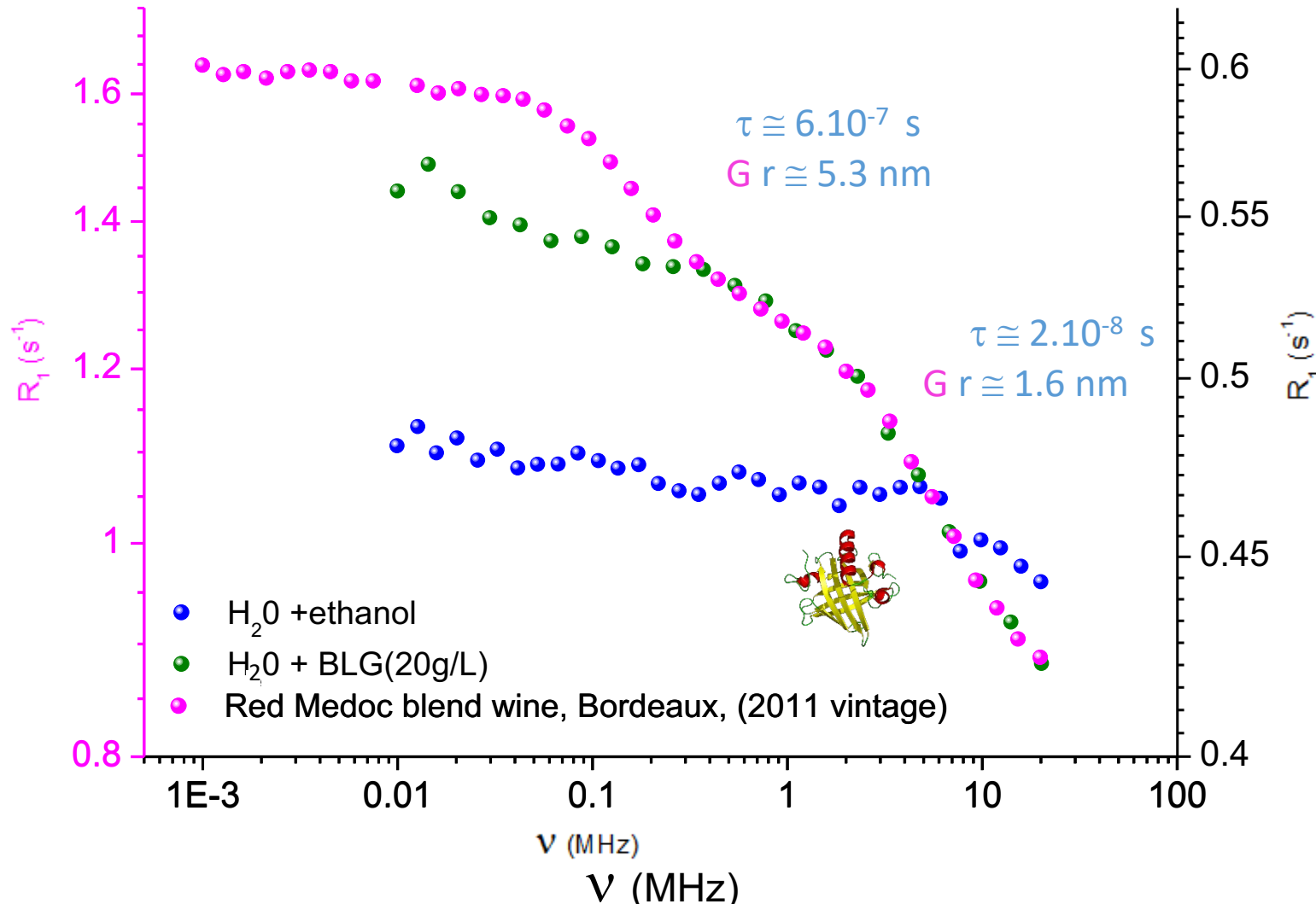


Rotational diffusion of big molecules
(proteins, polysaccharides) ?

NMRD profile of wine (red Medoc blend)



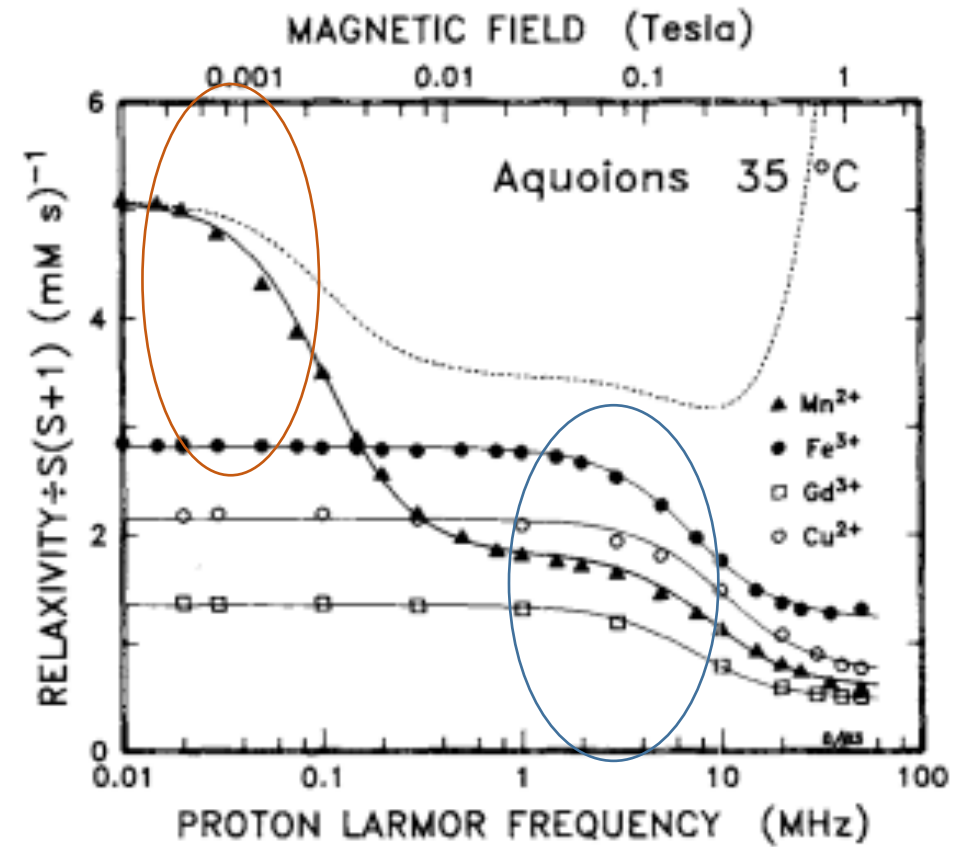
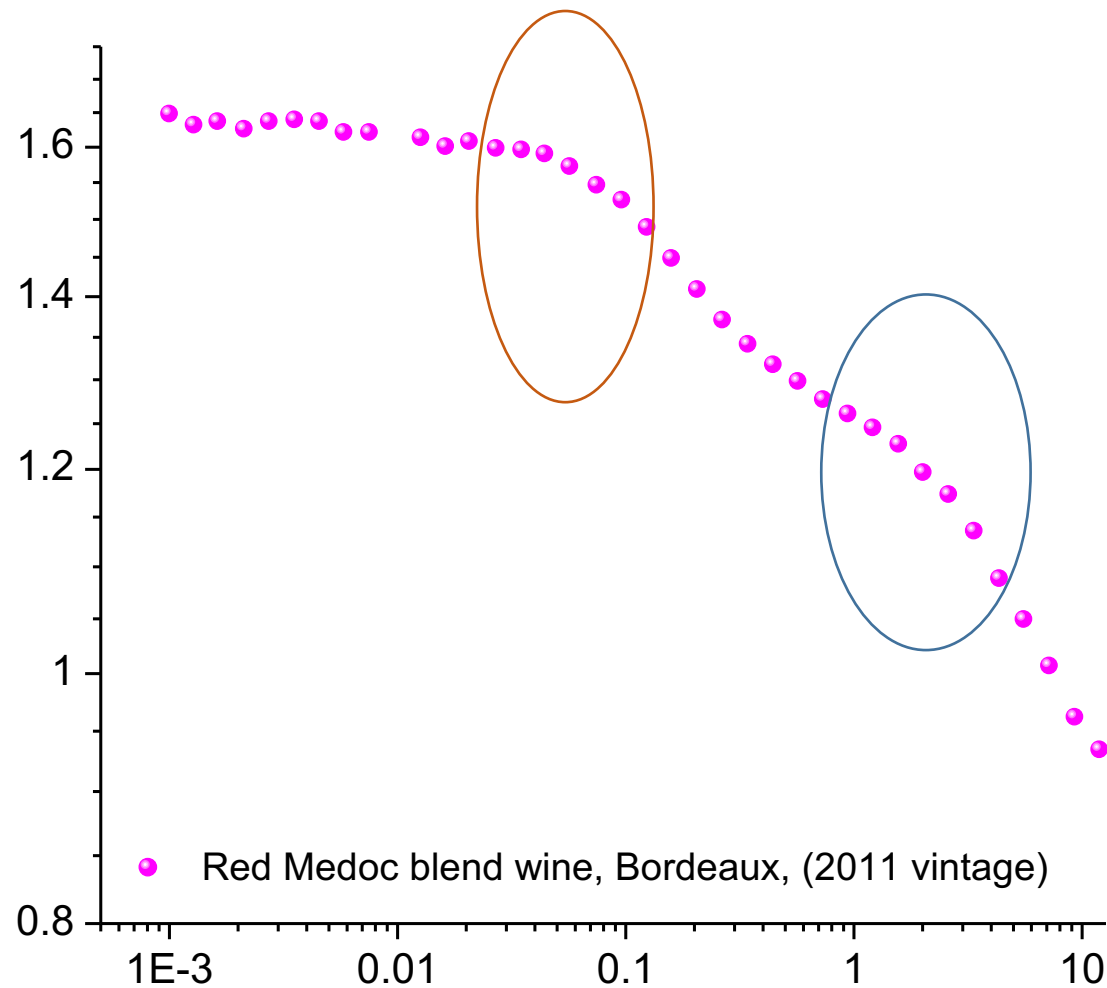
NMRD profile of wine (red Medoc blend)



Rotational diffusion of big molecules (proteins, polysaccharides) ?

The concentration and size distribution of such particles in wine would likely be insufficient to explain the NMRD profile features.

NMRD profile of wine (red Medoc blend)



S.H. Koenig, R.D. Brown, Relaxation of solvent protons by paramagnetic ions and its dependence on magnetic field and chemical environment: implications for NMR imaging, Magnetic Resonance in Medicine. 1 (1984) 478–495

Source of metal ions in wines.

Al (insecticide)

Zn (herbicides/ insecticides)

Cu (pesticide)



Cd (phosphate fertilizer)

Fe*

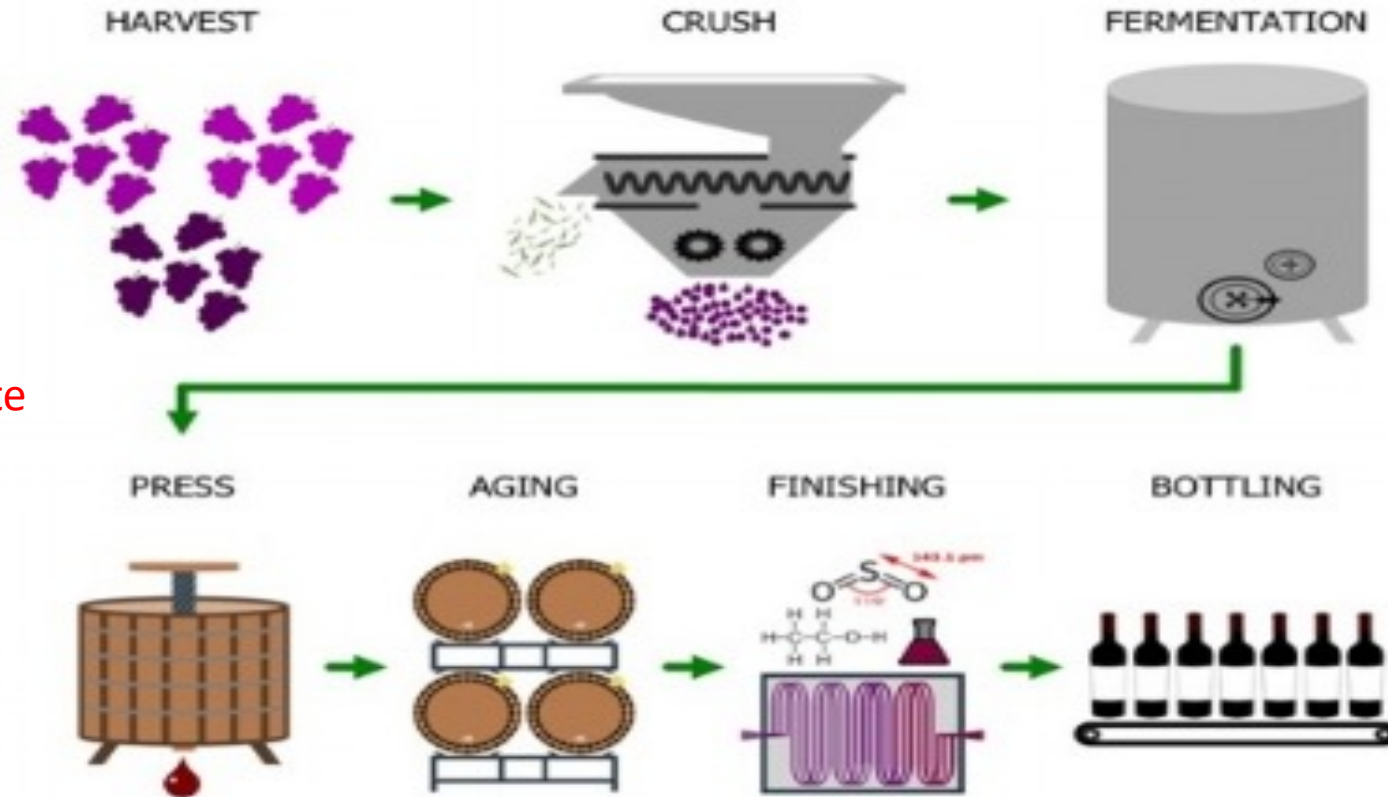
Mn*

Pb

Cr (stainless steel container)

Zn (container)

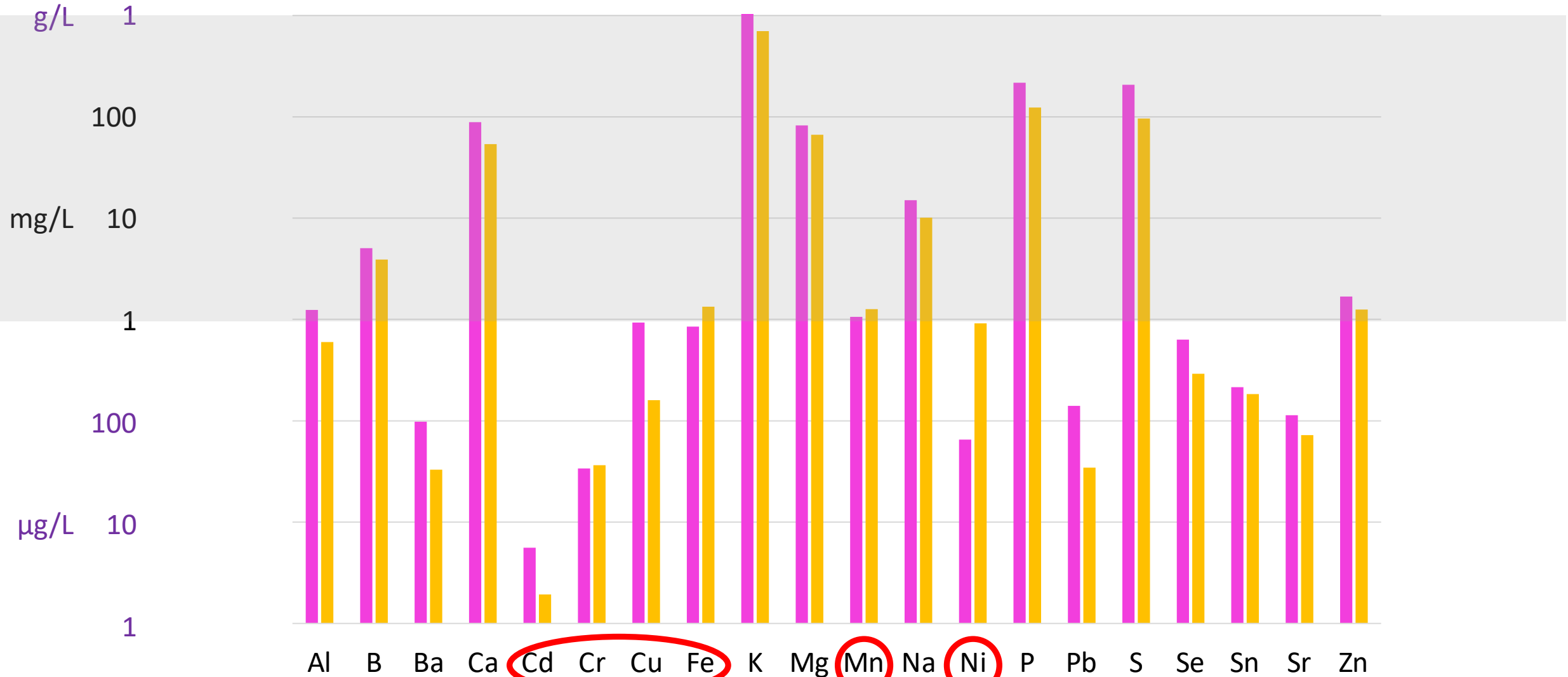
Cu (copper/ bronze materials)



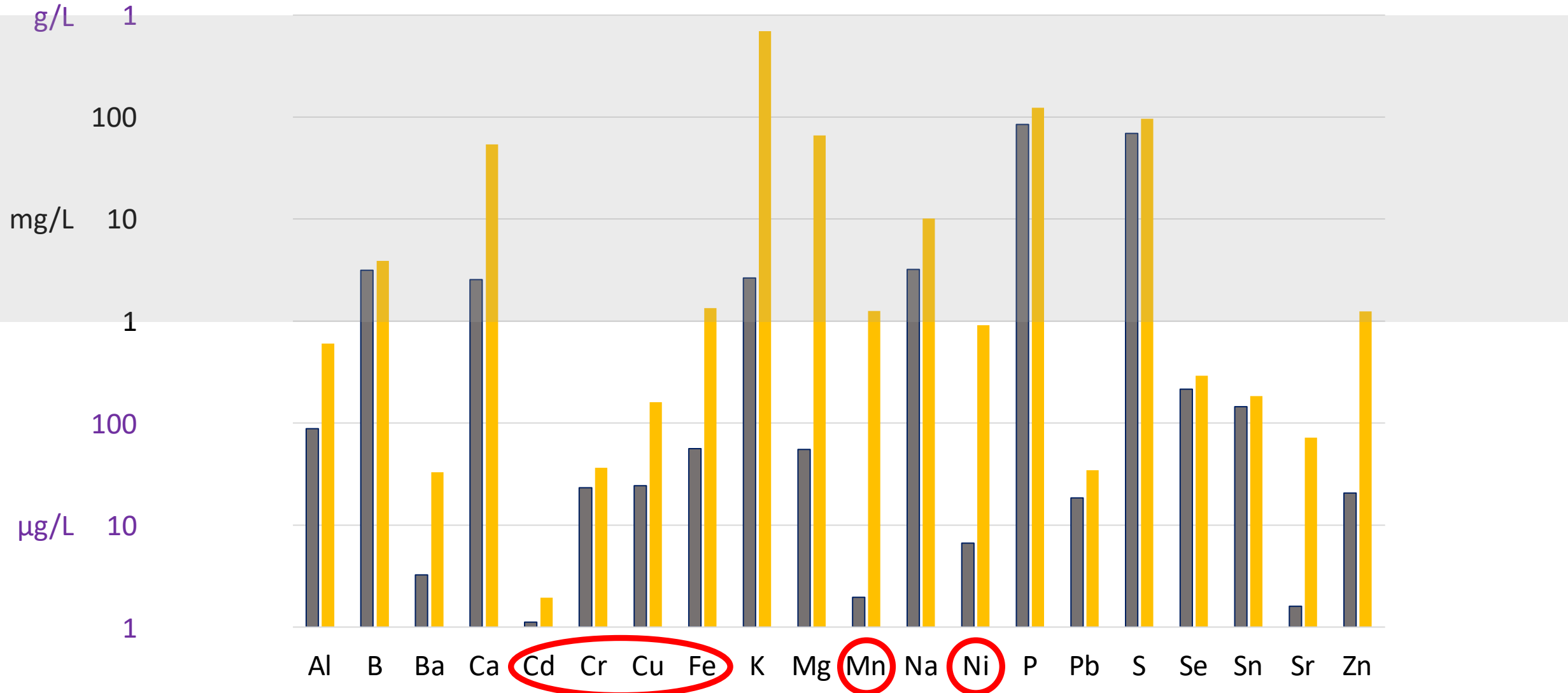
Cu (to eliminate smells from organic sulfur)

Al (use of bentonite for wine fining)

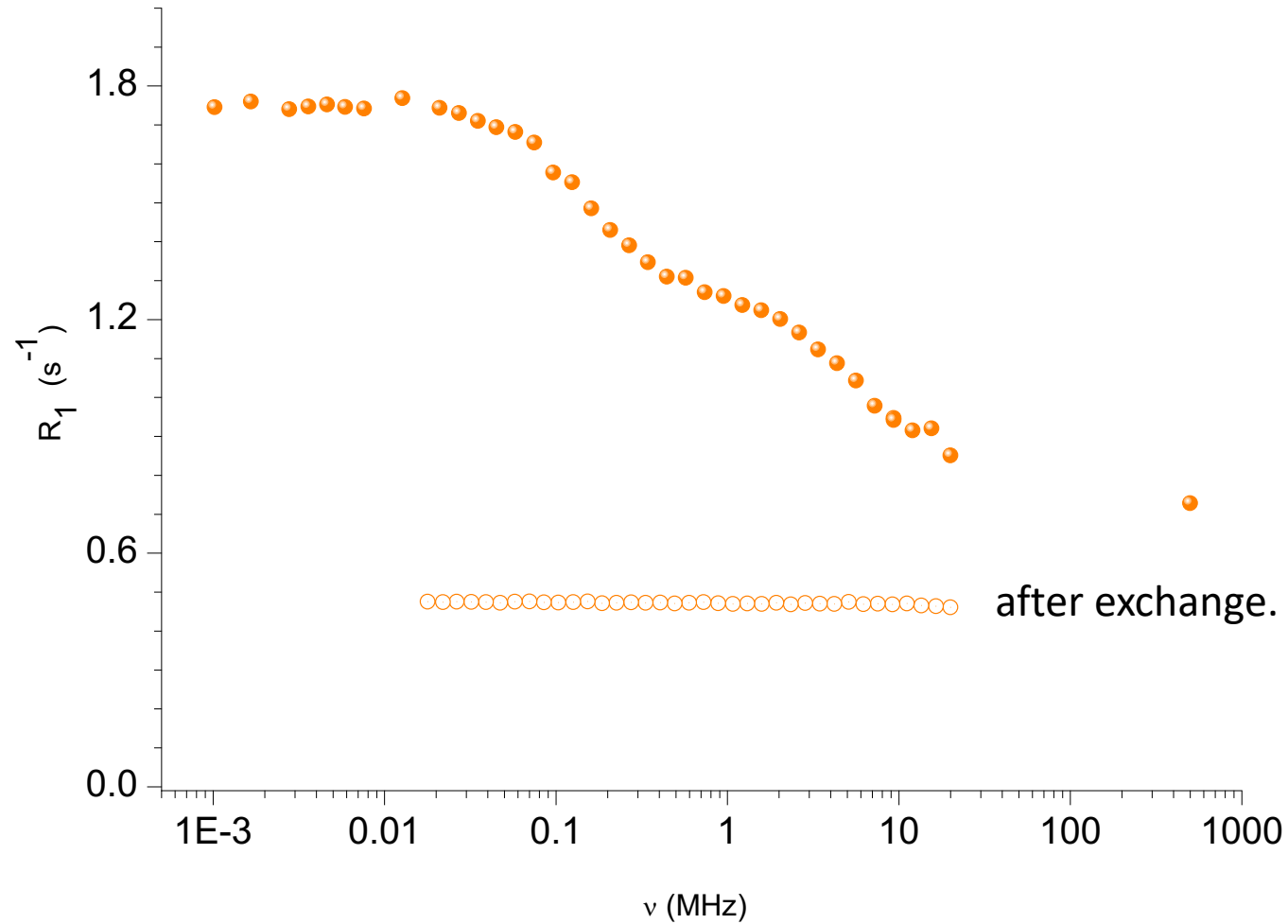
Metal ions in red Medoc blend & white Chardonnay (ICP-AES).



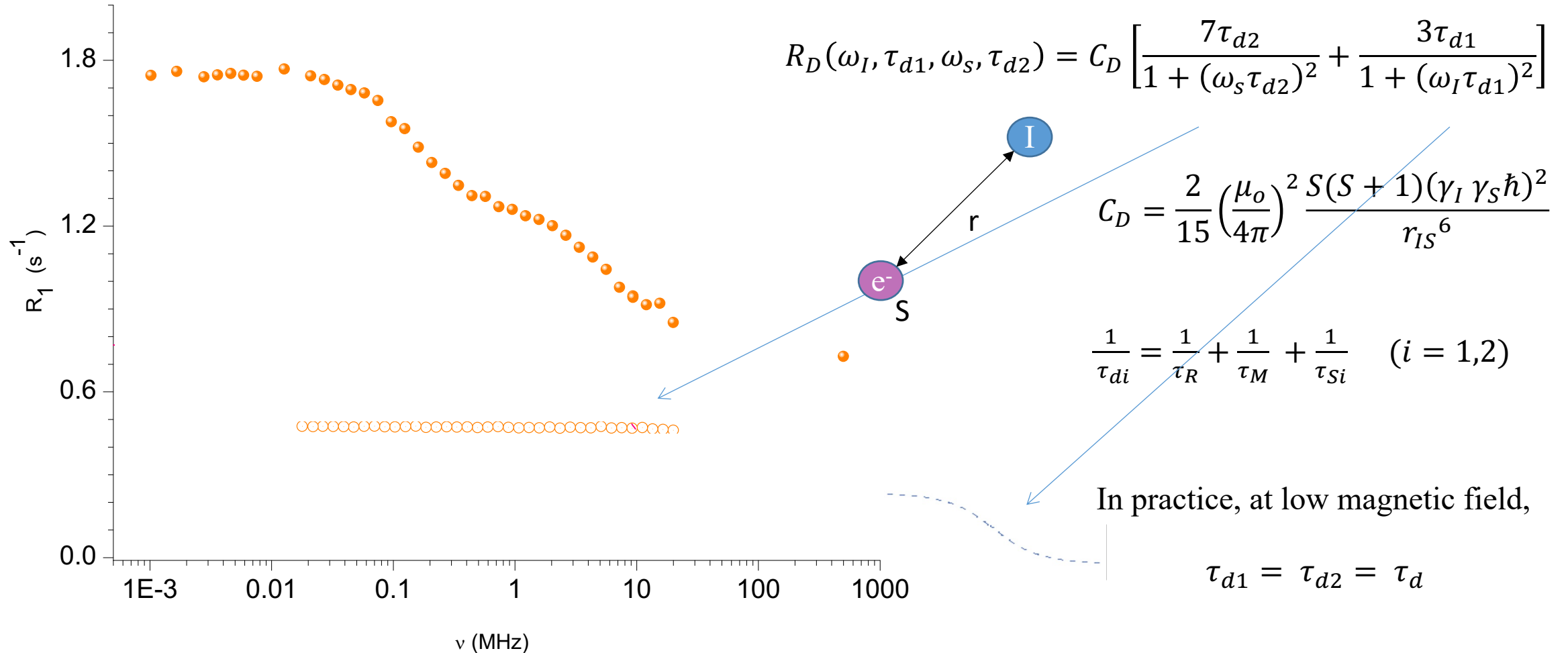
Metal ions in white Chardonnay before & after exchange (ICP-AES).



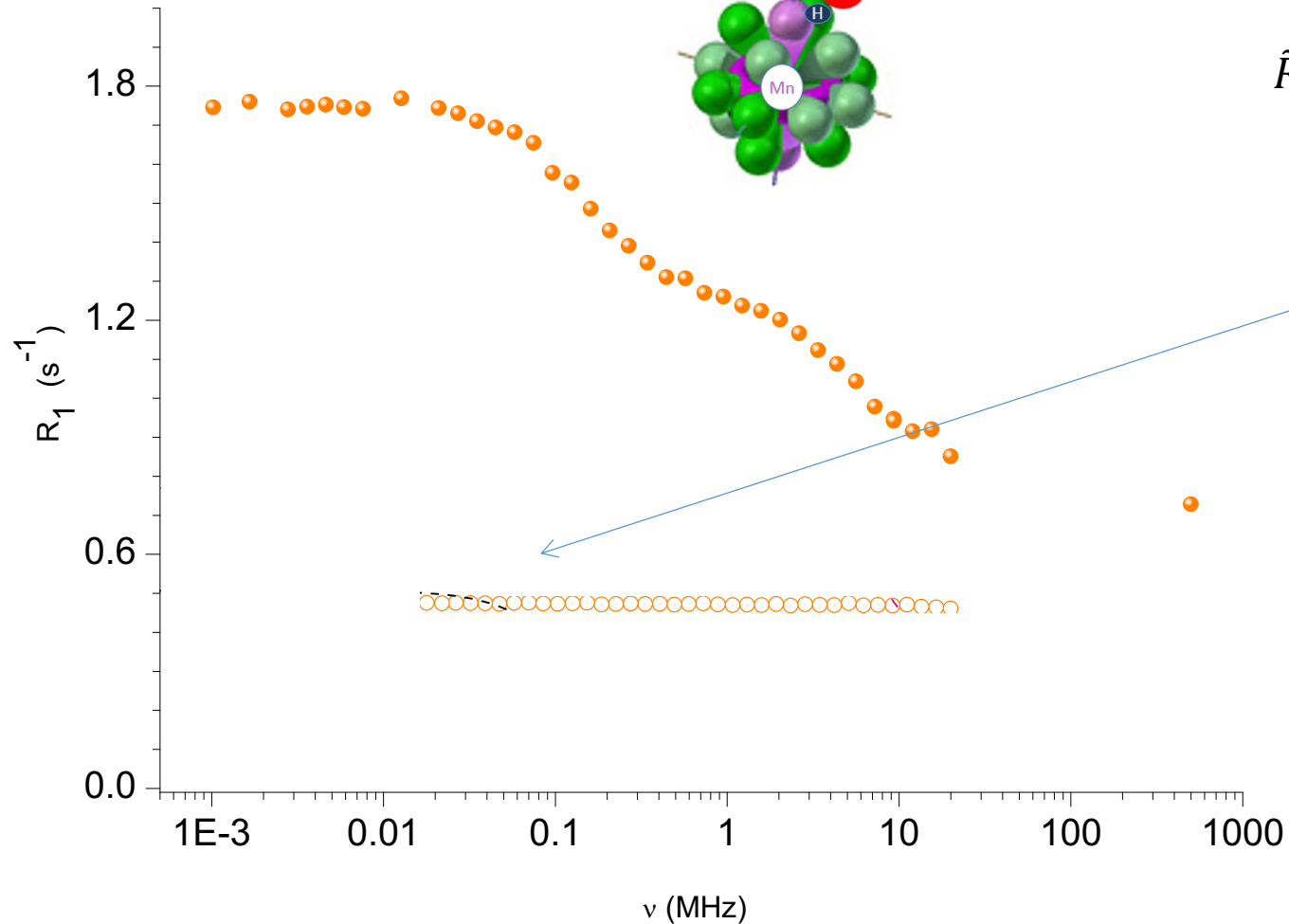
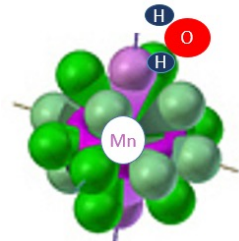
Chardonnay white wine.



Paramagnetic relaxation Solomon mechanism



Paramagnetic relaxation, Bloembergen mechanism

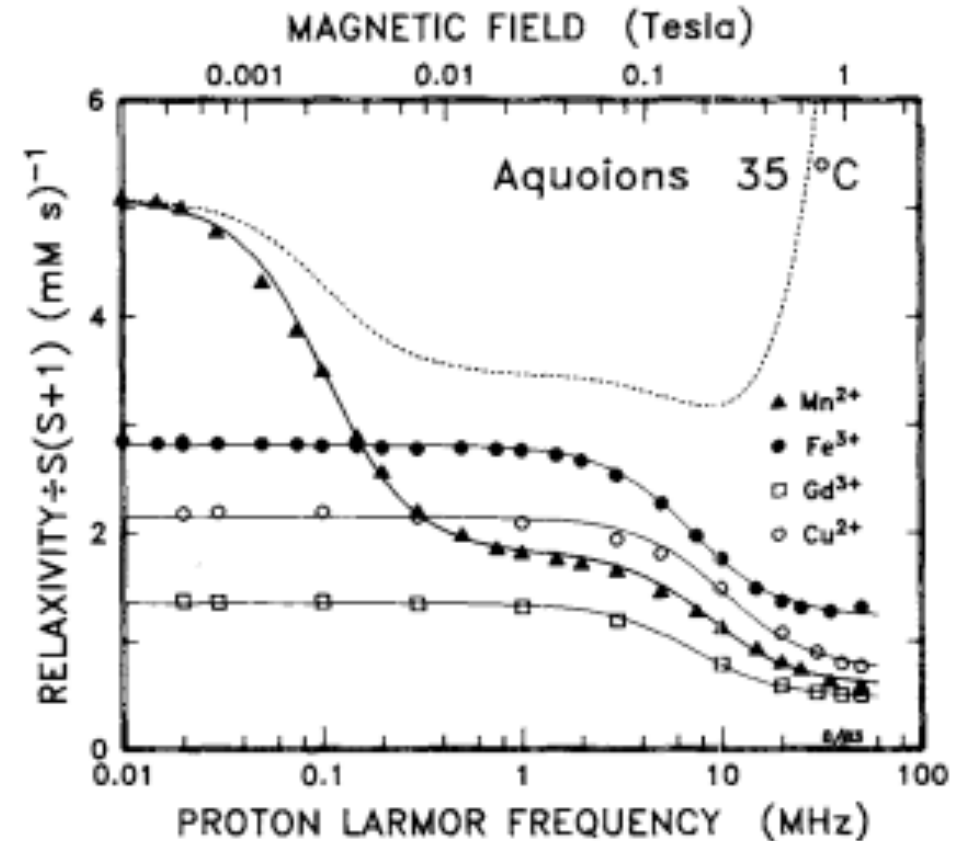
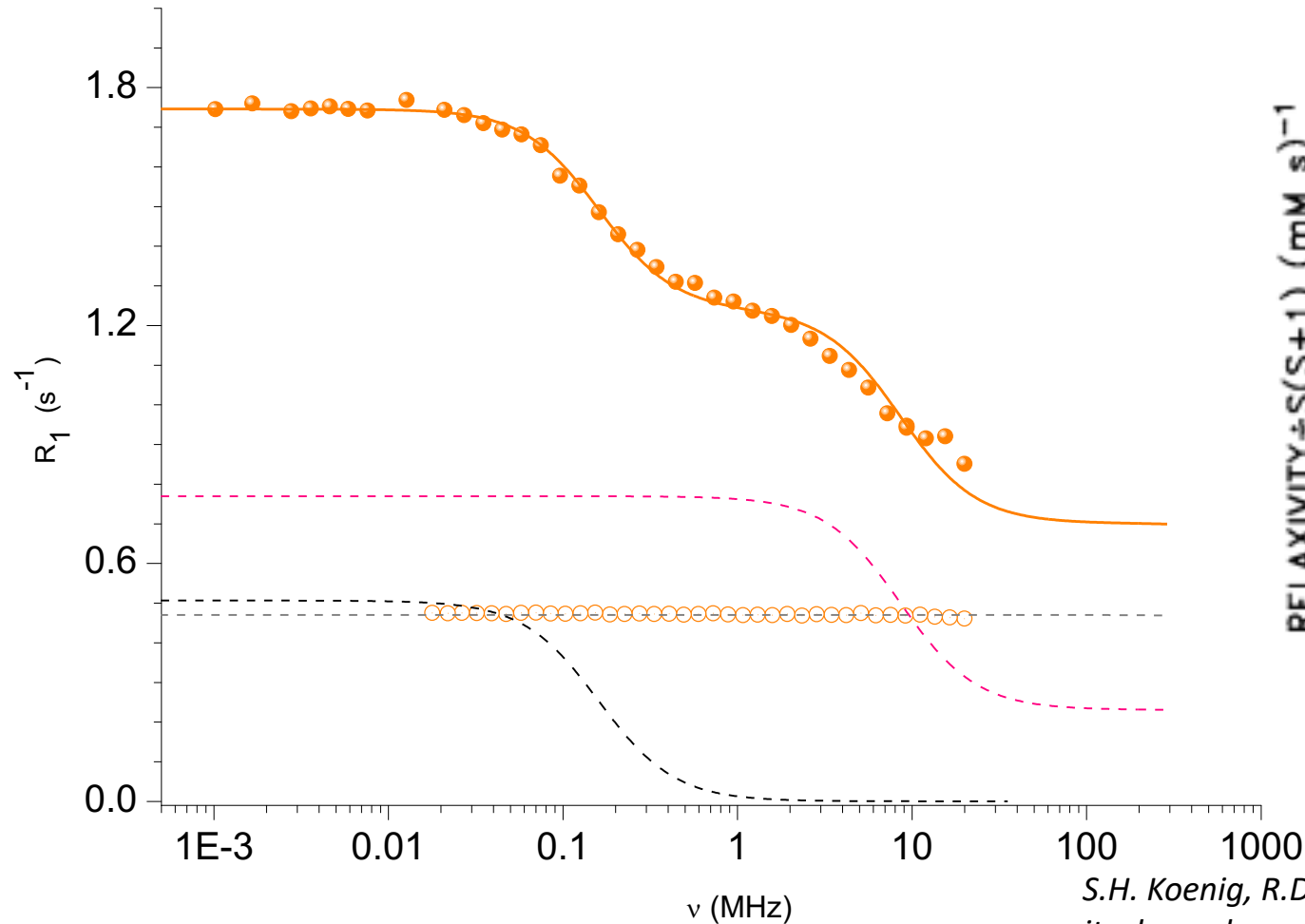


$$\tilde{R}_C(\omega_s, \tau_c) = \tilde{C}_C \left[\frac{\tau_c}{1 + (\omega_s \tau_c)^2} \right]$$

$$\tilde{C}_C = \frac{2A^2 S(S+1)}{3\hbar^2}$$

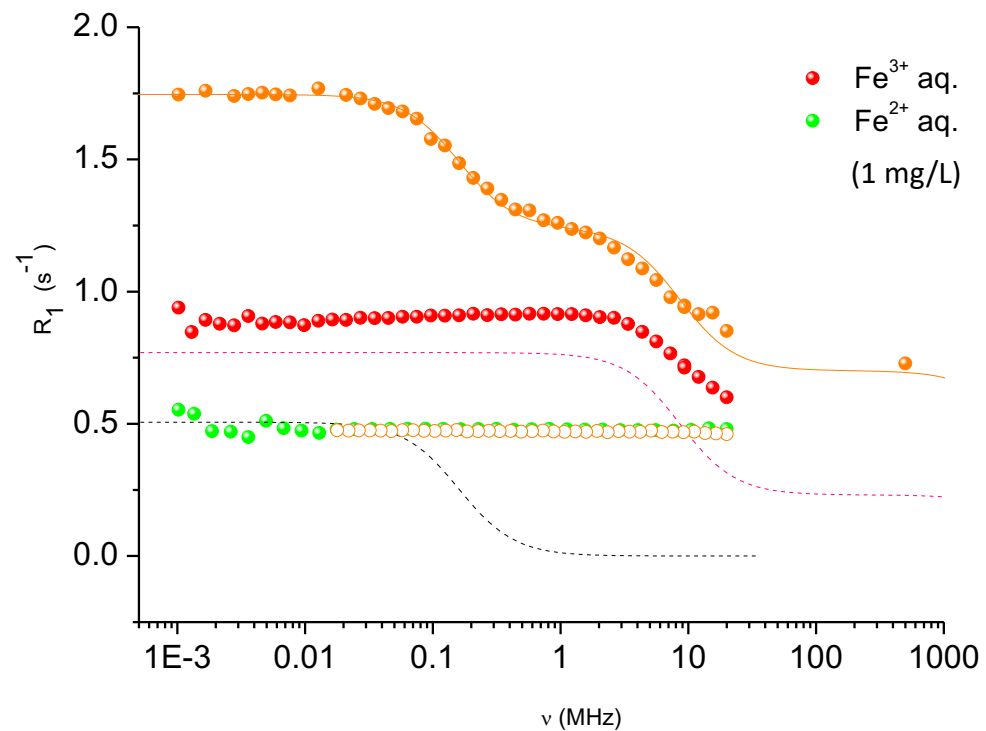
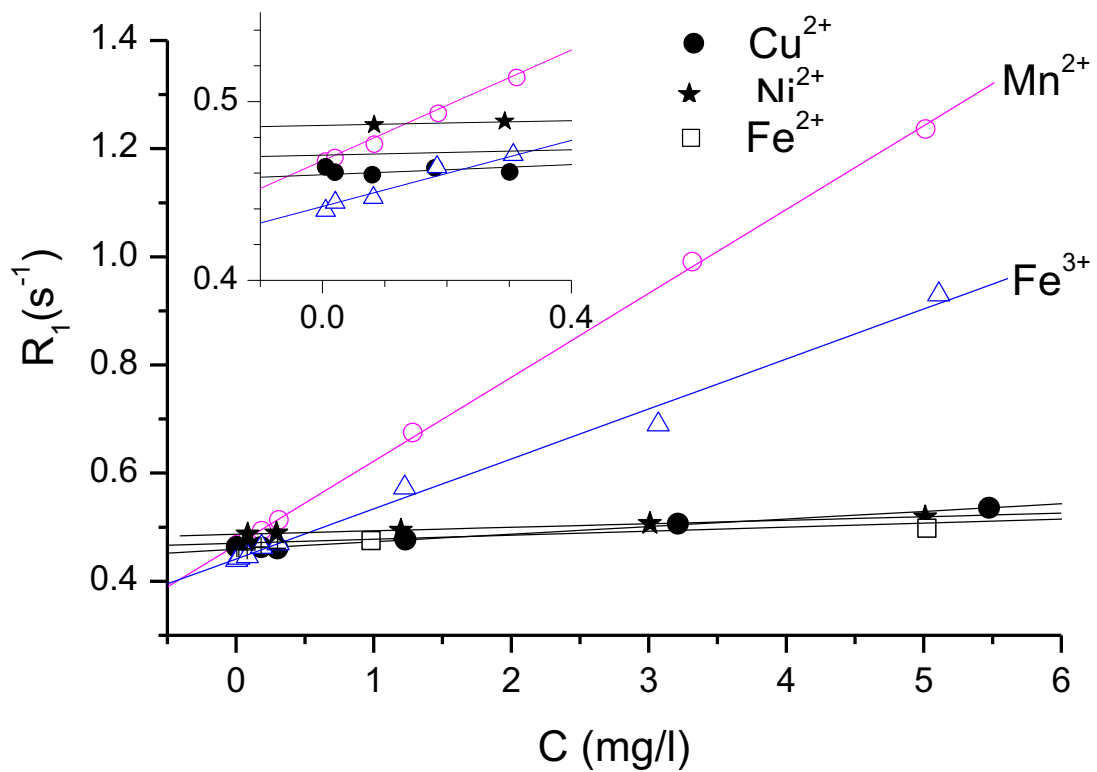
$$\frac{1}{\tau_c} = \frac{1}{\tau_M} + \frac{1}{\tau_{S2}}$$

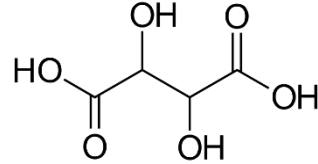
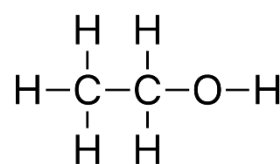
Dia and paramagnetic relaxations.



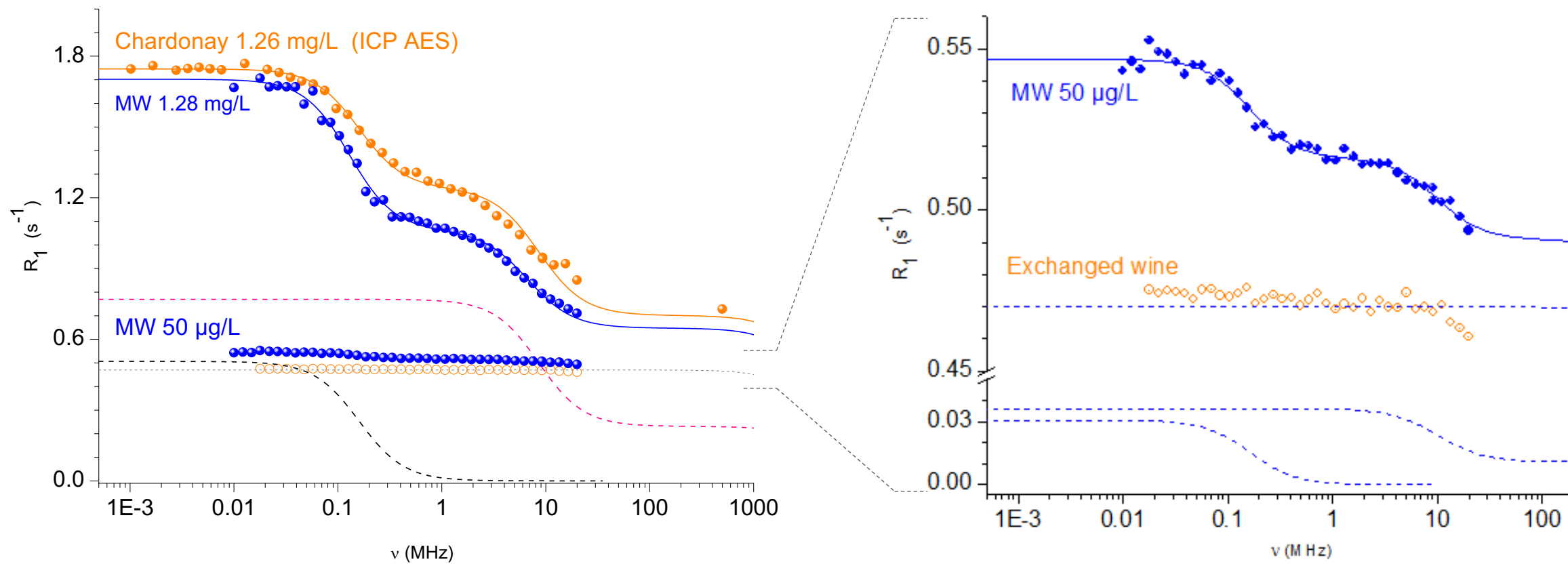
S.H. Koenig, R.D. Brown, Relaxation of solvent protons by paramagnetic ions and its dependence on magnetic field and chemical environment: implications for NMR imaging, Magnetic Resonance in Medicine. 1 (1984) 478–495

Other Contributions.





Model wines (H₂O, ethanol, tart. a. (5g/L))

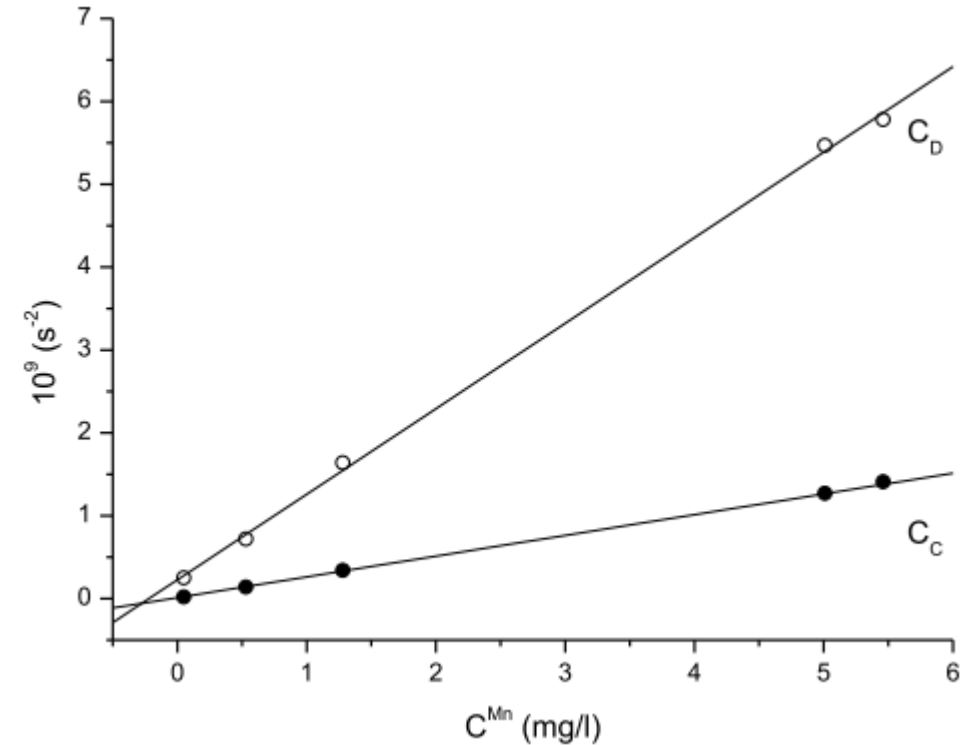


Model wines

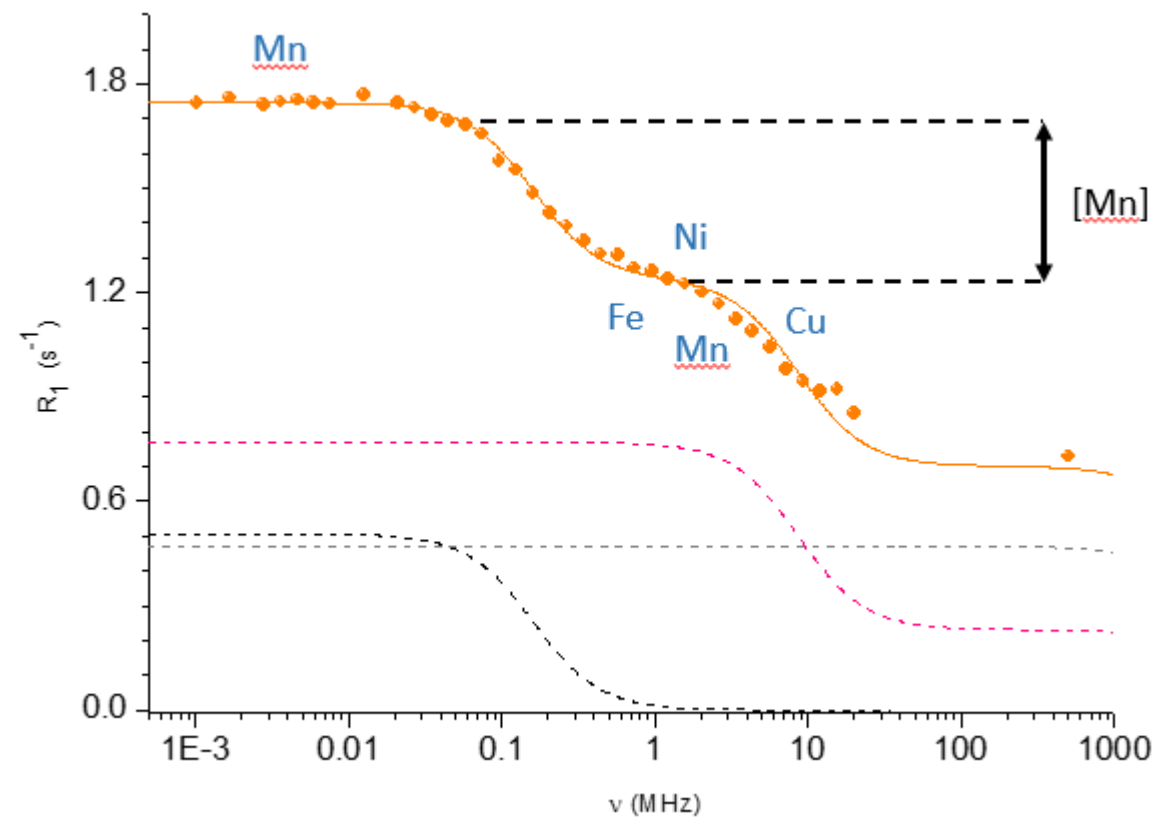
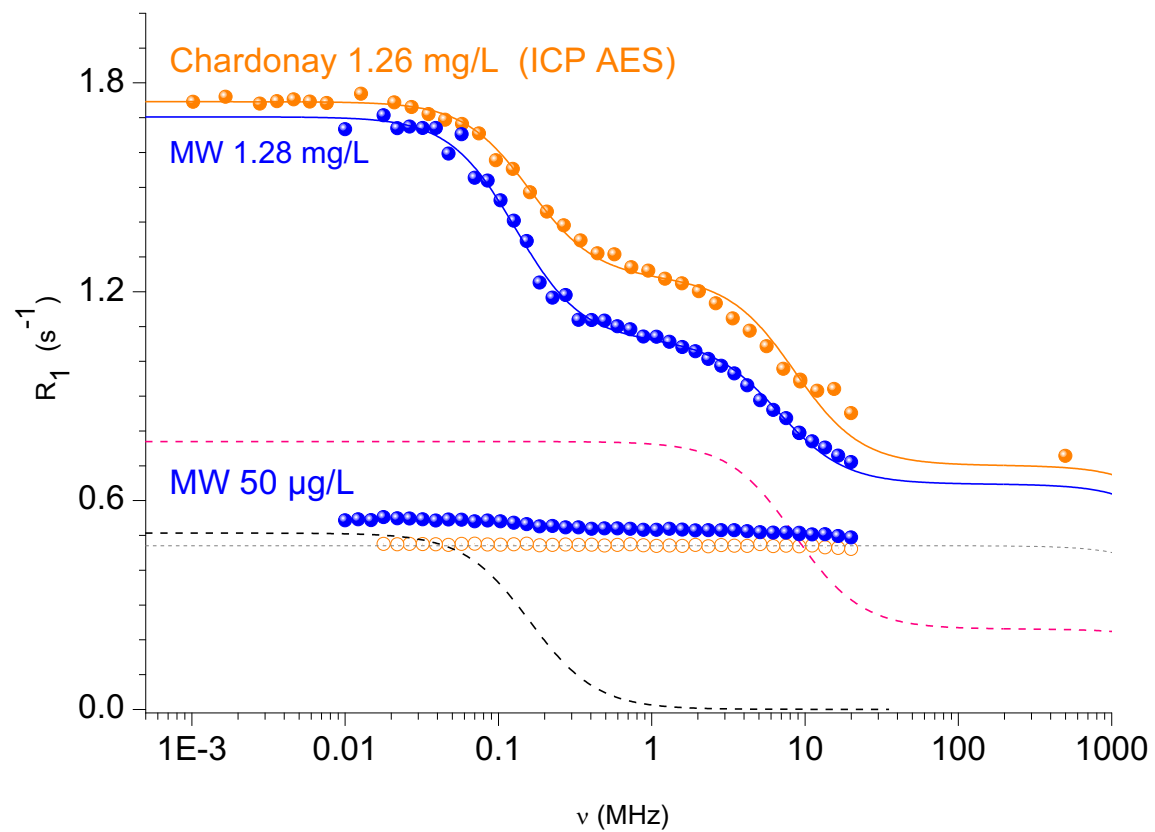
$$R_D(\omega_I, \tau_{d1}, \omega_S, \tau_{d2}) = C_D \left[\frac{7\tau_{d2}}{1+(\omega_S\tau_{d2})^2} + \frac{3\tau_{d1}}{1+(\omega_I\tau_{d1})^2} \right] + \tilde{C}_C \left[\frac{\tau_c}{1+(\omega_S\tau_c)^2} \right]$$

Parameters obtained from refinements of NMRD profiles for the white Chardonnay (W), the red Medoc blend (R) and model wines (MW). MWx refers to model wines containing x/100 mg/L of manganese. $C_{D/C} = pq\tilde{C}_{D/C}$ and numbers in parentheses are last-digit-uncertainties resulting purely from the numerical refinement.

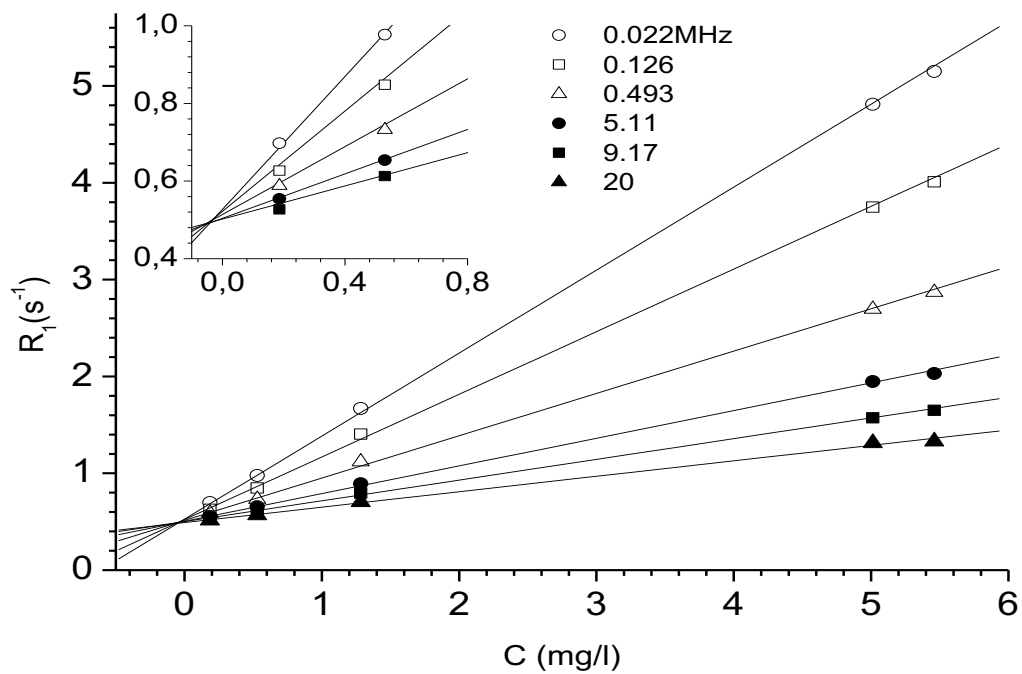
	R_D		R_C	
	$C_D (10^9 \text{ s}^{-2})$	$\tau_d (10^{-11} \text{ s})$	$C_C (10^9 \text{ s}^{-2})$	$\tau_c (10^{-9} \text{ s})$
MW546	5.78	3.81 (2)	1.41	1.88 (1)
MW501	5.47	3.78 (2)	1.27	1.86 (2)
MW128	1.64	3.60 (3)	0.34	1.87 (3)
MW053	0.72	3.43 (3)	0.14	1.82 (3)
MW005	0.25	1.80 (2)	0.02	1.50 (4)
Wa	2.73	2.82 (3)	0.33	1.51 (3)
Wb	2.69	2.92 (2)	0.36	1.43 (2)
Ra	2.97	2.56 (2)	0.30	1.28 (3)
Rb	2.07	3.22 (3)	0.30	1.38 (4)



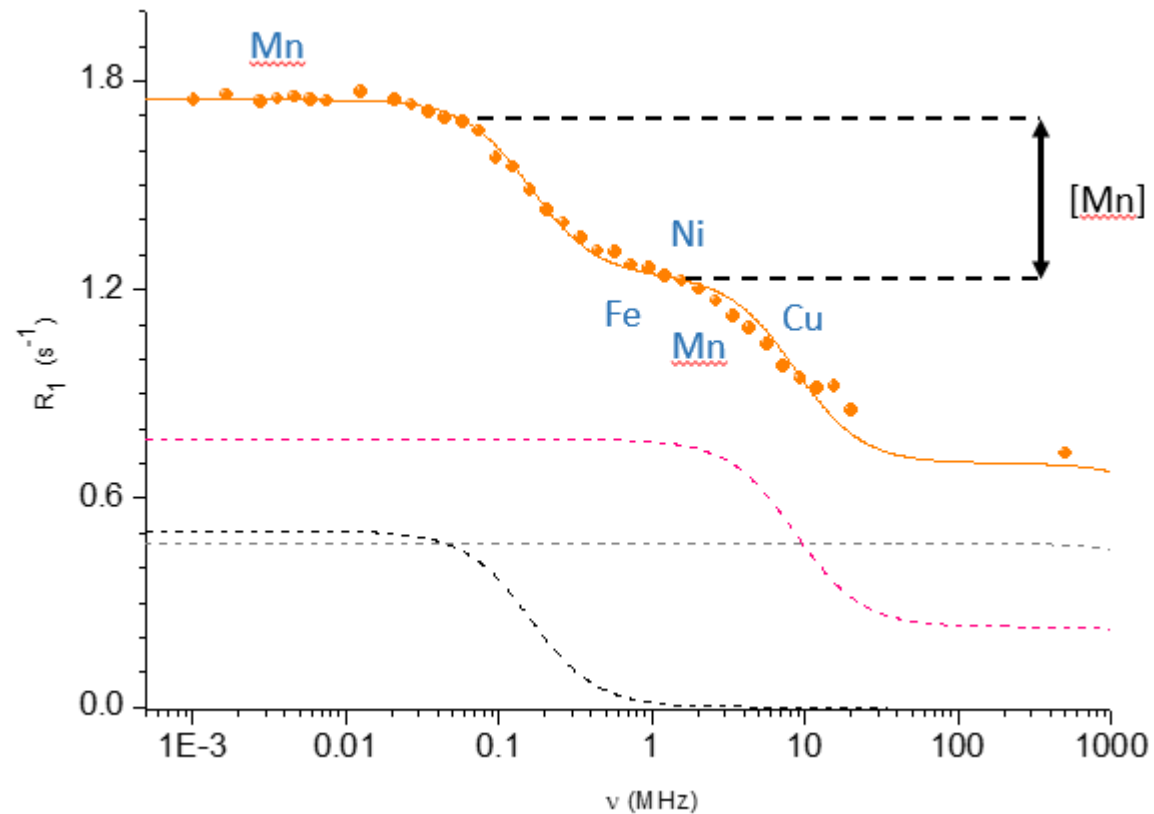
Quantification of Manganese



Quantification of Manganese

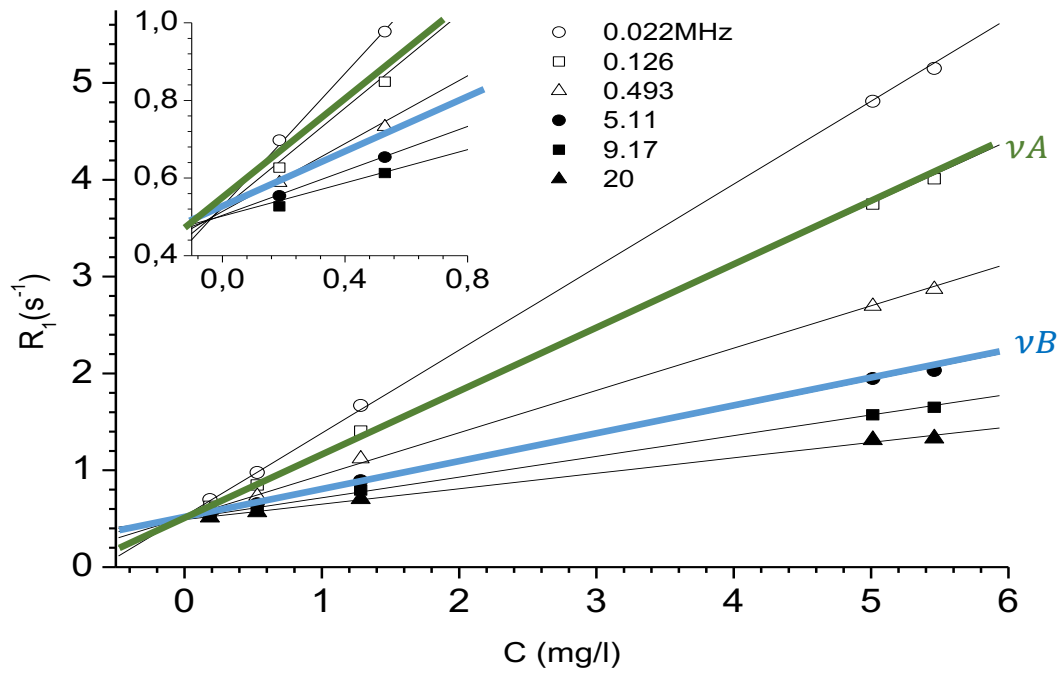


$$R_\nu = R_0 + r_\nu^{Mn} \cdot C^{Mn}$$

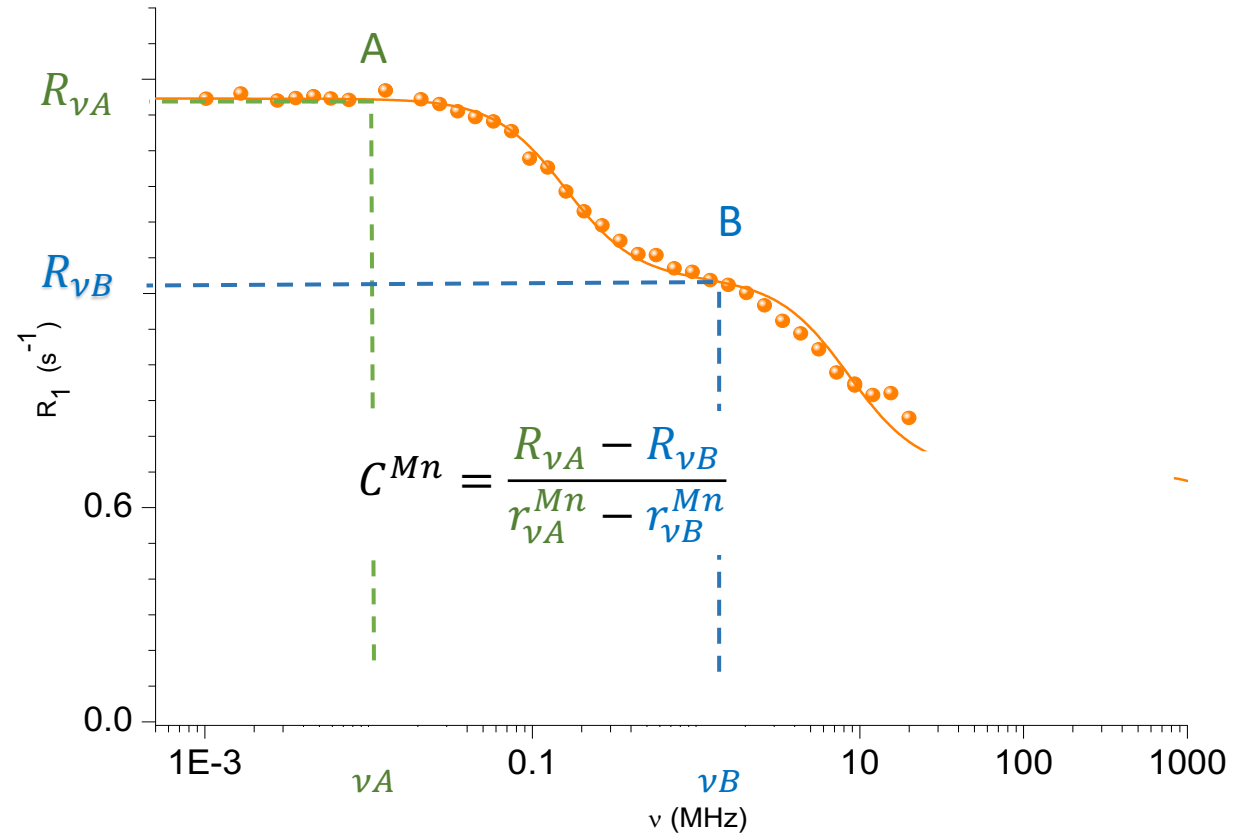


Quantification of Manganese

How the relaxation rate evolves with manganese concentration



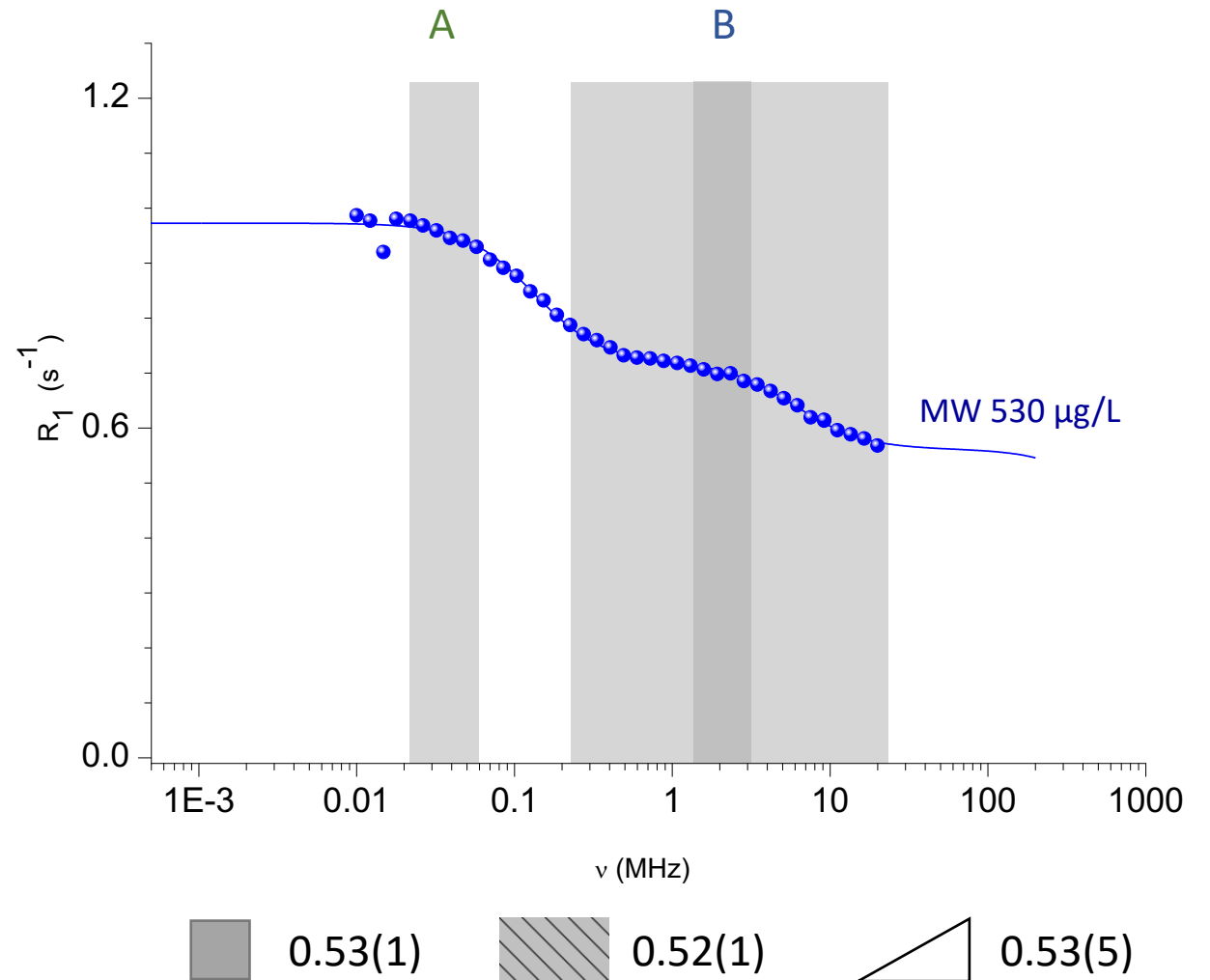
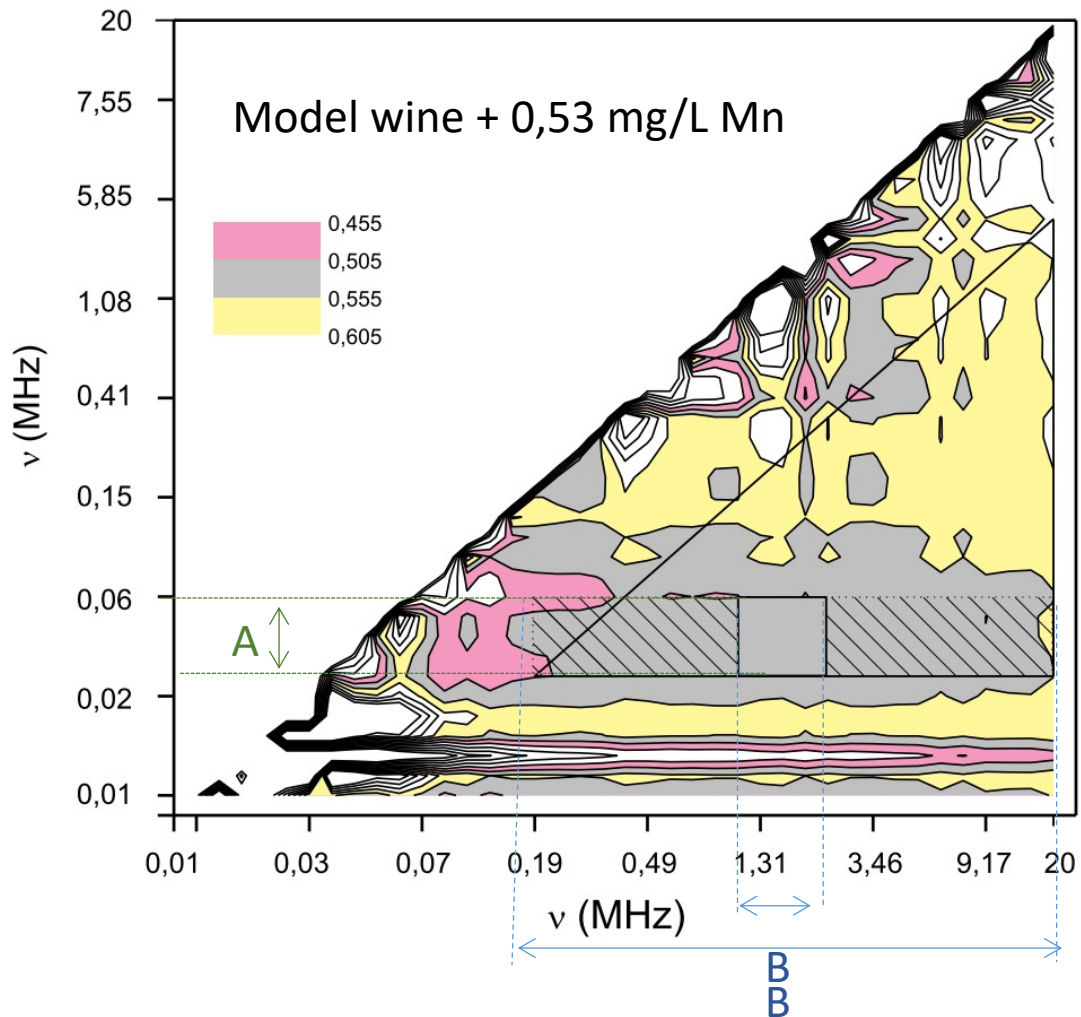
$$R_v = R_0 + \underline{r_v^{Mn}} \cdot C^{Mn}$$



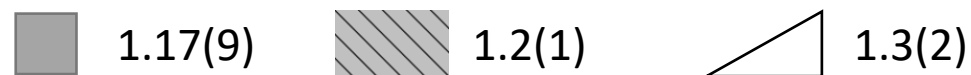
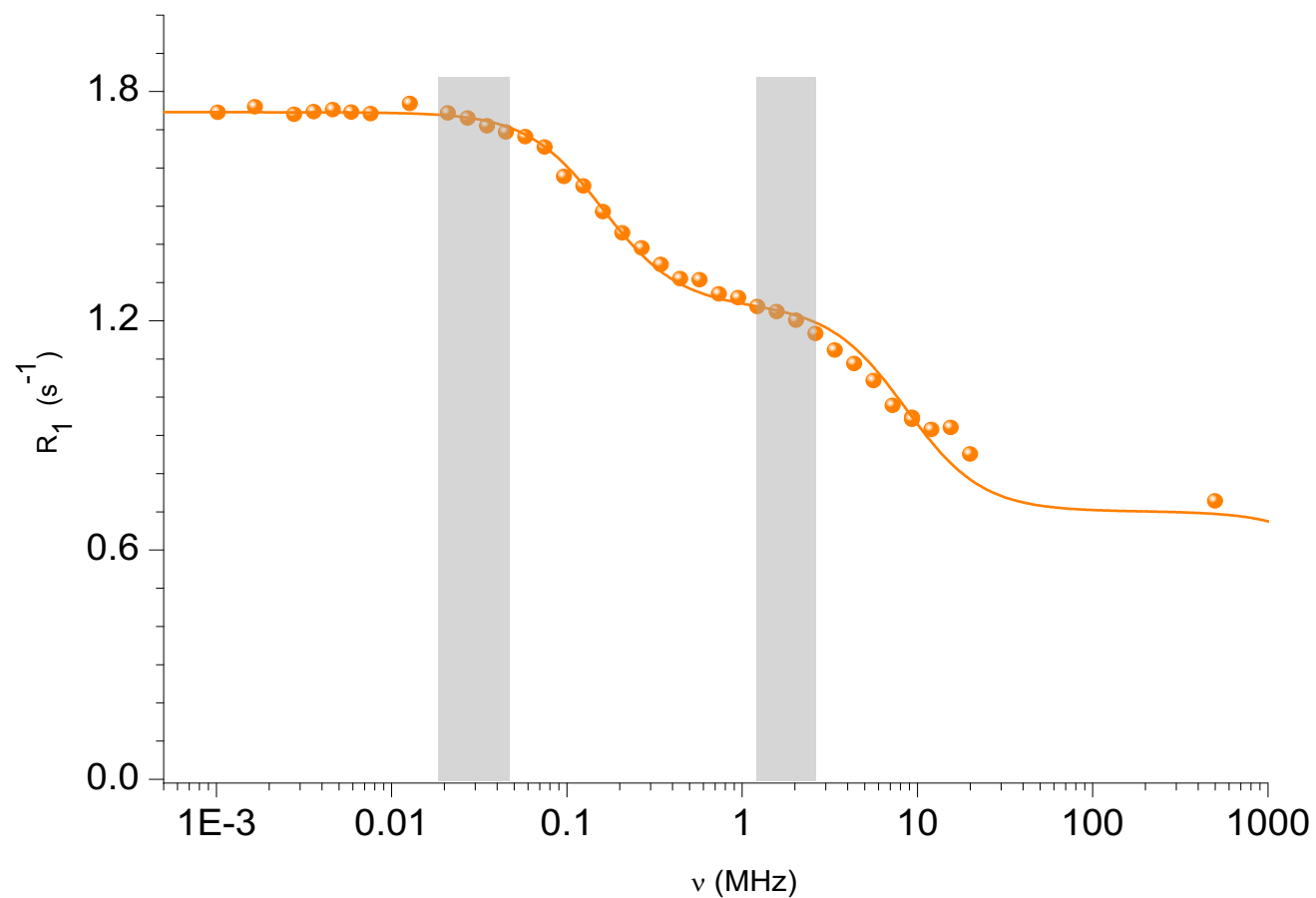
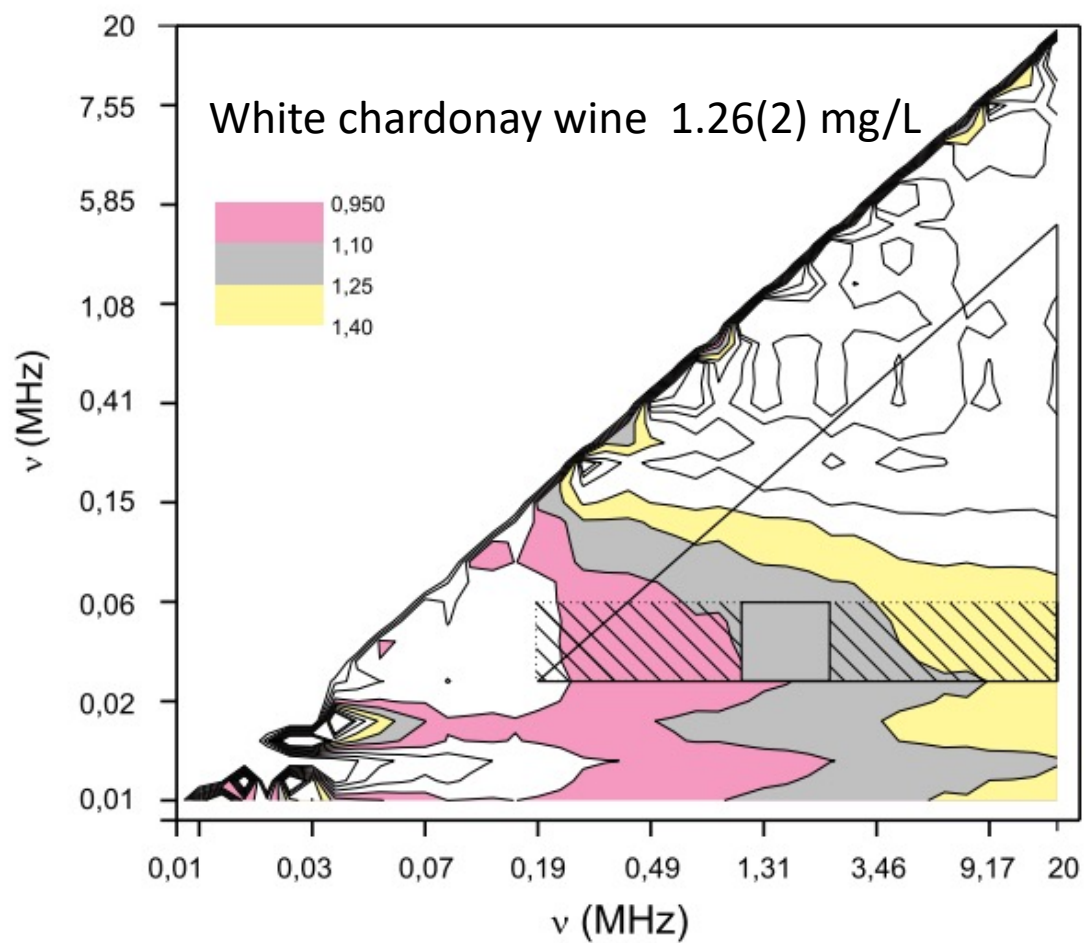
Quantification of Manganese

How the relaxation rate evolves with manganese concentration

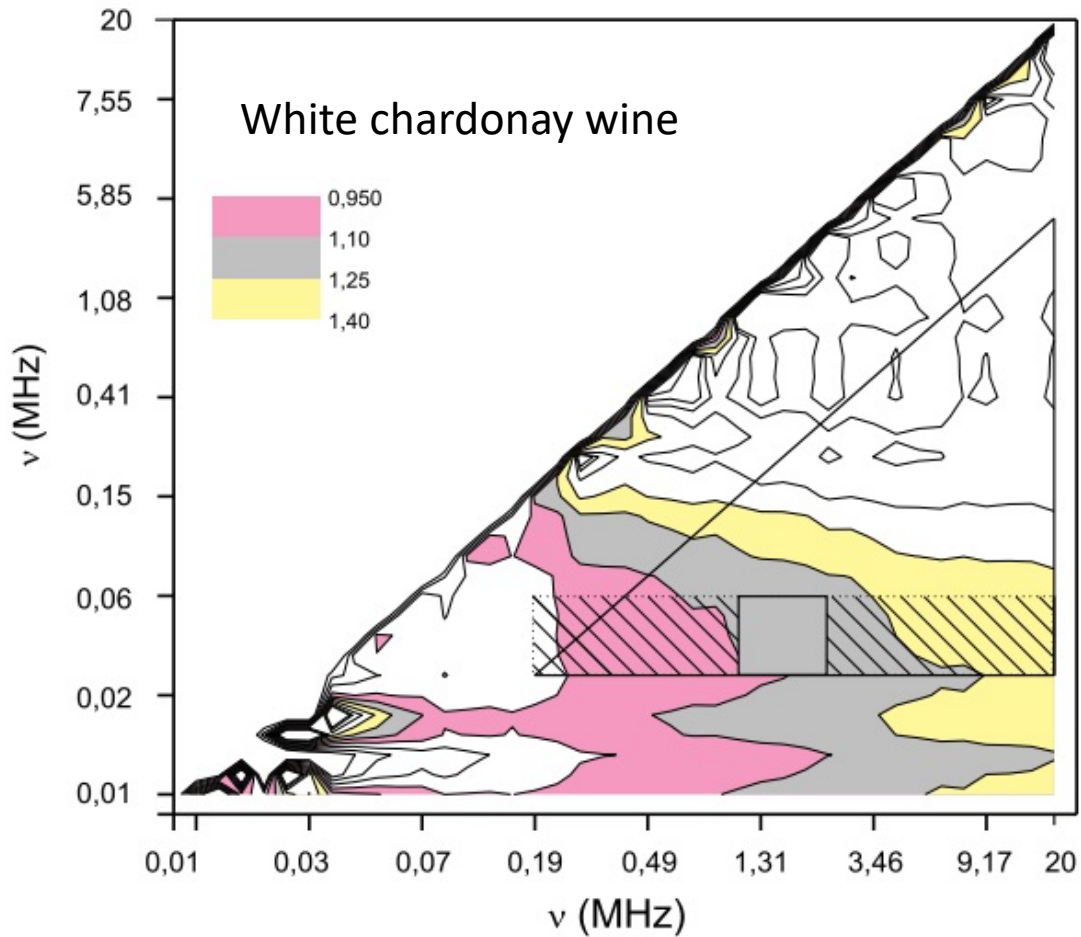
$$C^{Mn} = \frac{R_{\nu A} - R_{\nu B}}{r_{\nu A}^{Mn} - r_{\nu B}^{Mn}}$$



Quantification of Manganese



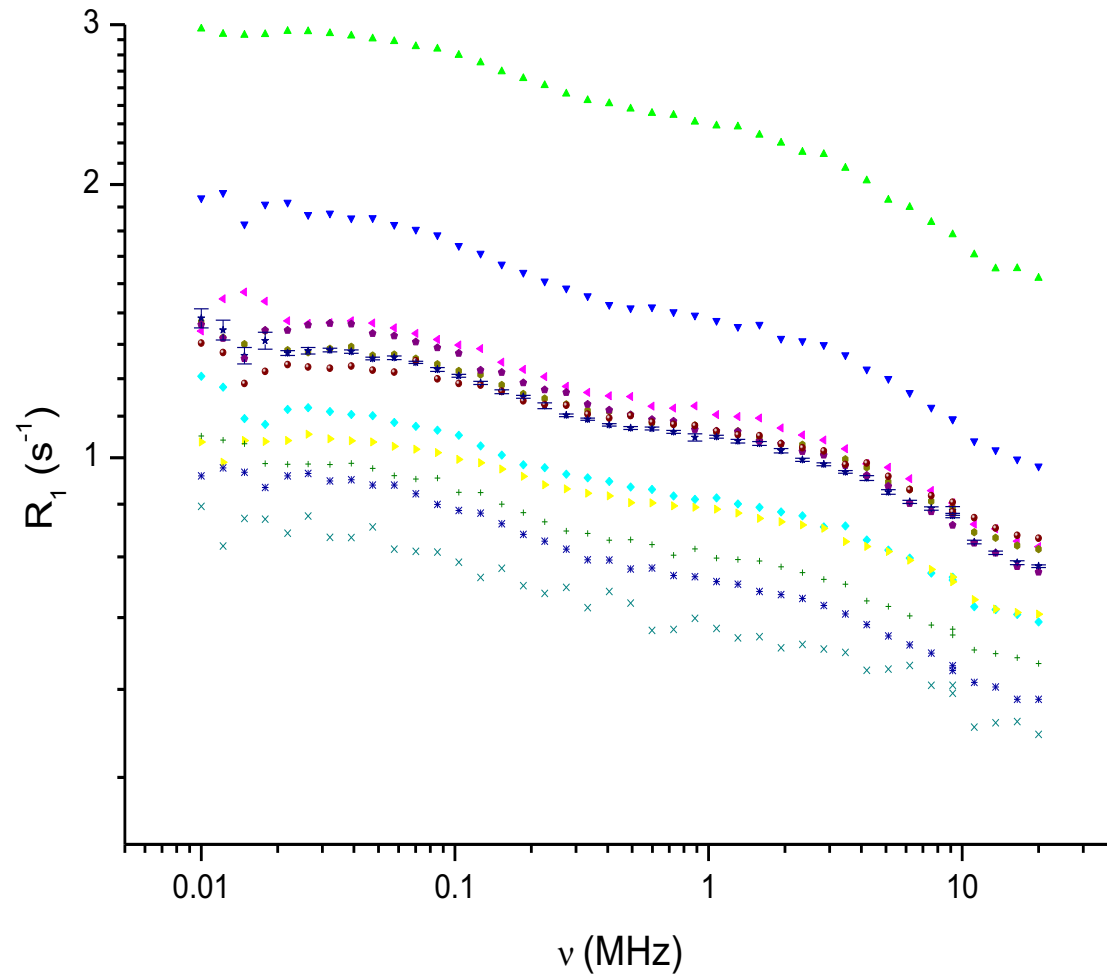
Quantification of Manganese



	Manganese concentration(mg/L)	Square zone	Rectangular zone	Triangular zone
MW546	5.46	5.46 (3)	5.45 (4)	5.5 (1)
MW501	5.01	4.97 (5)	4.97 (6)	5.0 (1)
MW128	1.28	1.34 (8)	1.3 (1)	1.3 (1)
MW053	0.53	0.53 (1)	0.52 (1)	0.53 (5)
MW005	0.05	0.063 (5)	0.063 (6)	0.06 (1)
Wa	1.26 (2) ^a	1.17 (9)	1.2 (1)	1.3 (2)
Wb		1.13 (3)	1.1 (1)	1.4 (2)
Ra	1.06 (2) ^a	0.83 (4)	0.9 (1)	1.2 (3)
Rb		0.91 (5)	0.9 (1)	1.2 (3)
EW	< 0.002 ^a	0.009 (6)	0.011 (4)	0.01 (1)

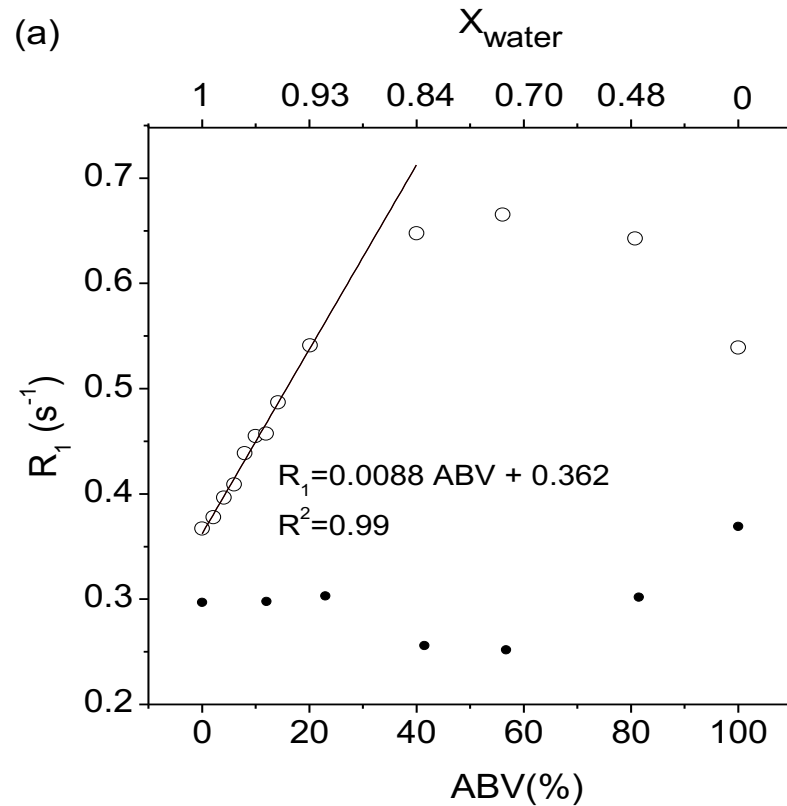
^a Concentration measured by ICP AES.

More wines ?



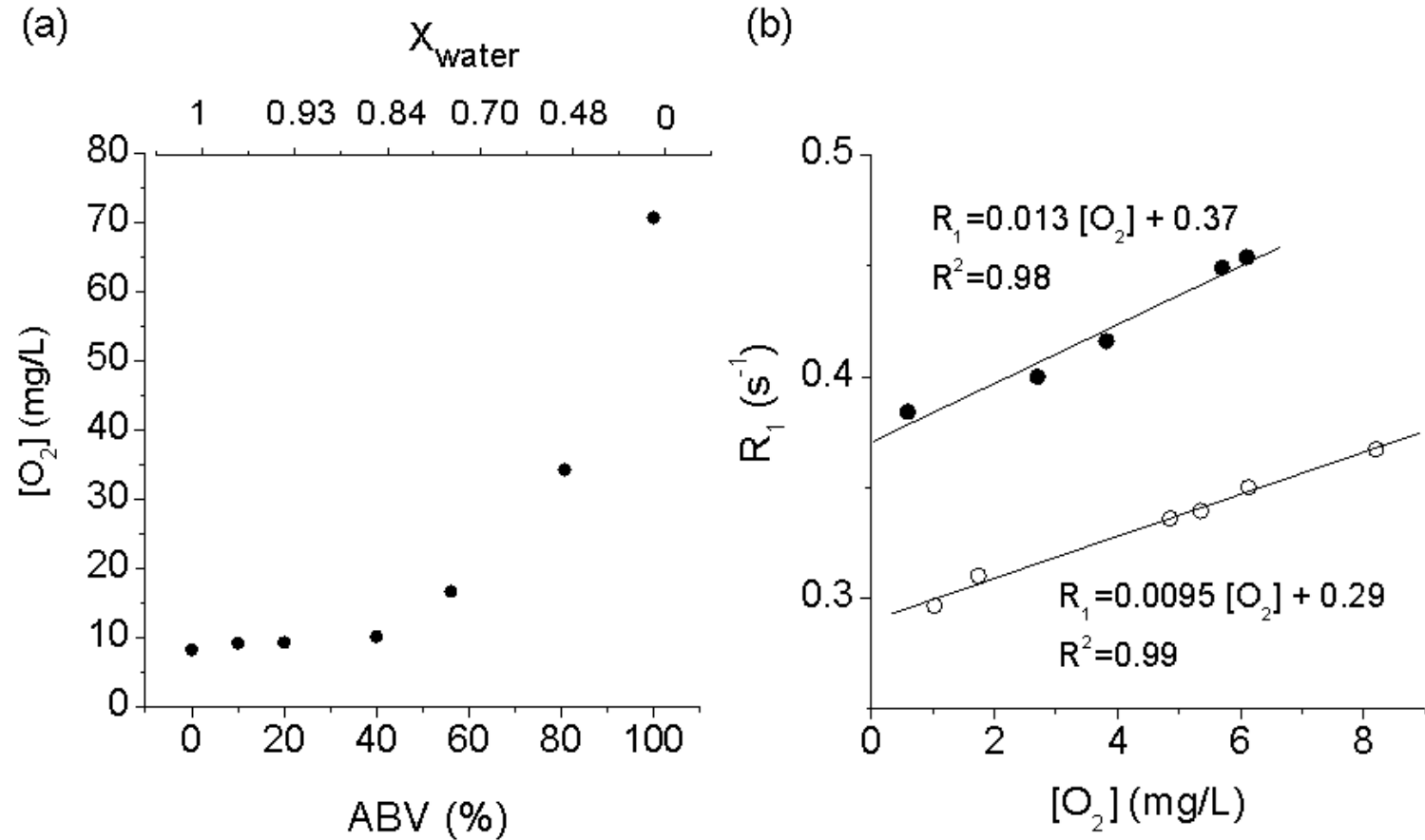
hydroalcoholic solutions (ABV)

- (a) Open circles (o) represent the proton spin–lattice relaxation rate at 19.65 MHz and 25 °C of hydroalcoholic solutions versus ABV and X_{water} . Filled circles (●) correspond to the ratio of the relaxation rate of the hydroalcoholic solution corrected by the dioxygen contribution over the viscosity
- (b) open circles (o) represent the dynamic viscosity of the hydroalcoholic solution, measured at 25 °C, versus ABV and X_{water}



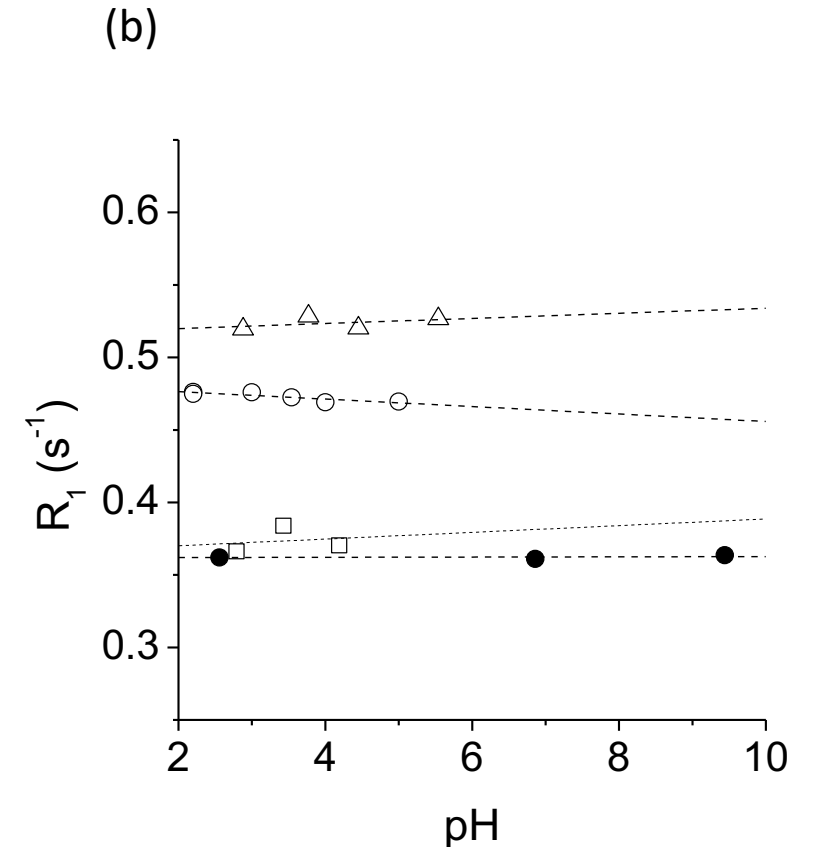
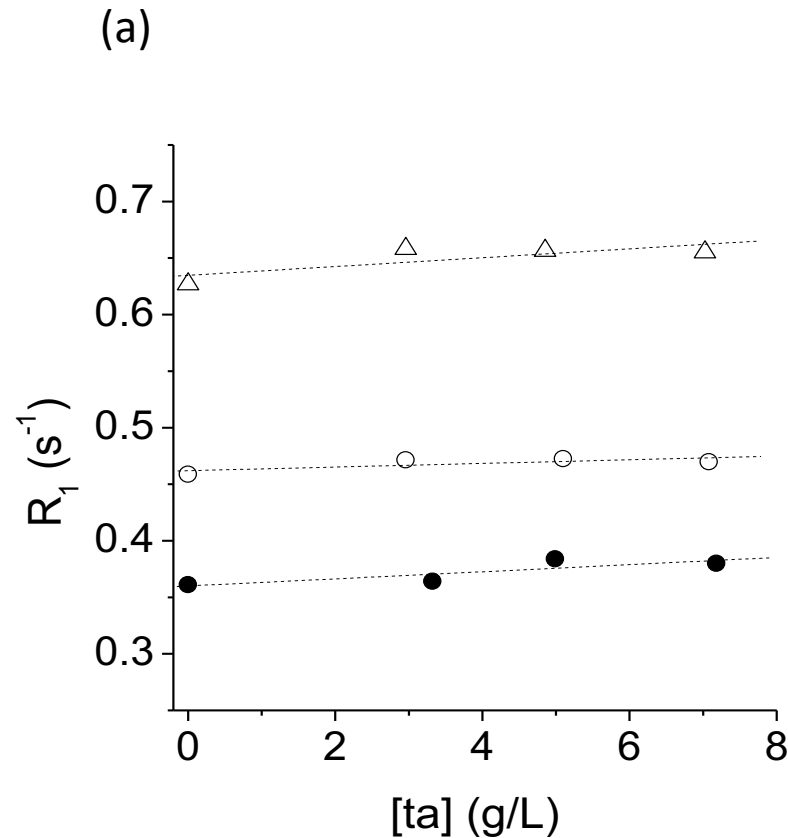
hydroalcoholic solutions ($[O_2]$)

- (a) Atmospheric equilibrium dissolved dioxygen concentration in hydroalcoholic solutions at 25 °C versus ABV and water molar fraction X_{water} .
- (b) Proton spin–lattice relaxation rate at 19.65 MHz and 25 °C versus the dissolved dioxygen concentration in water (○) and 12% ABV hydroalcoholic solution (●, E12)



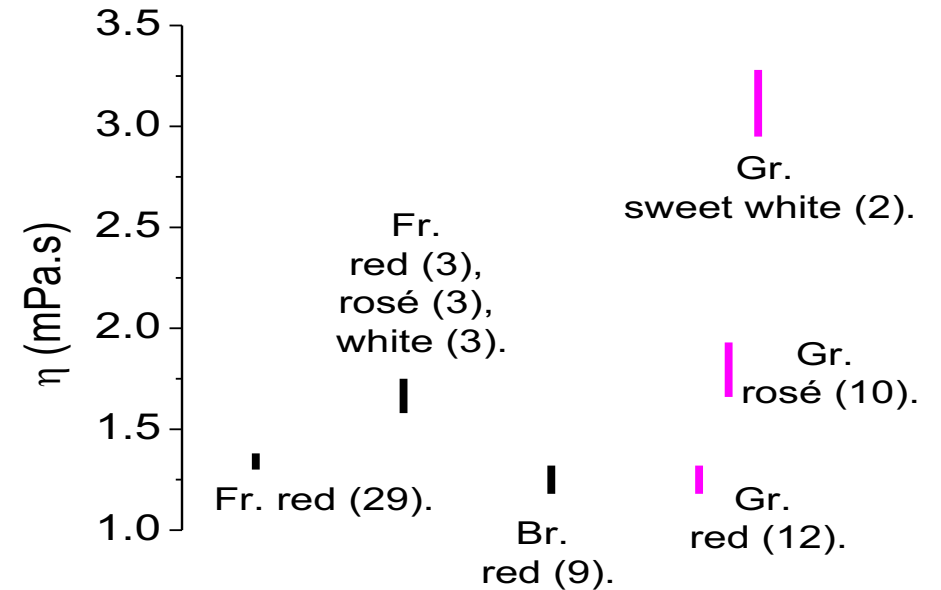
Model wine ([Tartaric acid / pH])

- (a) Proton spin–lattice relaxation rate at 19.65 MHz and 25 °C of water (●, Wta), hydroalcoholic solution (○, E12ta), and model wine containing 1.2 mg/L of manganese (Δ, E12taMn1.2) versus tartaric acid concentration. For each solution, the pH was fixed to 2.3, 3.5, and 3.4 for E12taMn1.2, E12ta, and Wta, respectively
- (b) Proton spin–lattice relaxation rates at 19.65 MHz and 25 °C of water (●), tartaric acid solutions (□, Wta5), hydroalcoholic solution (○, E12ta5), and manganese solutions (Δ, WMn1.2) versus pH values



Viscosity for various wines

Viscosity domains of various wines. Labels indicate the country, the type, and in brackets, the number of wines measured. (fr. red (29)) corresponds to 29 red wines of the same grape variety (Loire Valley Cabernet Franc) elaborated with a standard protocol but coming from two distinct areas, Anjou and Touraine (Siret et al. 2010); (Fr. red (3), rosé (3), and white (3)) reports 9 wines of 2 vintages from Loire Valley selected according to their typicity and probable differences in terms of viscosity and texture (Siret et al. 2008). (Br. Red (9)) is for 9 types of Brazilian dry red wines from different cultivars and produced by different vineries (Neto et al. 2015). Twentyfour different Greek wines (Yanniotis et al. 2007) of 2 vintages (in fuchsia) are also reported but the measurement was done at 16 °C whilst they were done at 23 and 26 °C for French and Brazilian wines, respectively



Some conclusions

Manganese in wine comes primarily from the soil.
Its concentration is not affected by wineries practices.
It does not seem to form many stable complexes.
Manganese seems to be observable on many type of wine.

Manganese could be a valuable fingerprint for wines.

Relaxometry that could allow easy and precise in situ concentration measurement would then be a technique of choice for wine control.

Some conclusions

An important viscosity variability of the wine can complicate the interpretation of NMRD profiles and relaxation times, (e.g. precluding the determination of the manganese concentration by NMR relaxometry). However, the literature shows that a rather low and narrow range of viscosity (particularly for red and dry white wines) characterises wines and the relaxation times could be interpreted with ease.

As the alcoholic strength increases (e.g. in distilled alcohols), the situation is less straightforward.

- (i) The amount of dissolved dioxygen strongly increases and has to be taken into account;
- (ii) (ii) the viscosity increases and relaxation mechanisms are further complicated;
- (iii) (iii) two main sources of proton may have to be considered simultaneously: ethanol & water



ELSEVIER

Contents lists available at [ScienceDirect](https://www.sciencedirect.com)

Talanta

journal homepage: www.elsevier.com/locate/talanta



Quantification of manganese ions in wine by NMR relaxometry

Philippe R. Bodart^{a,b,*}, Adam Rachocki^c, Jadwiga Tritt-Goc^c, Bernhard Michalke^d,
Philippe Schmitt-Kopplin^{d,e}, Thomas Karbowski^a, Régis D. Gougeon^a

^a Univ. Bourgogne Franche-Comté, Agrosup Dijon, UMR PAM A02.102, 1 Esplanade Erasme, 21000, Dijon, France

^b IUT A - Université des Sciences et Technologies de Lille, Villeneuve d'Ascq, 59655, France

^c Institute of Molecular Physics Polish Academy of Sciences, M. Smoluchowskiego 17, 60-179, Poznan, Poland

^d Research Unit Analytical BioGeoChemistry, Helmholtz Zentrum München, Ingolstaedter Landstrasse 1, Neuherberg, 85764, Germany

^e Chair of Analytical Food Chemistry, Technische Universität München, Alte Akademie 10, 85354, Freising-Weihenstephan, Germany



Food Analytical Methods (2022) 15:266–275

<https://doi.org/10.1007/s12161-021-02118-w>



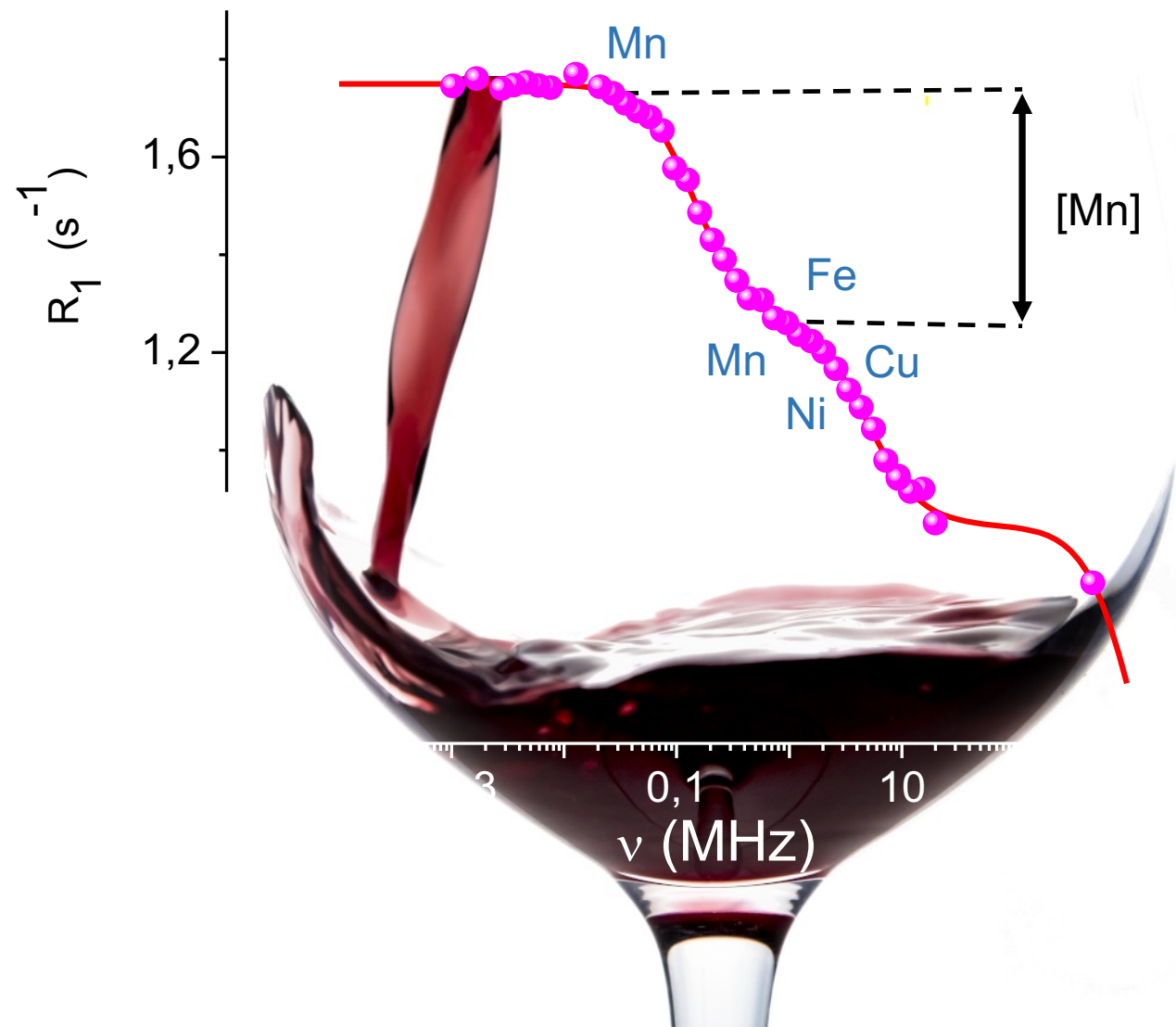
Analysis of the Proton Spin–Lattice Relaxation in Wine and Hydroalcoholic Solutions

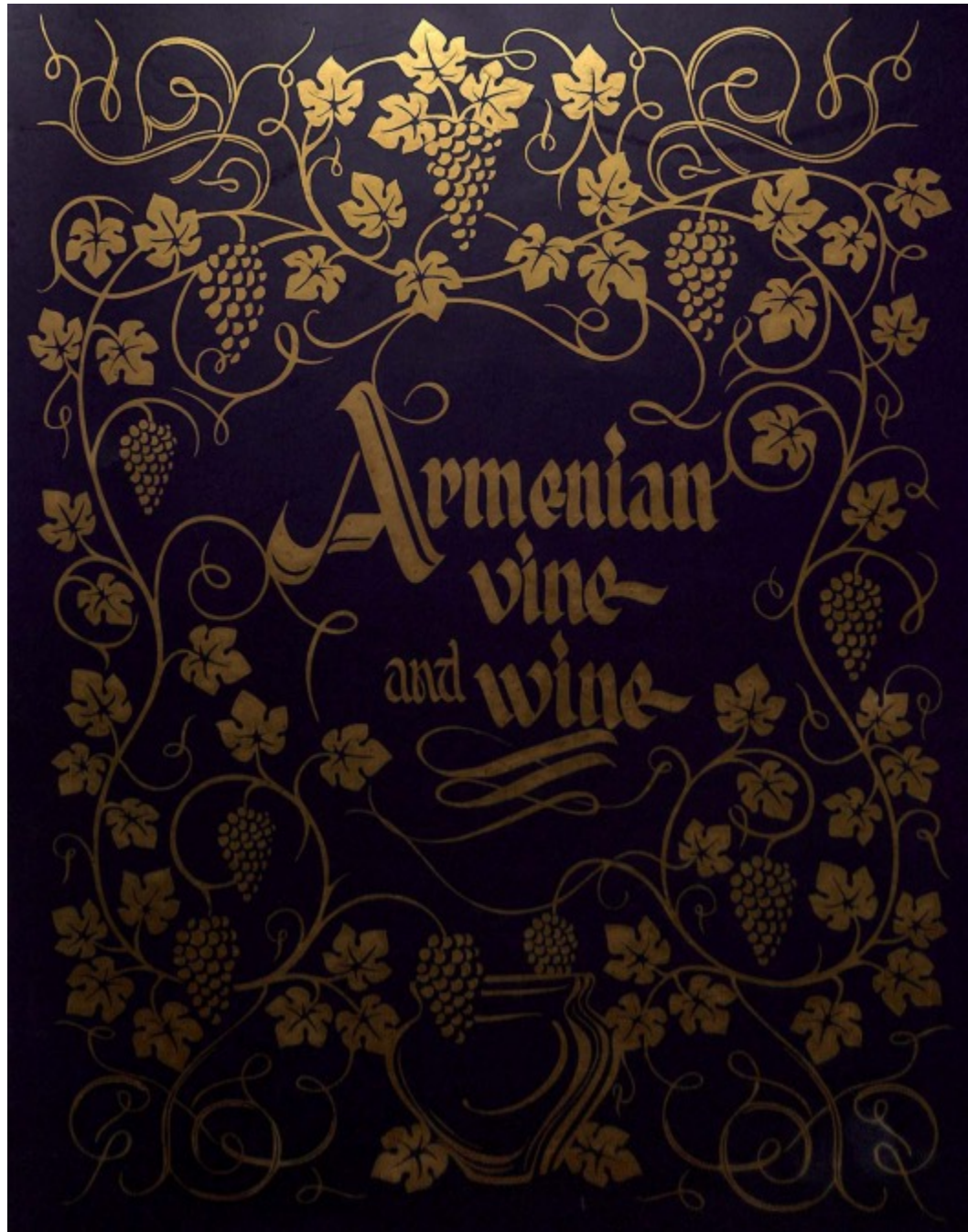
Philippe R. Bodart¹  · Aymeric Batlogg¹ · Eric Ferret¹ · Adam Rachocki² · Magdalena Knapkiewicz² · Syuzanna Esayan^{1,3} · Nelli Hovhannisyanyan⁴ · Thomas Karbowski¹ · Régis D. Gougeon⁵



Interaction between Armenian clay-based ceramics and model wine during storage

Syuzanna Esayan^{1,2}, Camille Loupiac¹, Nelli Hovhannisyanyan², Régis D. Gougeon³, Thomas Karbowski¹, Bernhard Michalke⁴,
Philippe Schmitt-Kopplin^{4,5}, Claude Fontaine⁶, Sabine Valange⁶ and Philippe R. Bodart^{1*}





Nelli .A. Hovhannisyan, A.A. Yesayan, A. Bobokhyan, M.V. Dallakyan, S. Hobosyan, B.Z. Gasparyan, A. Danielyan, Z. Muradyan, V. Ter-Ghazaryan, Backbone Branding (Firm), Deutsche Gesellschaft für Internationale Zusammenarbeit, Armenian vine and wine, 2017.

In conclusion

- Manganese in wine comes primarily from the soil.
- Its concentration is not affected by wineries practices.
- It does not seem to form many stable complexes.
- Manganese seems to be observable on many type of wine.

Manganese could be a valuable fingerprint for wines.

] Relaxometry that could allow easy and precise in situ concentration measurement would then be a technique of choice for wine control.

- Professor Regis D. Gougeon – Thomas Karbowiac
- Adam Rachocki – Jadviga tritt-Got

Master students

- Aymerick Batlogg
- Manouella Alakik

PhD. Students

- Pierre Fouilloux
- Syuzanna Essoyan

1. Tariba, Blanka. 2011. “Metals in Wine—Impact on Wine Quality and Health Outcomes.” *Biological Trace Element Research* 144 (April): 143–56. <https://doi.org/10.1007/s12011-011-9052-7>.

Wine can be made from any form of fermented fruit.



In most cases, wine is produced from grapes.



<https://pxhere.com/fr/photo/961549>

European grape vine or *Vitis vinifera*.




Cabernet, Merlot, Chardonnay, Pinot Grigio, etc.

Wine grapes contain seeds, are smaller, sweeter, and have thicker skins than table grapes.

In popular (or advertising) culture, many virtues are associated with a moderate wine consumption.

10 HEALTH BENEFITS OF DRINKING WINE



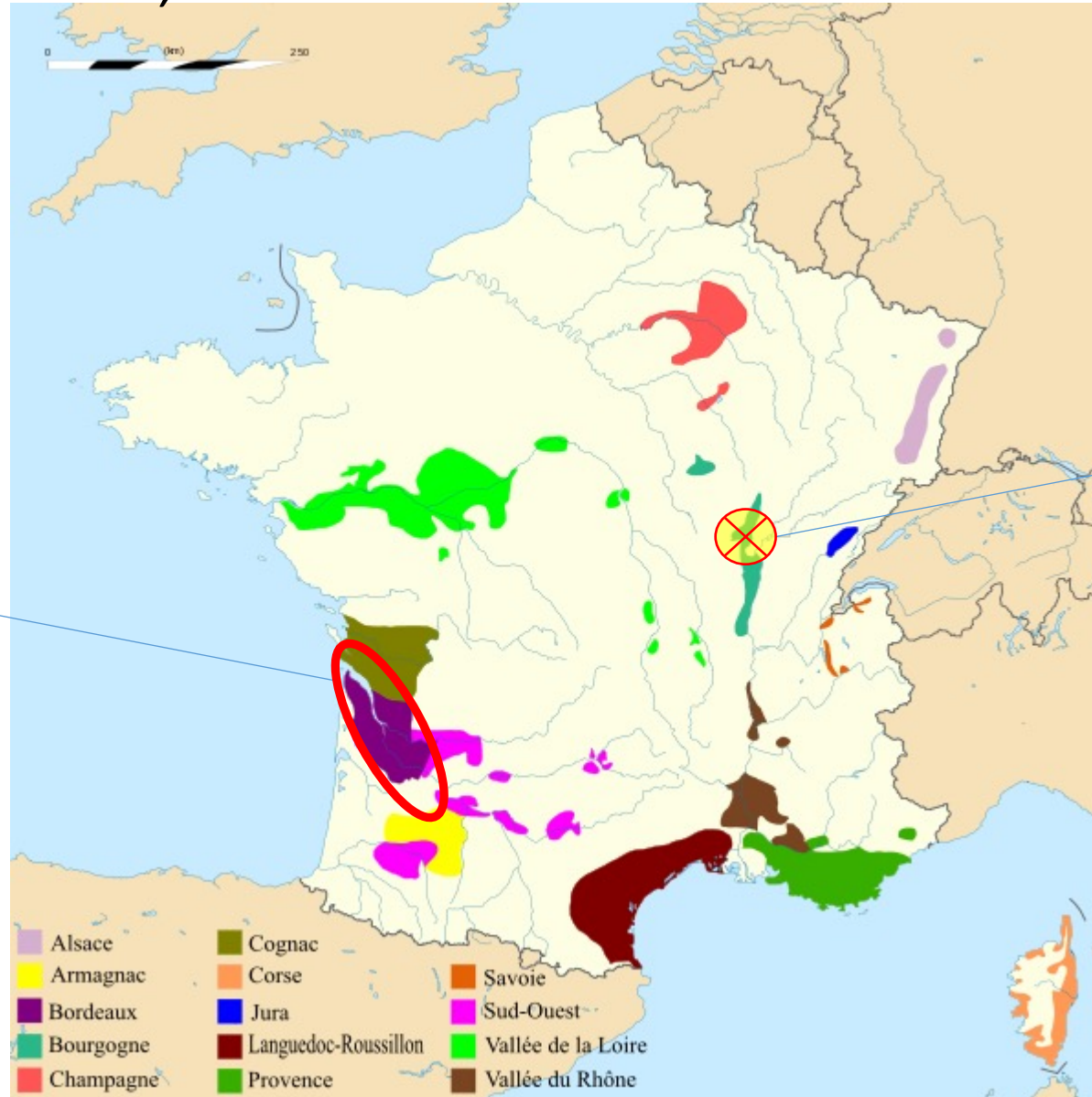
- Lowers risk of cancer
- Promotes mental health
- Increases bone density
- Protects teeth
- Fosters good eyesight
- Healthy Heart
- Encourages Longevity
- Anti-aging effects
- Reduces stress
- Reduces risk of diabetes



<https://www.austwinetourco.com.au/10-health-benefits-of-drinking-wine/>

Two distinct wines, red Medoc blend & white Chardonnay

Red Medoc blend wine
(2011 vintage),
Bordeaux.



Chardonnay white wine
(2014 vintage),
University of Burgundy.



EURELAX
COST ACTION CA15209



COST is supported by
the EU Framework Programme
Horizon 2020

European Network on NMR Relaxometry

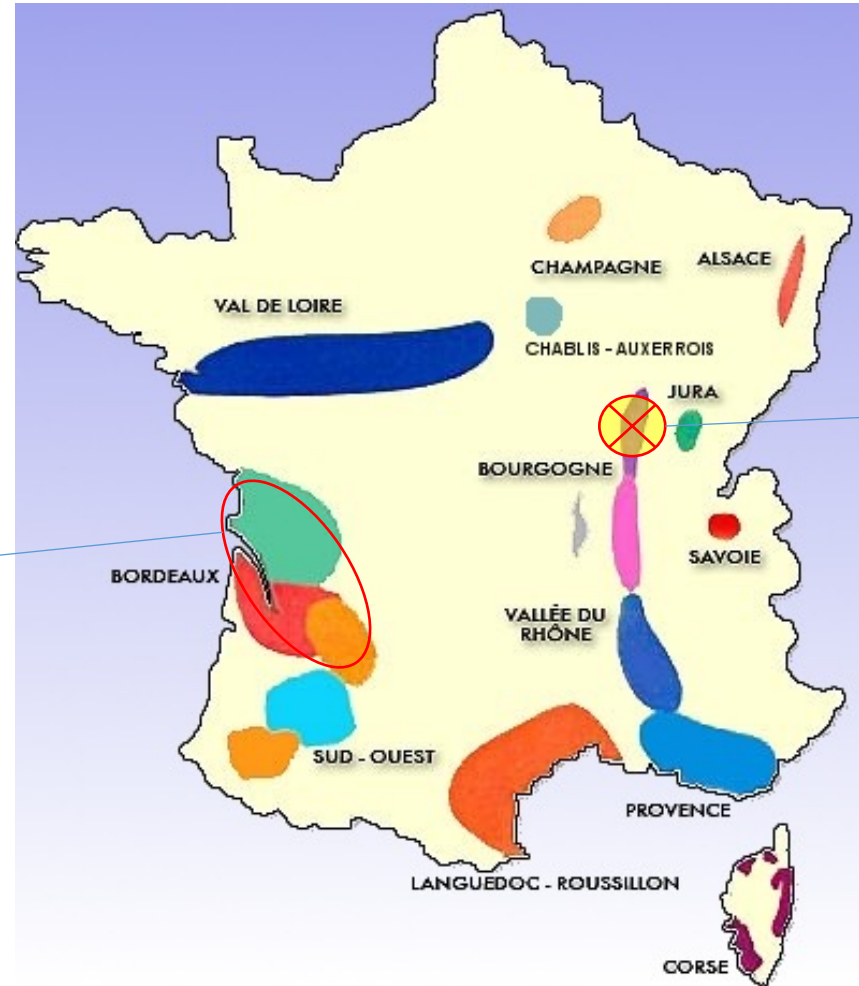
http://www.cost.eu/COST_Actions/ca/CA15209

<http://eurelax.uwm.edu.pl/>



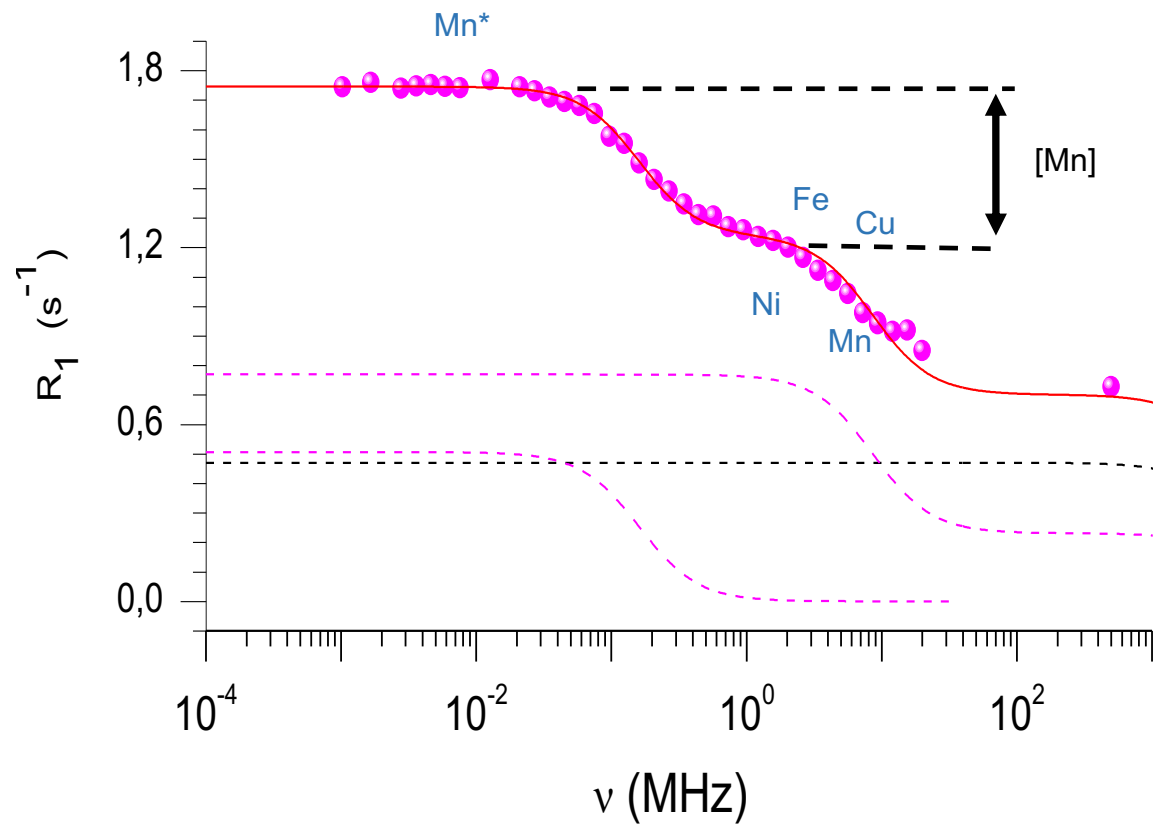
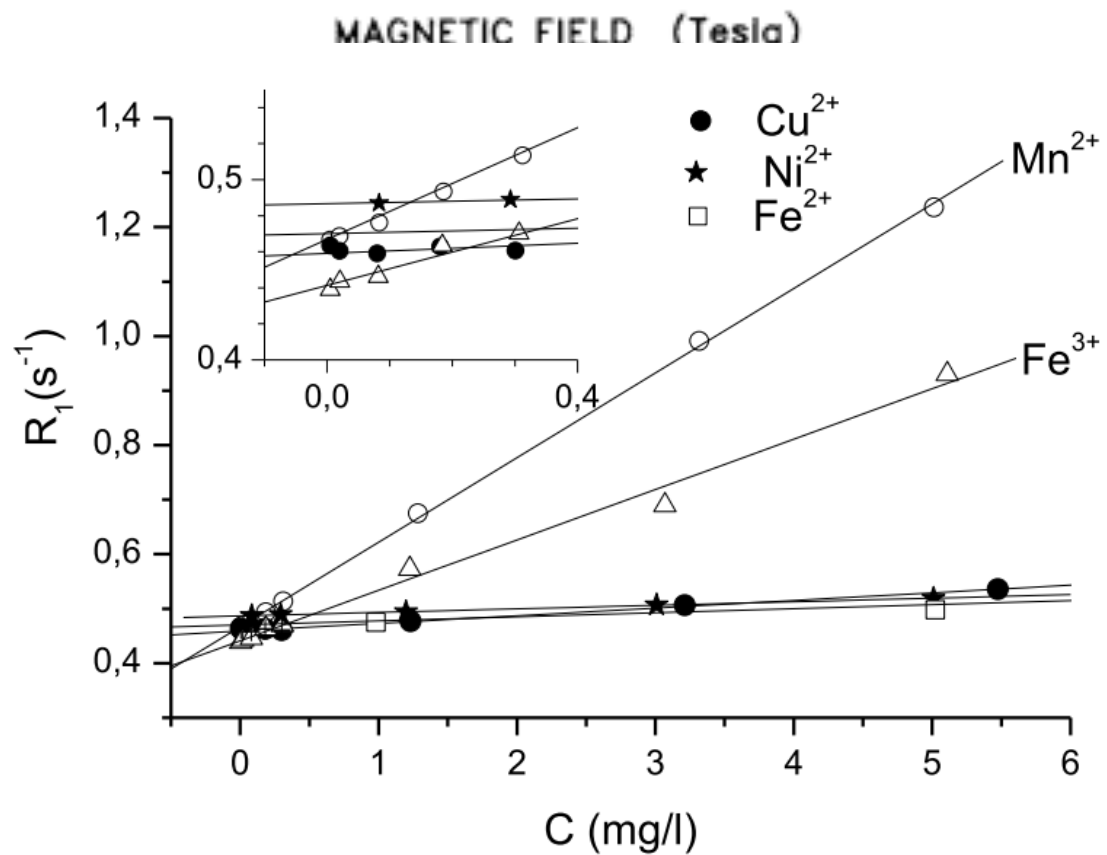
Two distinct wines red Medoc blend & white Chardonnay

Red Medoc blend wine
(2011 vintage),
Bordeaux.



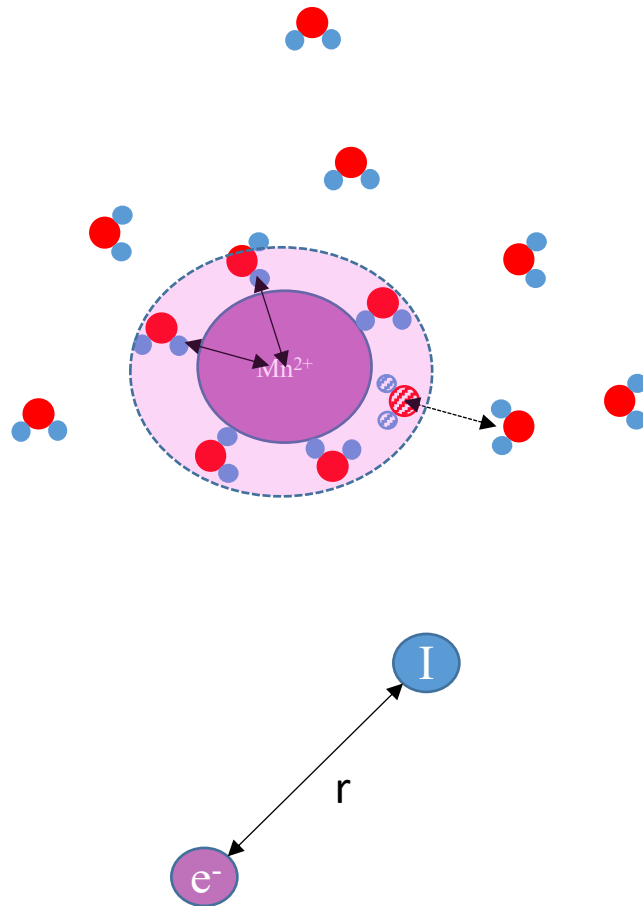
Chardonnay white wine
(2014 vintage),
University of Burgundy.

Quantification of Manganese



Paramagnetic relaxation Solomon mechanism

the unpaired electrons are localized at the paramagnetic ion.
The relaxation is described by an interaction between
an electronic point dipole and a nuclear point dipole



$$\tilde{R}_D(\omega_I, \tau_{d1}, \omega_S, \tau_{d2}) = \tilde{C}_D \left[\frac{7\tau_{d2}}{1 + (\omega_S \tau_{d2})^2} + \frac{3\tau_{d1}}{1 + (\omega_I \tau_{d1})^2} \right]$$

$$\tilde{C}_D = \frac{2}{15} \left(\frac{\mu_0}{4\pi} \right)^2 \frac{S(S+1)(\gamma_I \gamma_S \hbar)^2}{r_{IS}^6}$$

$$\frac{1}{\tau_{di}} = \frac{1}{\tau_R} + \frac{1}{\tau_M} + \frac{1}{\tau_{Si}}$$

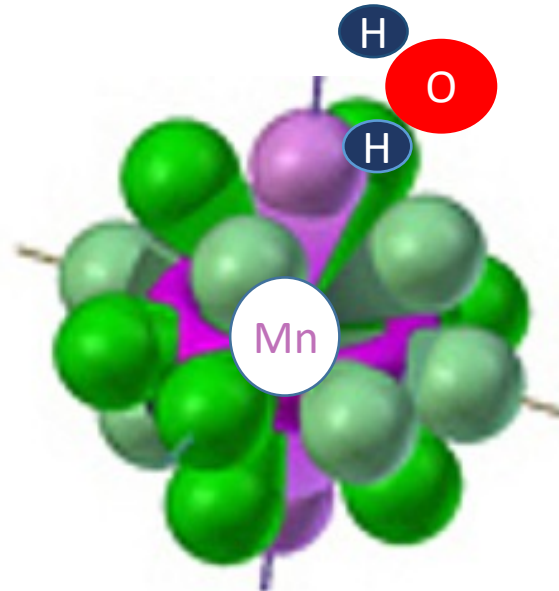
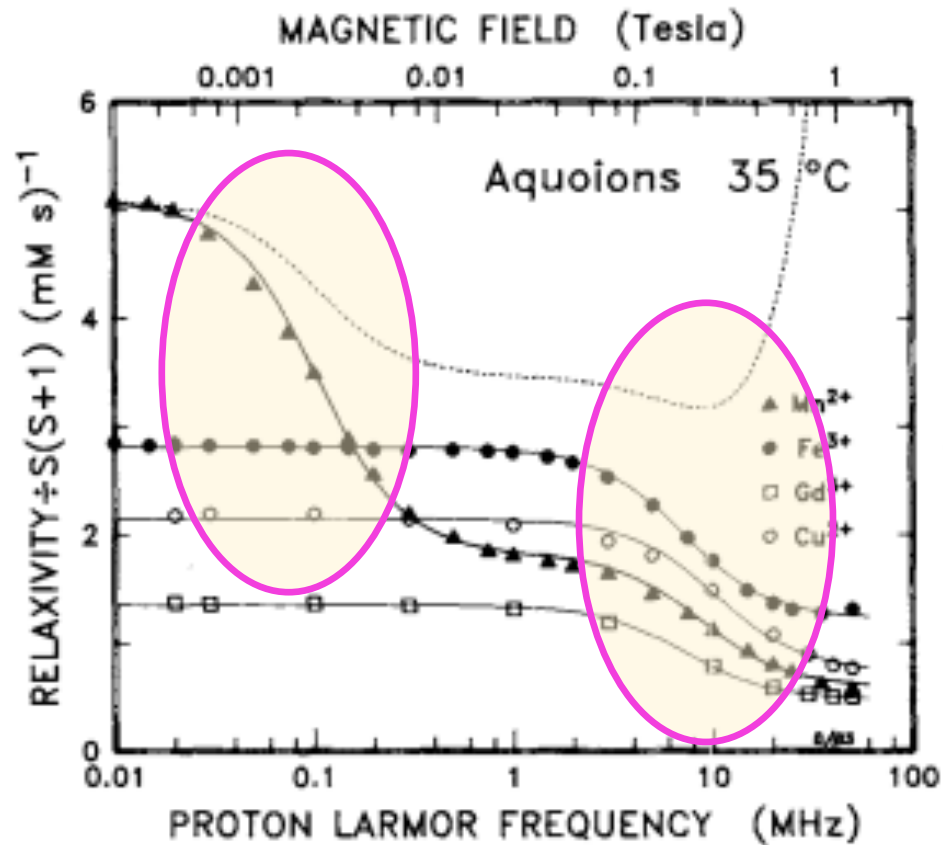
In practice, at low magnetic field,

$$\tau_{d1} = \tau_{d2} = \tau_d$$

What is the spin of the electron ?, what is a dipole

Paramagnetic relaxation Bloembergen mechanism

Delocalization of the electronic wave function of the paramagnetic nuclei to the physical location of I-nuclei (fermi contact interaction)



$$\tilde{R}_C(\omega_s, \tau_c) = \tilde{C}_C \left[\frac{\tau_c}{1 + (\omega_s \tau_c)^2} \right]$$

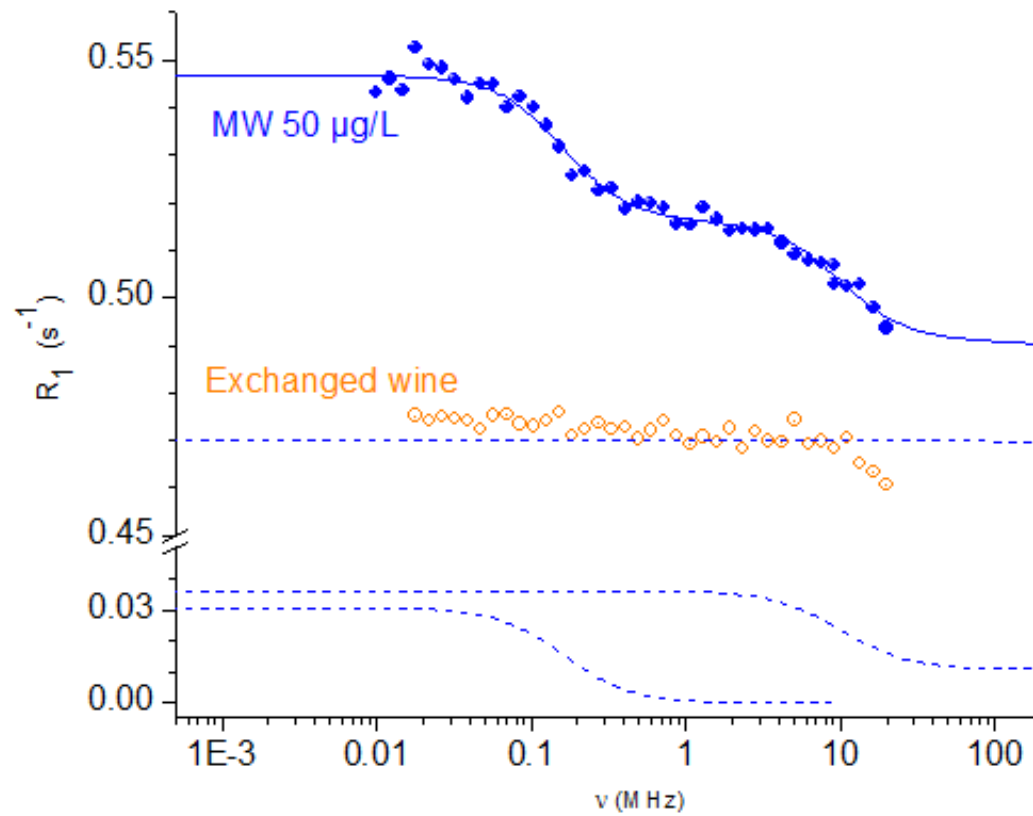
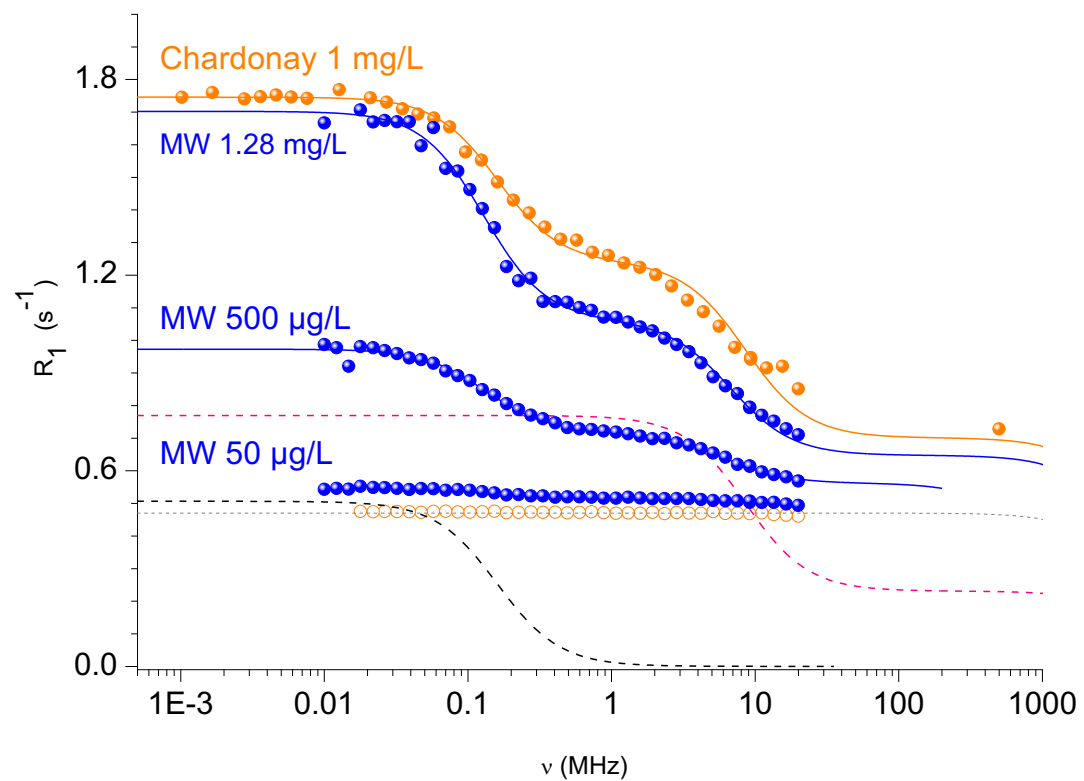
$$\tilde{C}_C = \frac{2A^2 S(S+1)}{3\hbar^2}$$

$$\frac{1}{\tau_c} = \frac{1}{\tau_M} + \frac{1}{\tau_{S2}}$$

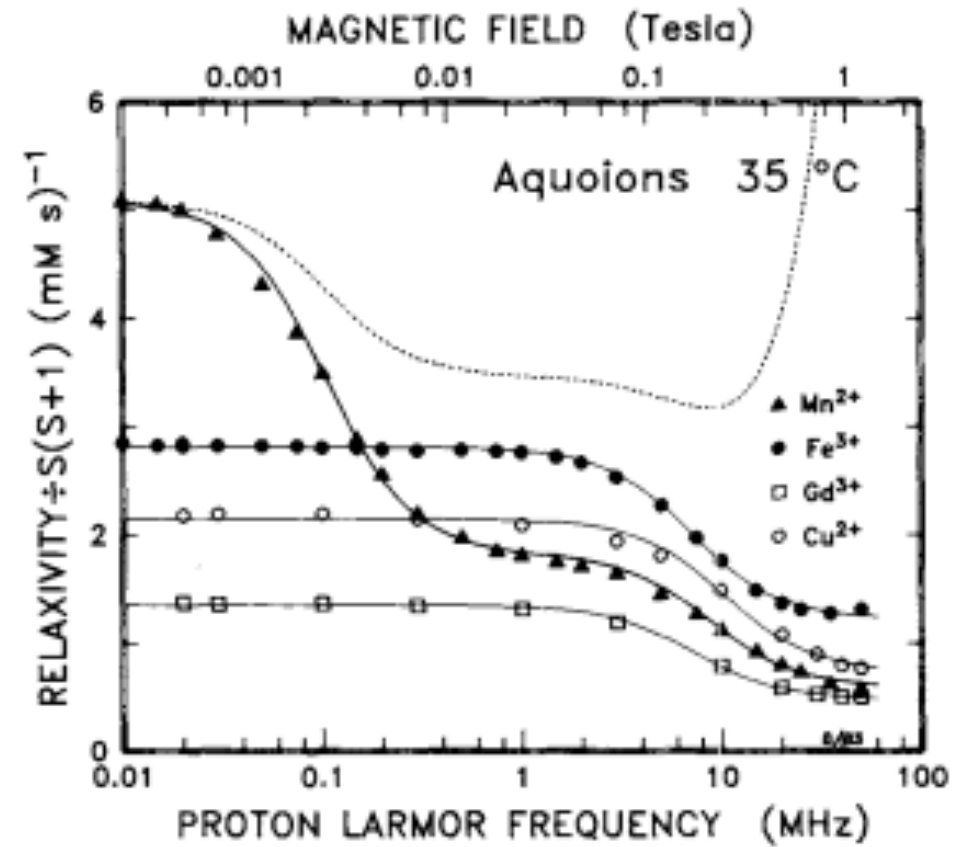
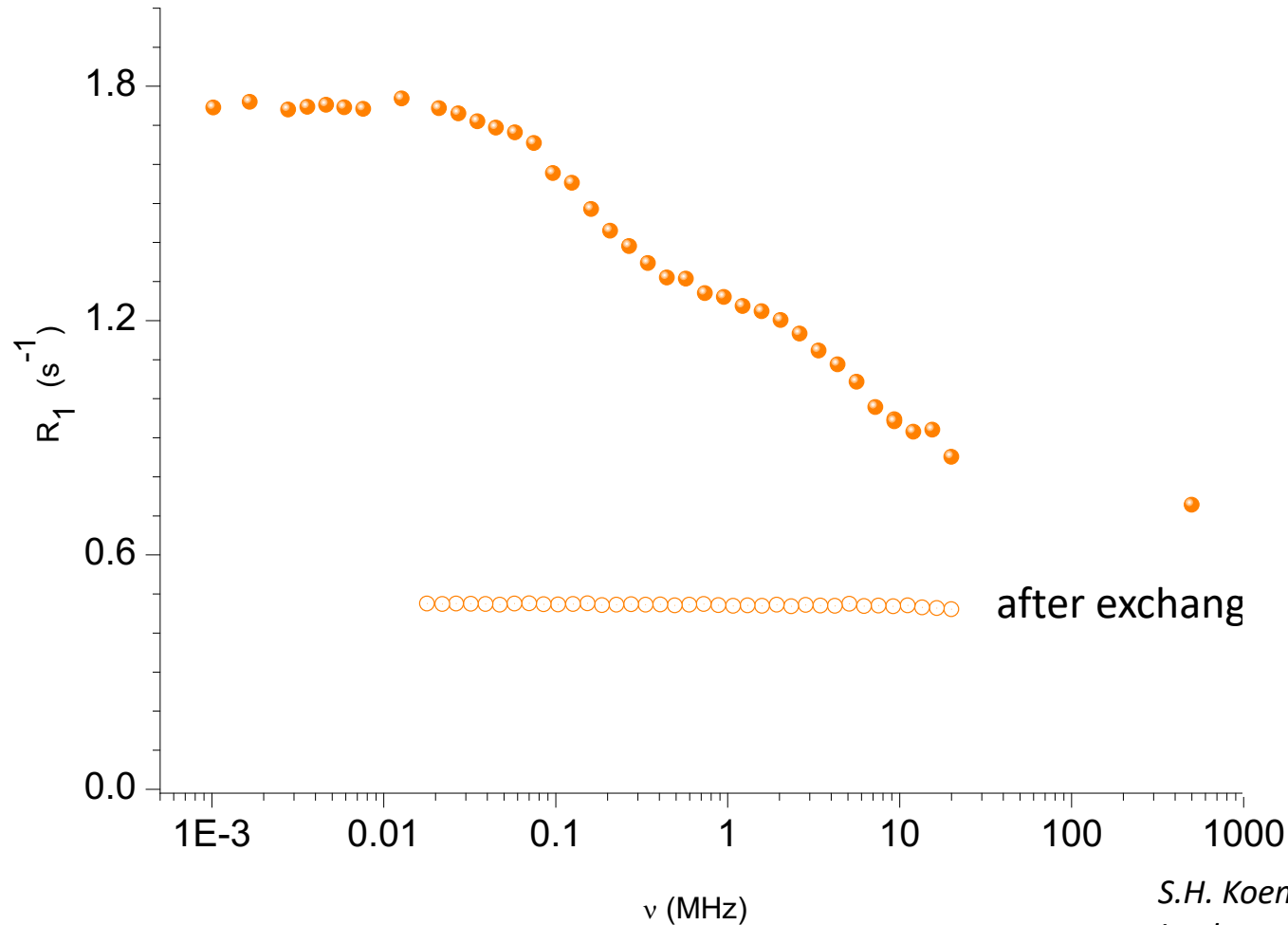
Bloembergen mechanism Solomon mechanism

What is tau s2

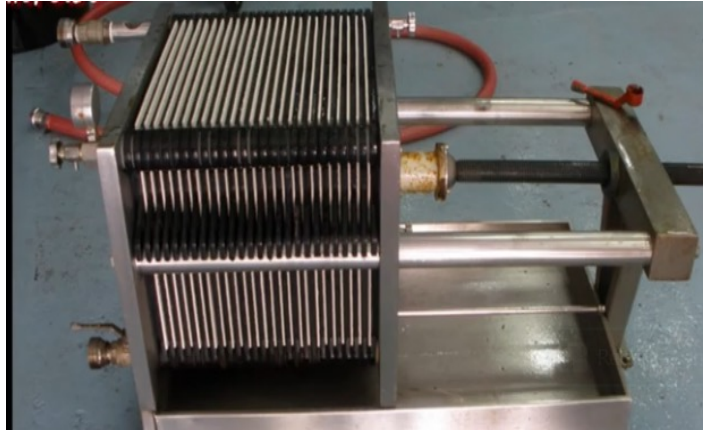
Model wines



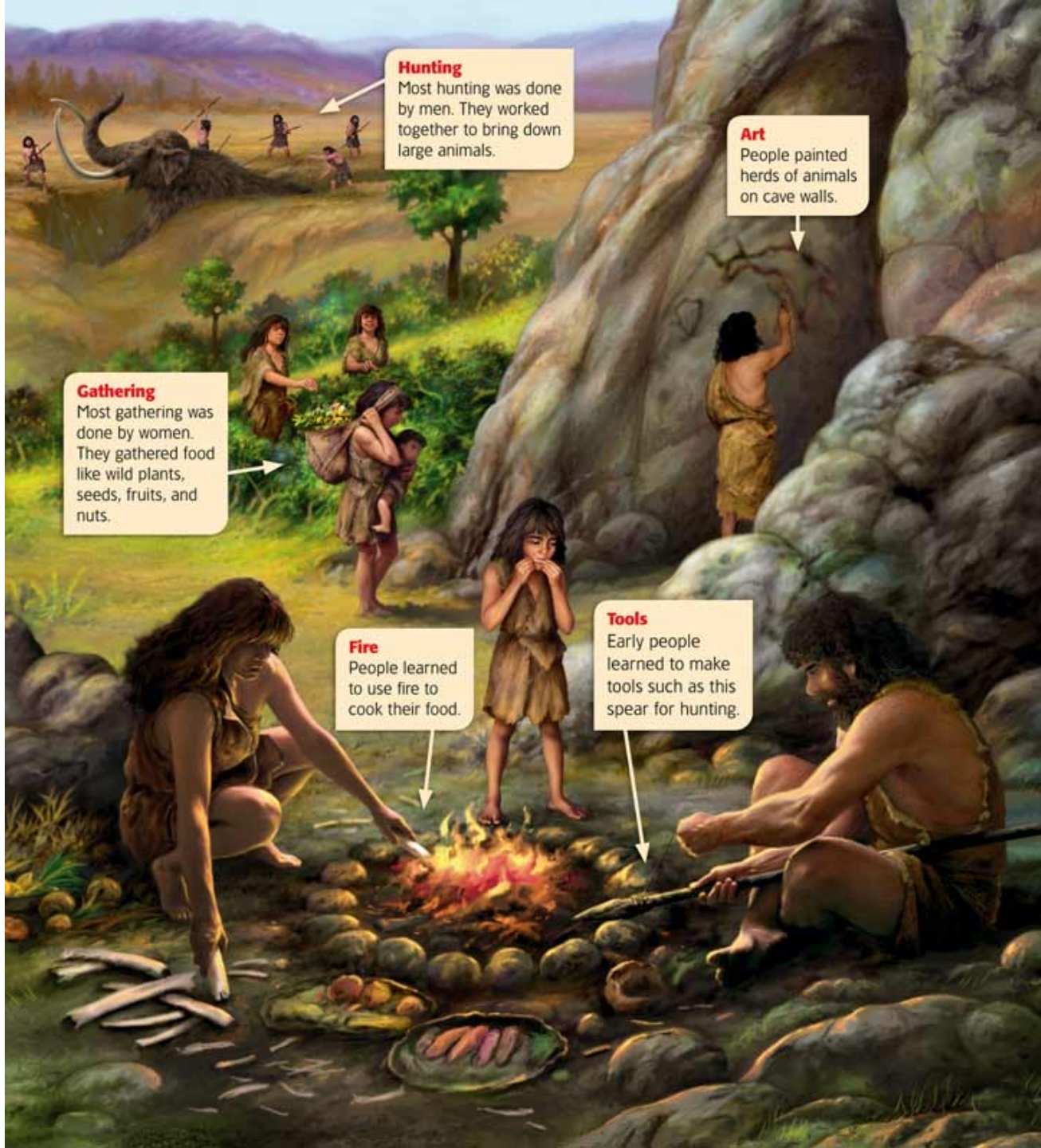
Chardonnay white wine.



S.H. Koenig, R.D. Brown, Relaxation of solvent protons by paramagnetic ions and its dependence on magnetic field and chemical environment: implications for NMR imaging, Magnetic Resonance in Medicine. 1 (1984) 478–495







Hunting
Most hunting was done by men. They worked together to bring down large animals.

Art
People painted herds of animals on cave walls.

Gathering
Most gathering was done by women. They gathered food like wild plants, seeds, fruits, and nuts.

Fire
People learned to use fire to cook their food.

Tools
Early people learned to make tools such as this spear for hunting.

Harvesting and wine production scene, Etruscan plate, 600 BC, (Cabinet des médailles de la bibliothèque nationale de France Paris)





Caravaggio's 1595 masterpiece Bacchus



Illumination from a copy of *Li livres dou santé* by Aldobrandino of Siena (XIII century).

In popular (or advertising) culture many virtues are associated with moderate wine consumption.

10 HEALTH BENEFITS

OF DRINKING WINE



Does wine helps to relax?
Is wine a good relaxing agent?

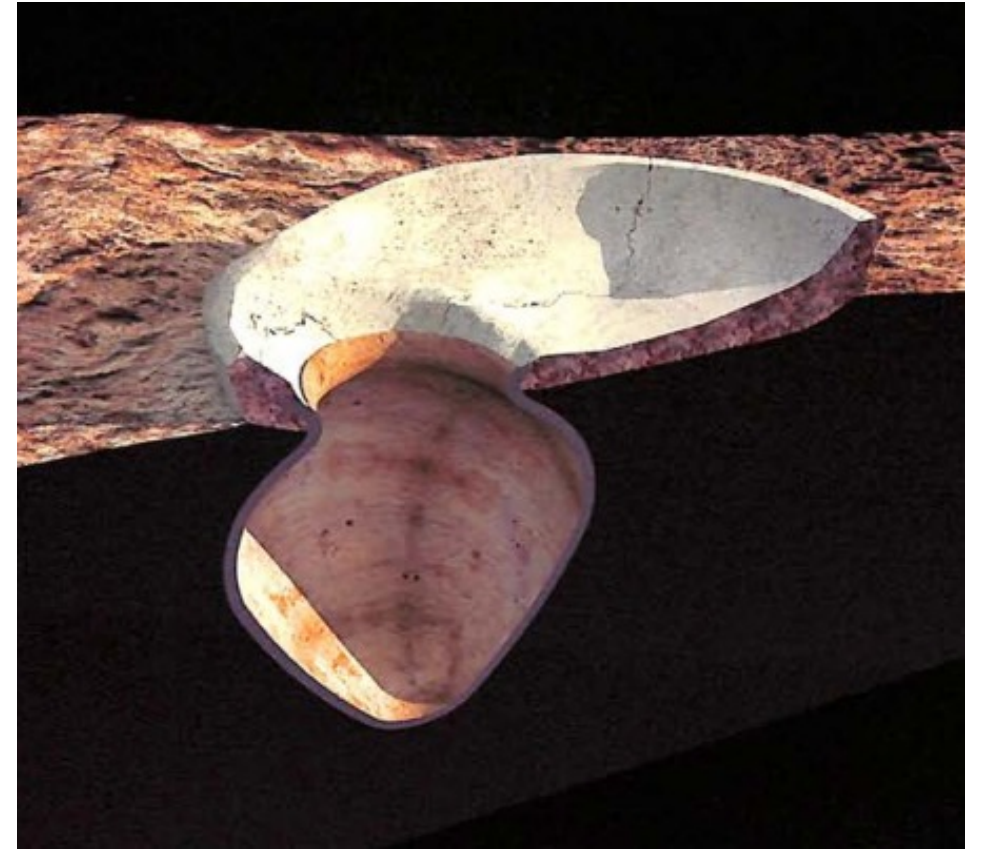


Relaxometry experiments ...

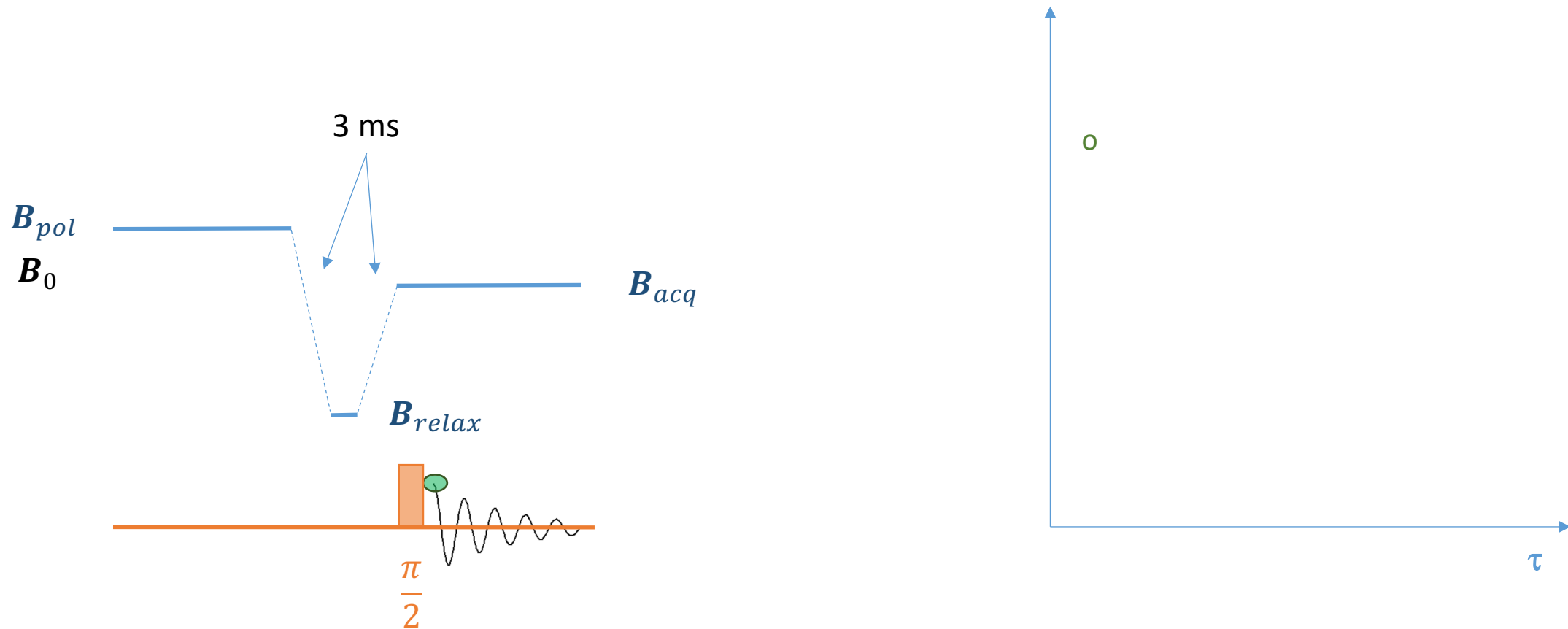
JOKE



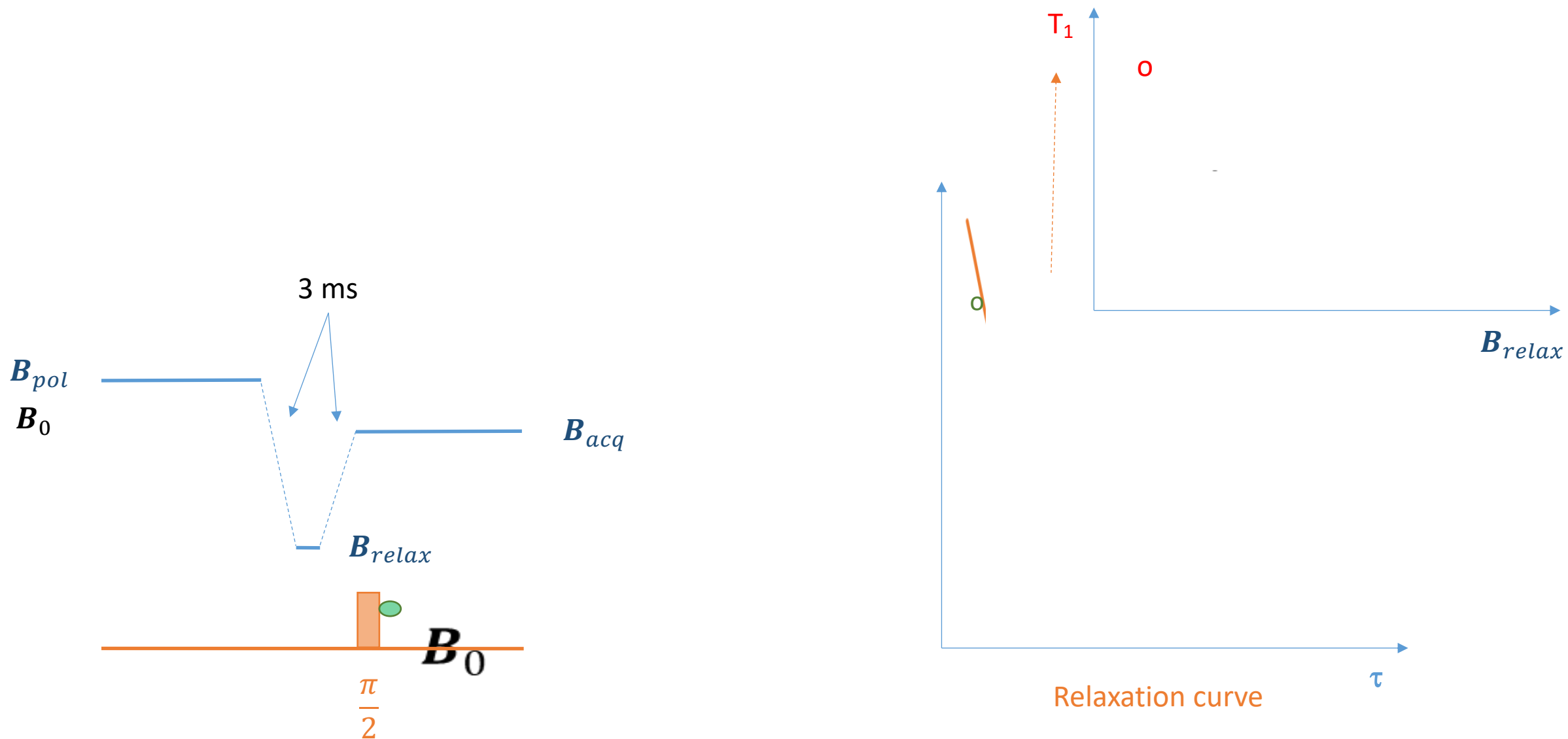
Oldest winery (4100 BC – Areni, Armenia)



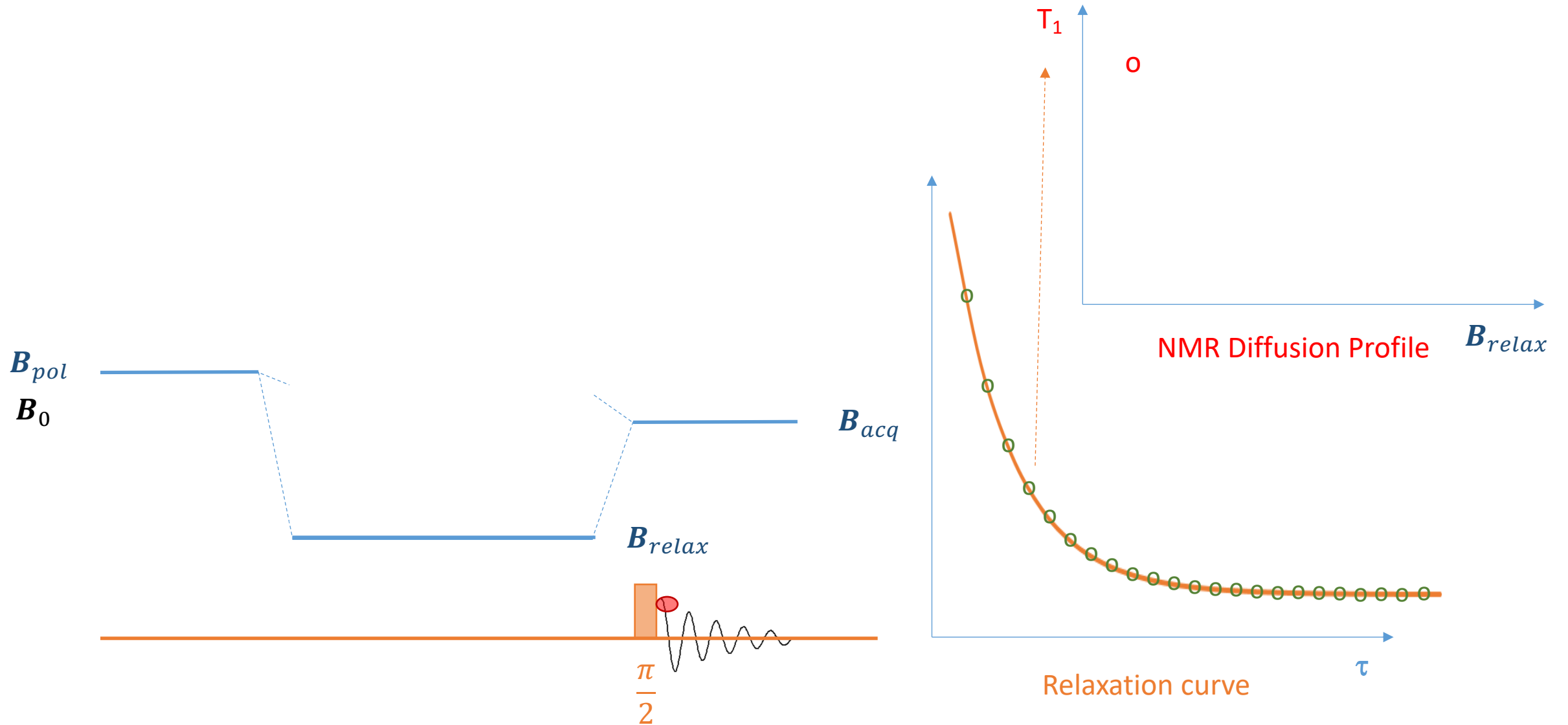
What relaxometry experiment did we perform?

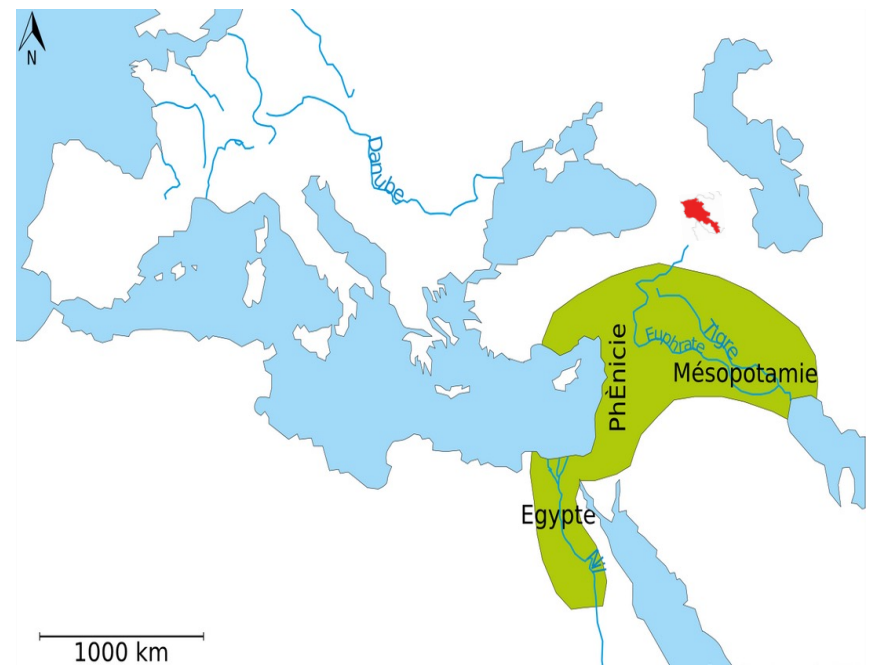


principle of relaxometry experiment



principle of relaxometry experiment







Sea

Mediterranean
Sea

Fertile
Crescent
Euphrates River
Tigris River

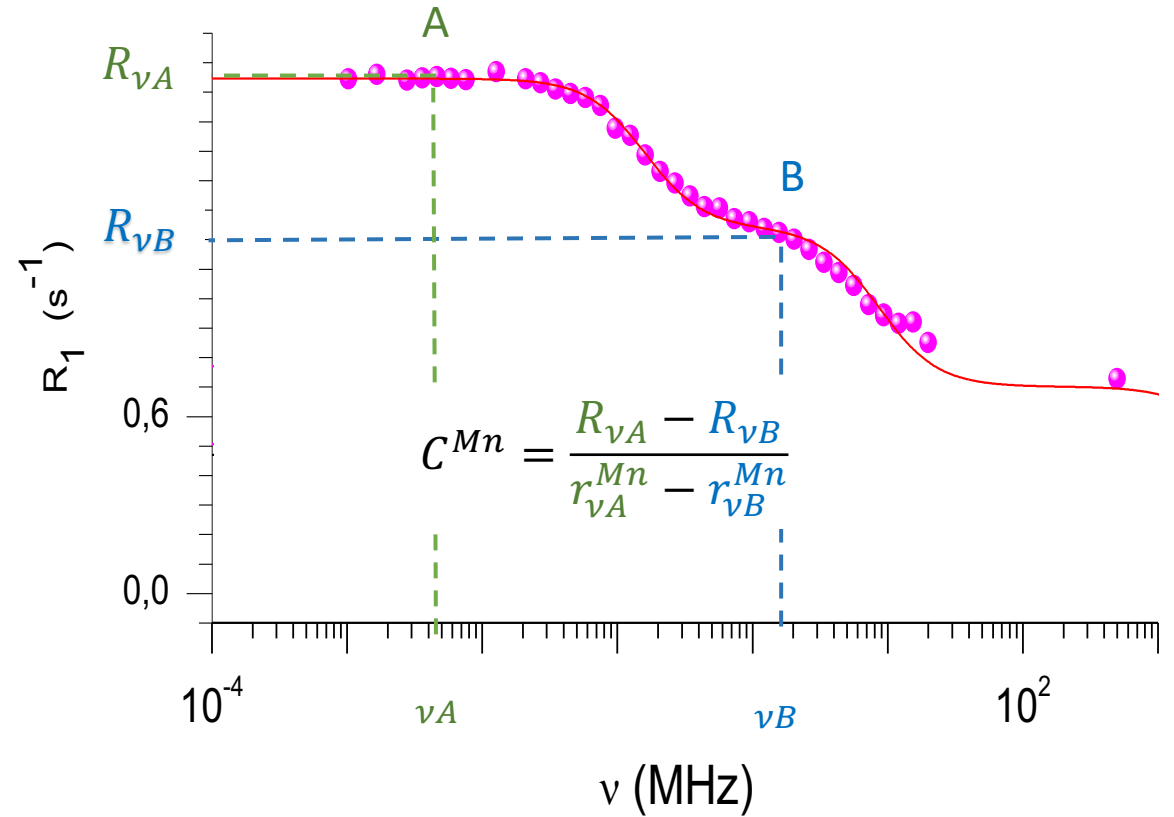
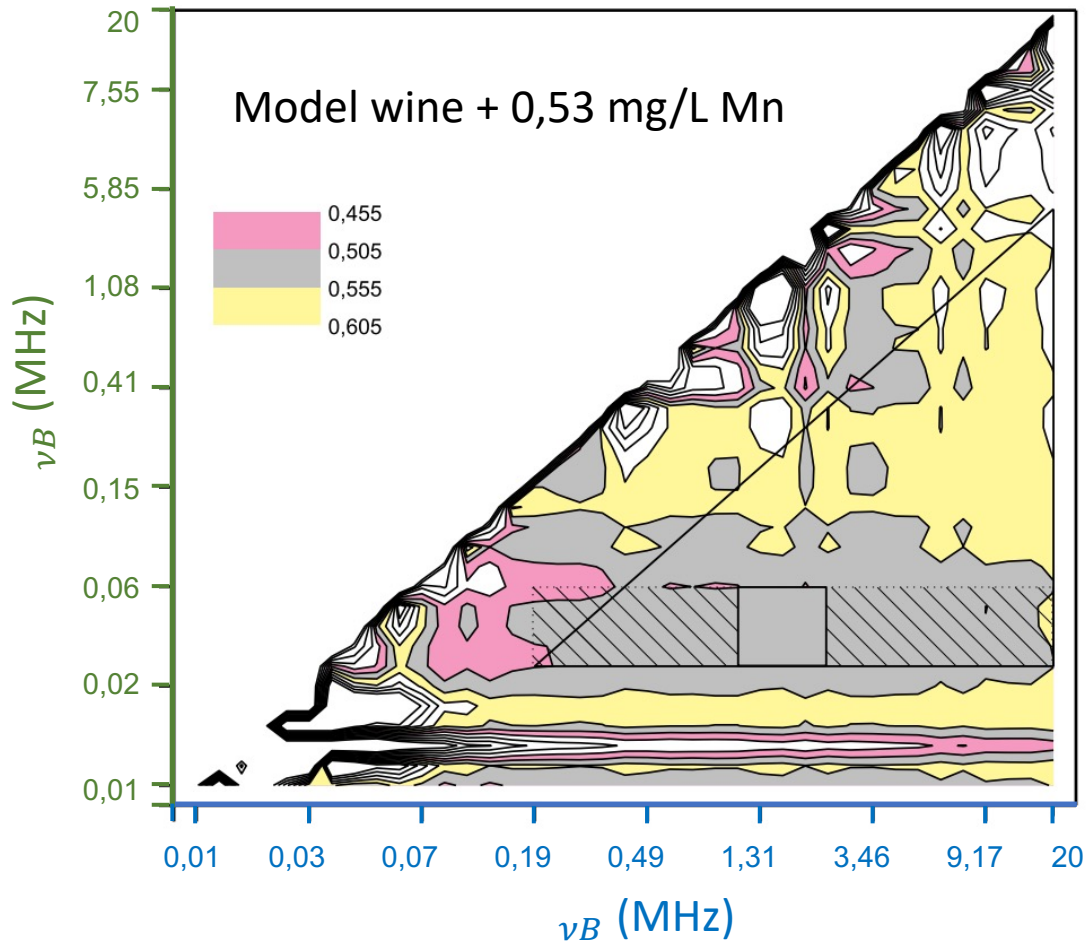
Persian Gulf



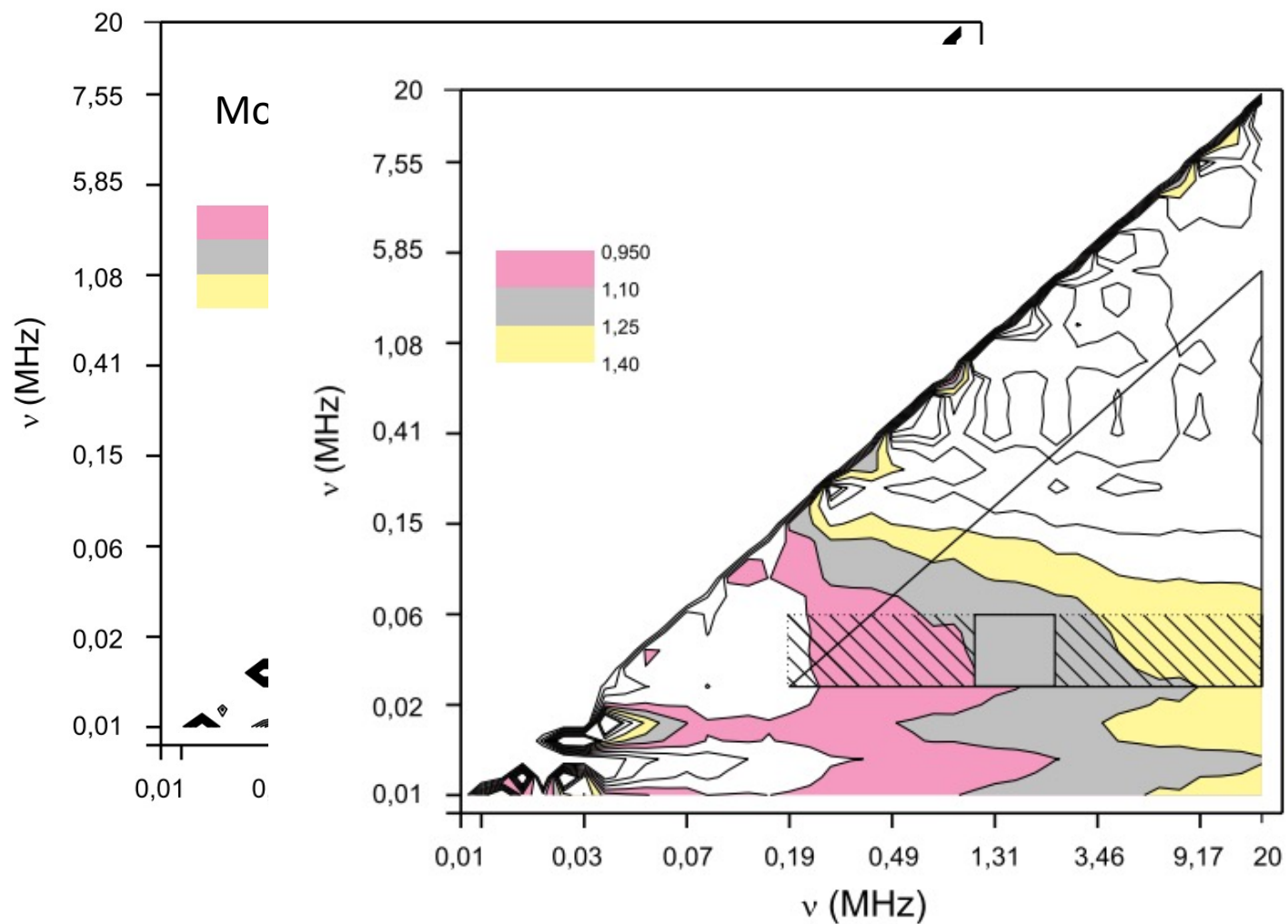
Nile River

Red Sea

Quantification of Manganese



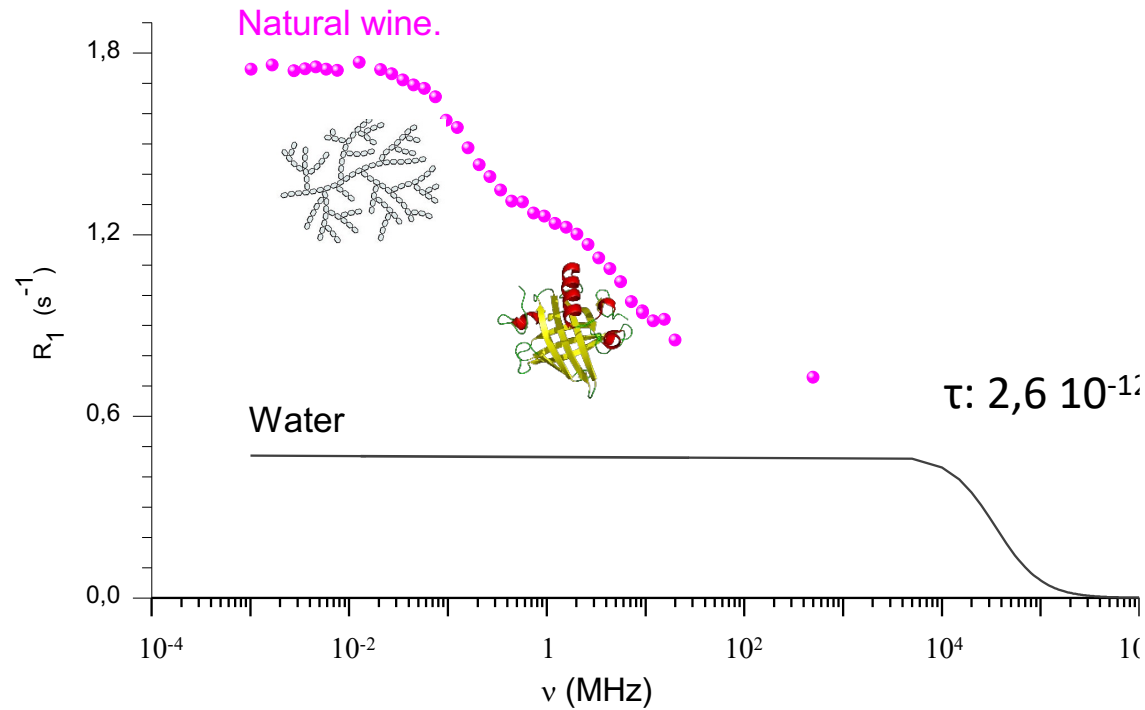
Quantification of Manganese



Manganese concentration	Square zone	Rectangular zone	Triangular zone
0.46	5.46 (3)	5.45 (4)	5.5 (1)
0.01	4.97 (5)	4.97 (6)	5.0 (1)
0.28	1.34 (8)	1.3 (1)	1.3 (1)
0.53	0.53 (1)	0.52 (1)	0.53 (5)
0.05	0.063 (5)	0.063 (6)	0.06 (1)
0.26 (2) ^a	1.17 (9)	1.2 (1)	1.3 (2)
	1.13 (3)	1.1 (1)	1.4 (2)
0.06 (2) ^a	0.83 (4)	0.9 (1)	1.2 (3)
	0.91 (5)	0.9 (1)	1.2 (3)
< 0.002 ^a	0.009 (6)	0.011 (4)	0.01 (1)

concentration measured by ICP AES.

NMRD profile of wine (white Chardonnay)

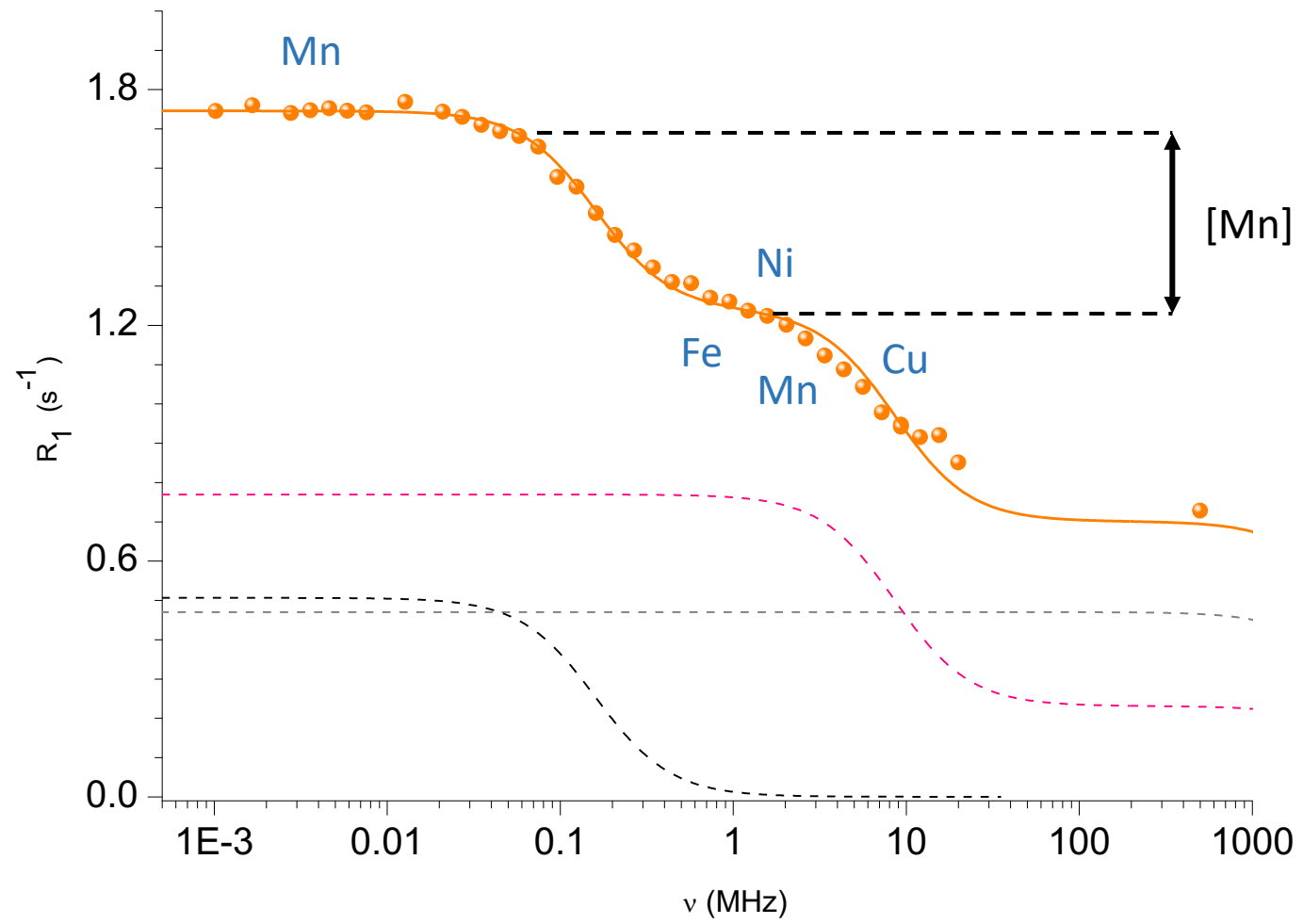


Concentrations (mg/L) of paramagnetic elements measured in the white Chardonnay (W), the red Medoc (R) and the exchanged wine (EW) by ICP-AES.

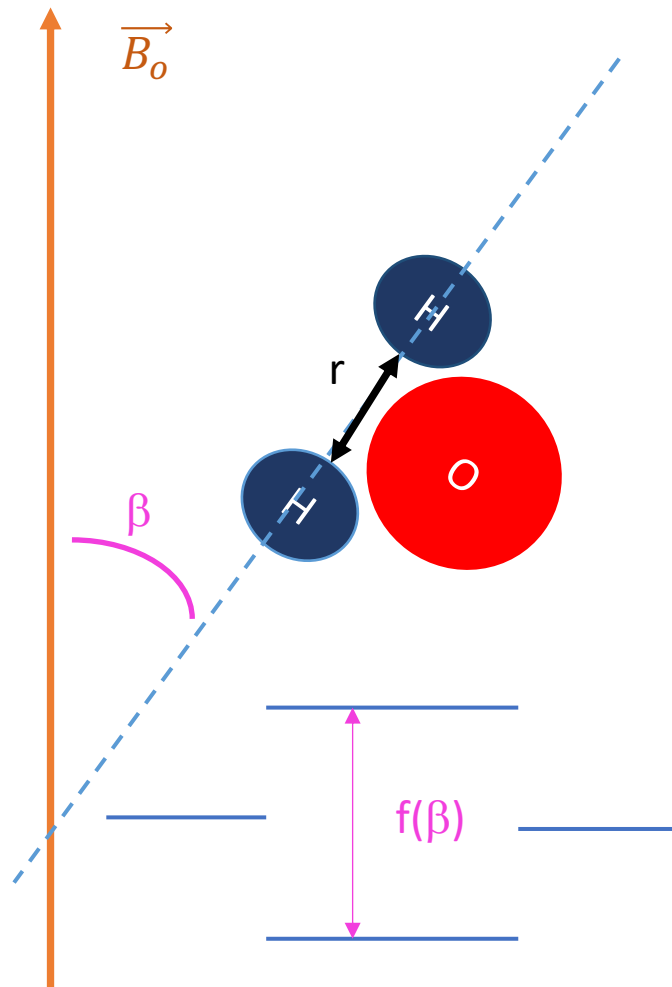
	Mn	Fe	Cu	Ni	Cd
W	1.26 (2)	1.34 (2)	0.160 (2)	0.91 (1)	0.0019 (1)
EW	< 0,002	0.056 (3)	0.024 (1)	< 0,007	< 0,001
R	1.06 (2)	0.85 (1)	0.93 (1)	0.065 (1)	0.0056 (3)

Basic dipolar relaxation mechanism



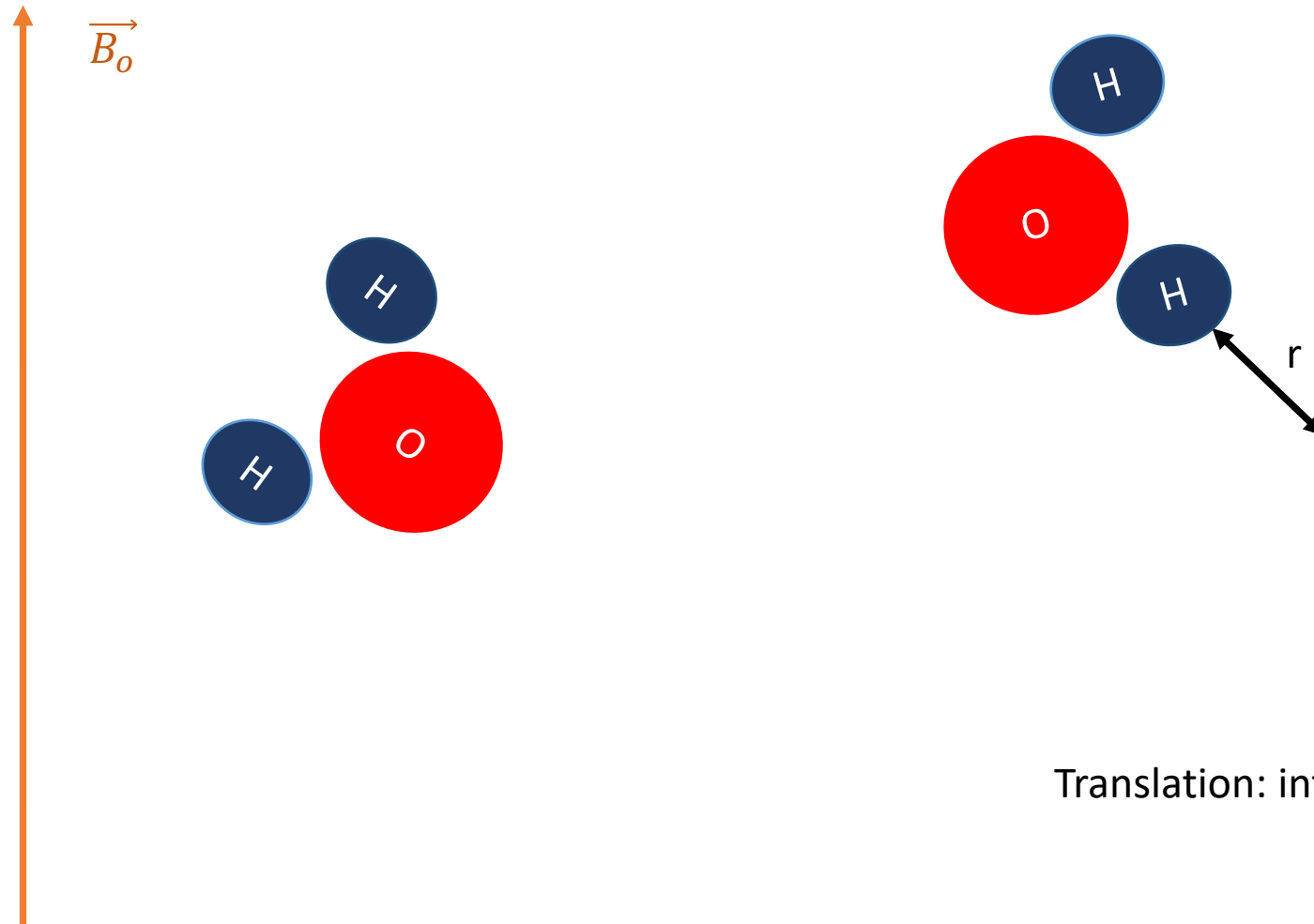


Basic dipolar relaxation mechanism



Rotation: intra molecular relaxation
Rotational isotropic diffusion

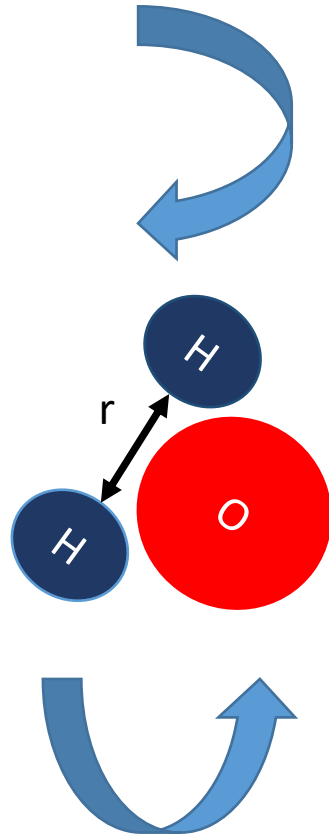
Basic dipolar relaxation mechanism



Translation: inter molecular relaxation

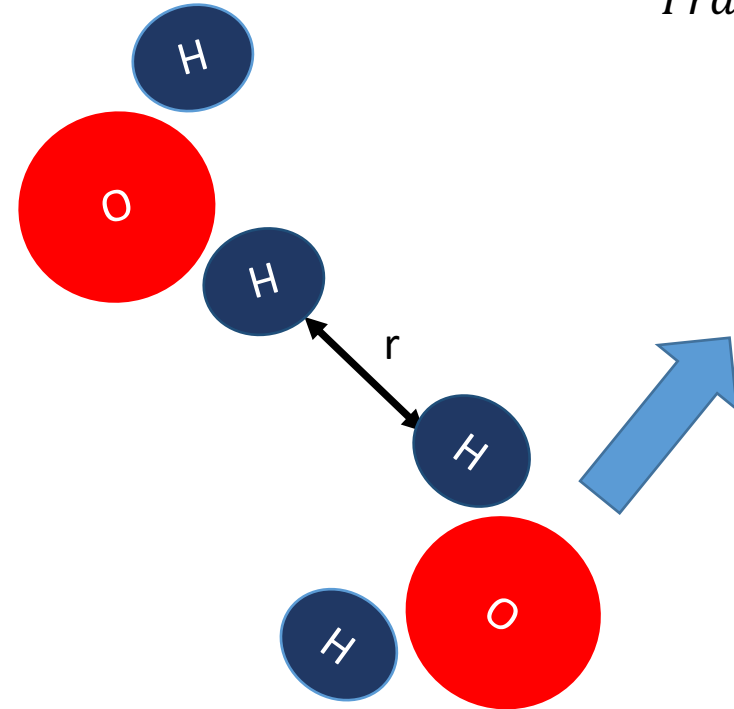
Basic dipolar relaxation mechanism

Rotation



$$R_1 = \frac{1}{T_1}$$

Translation



$$R_1 = R_1^{intra} + R_1^{inter}$$

BPP relaxation model

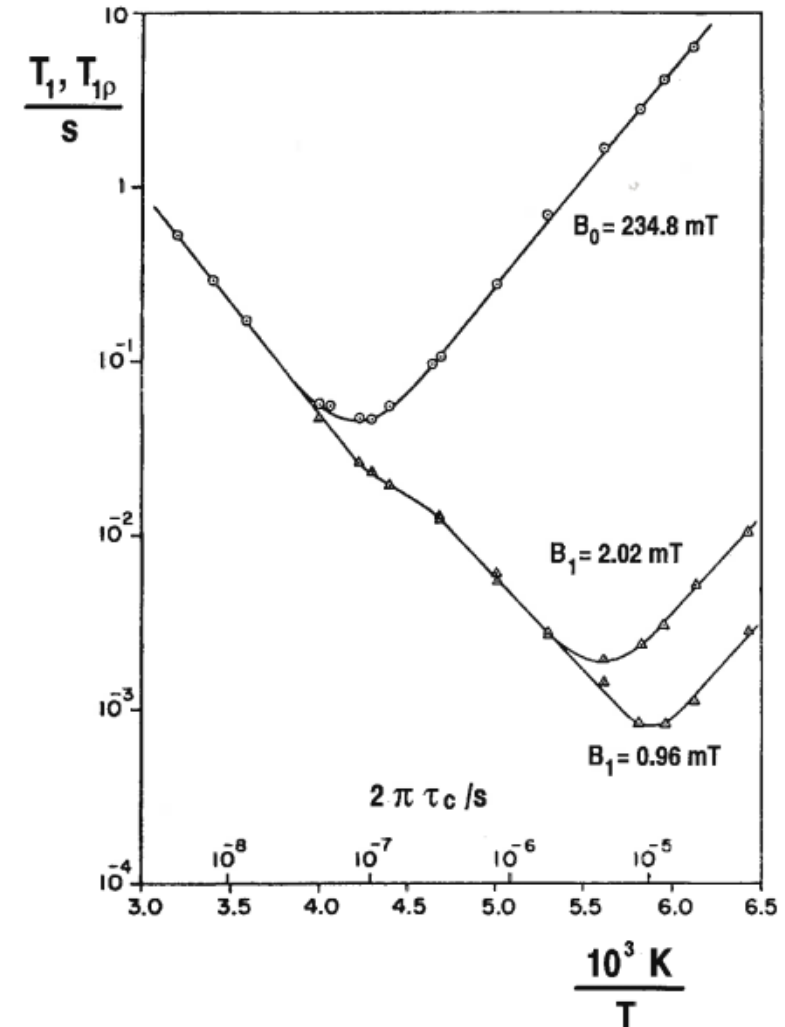
Dipolar interaction (H₂O),
intramolecular contribution
Isotropic rotational diffusion

$$\frac{1}{T_1}(\omega_I, \tau_c) = R_1(\omega_I, \tau_c) = \tilde{C}_o \left[\frac{\tau_c}{1 + (\omega_I \tau_c)^2} + \frac{4\tau_c}{1 + 4(\omega_I \tau_c)^2} \right]$$

$$\tilde{C}_o = \frac{3}{10} \left(\frac{\mu_o}{4\pi} \right)^2 \frac{\gamma_I^4 \hbar^2}{r_{II}^6}$$

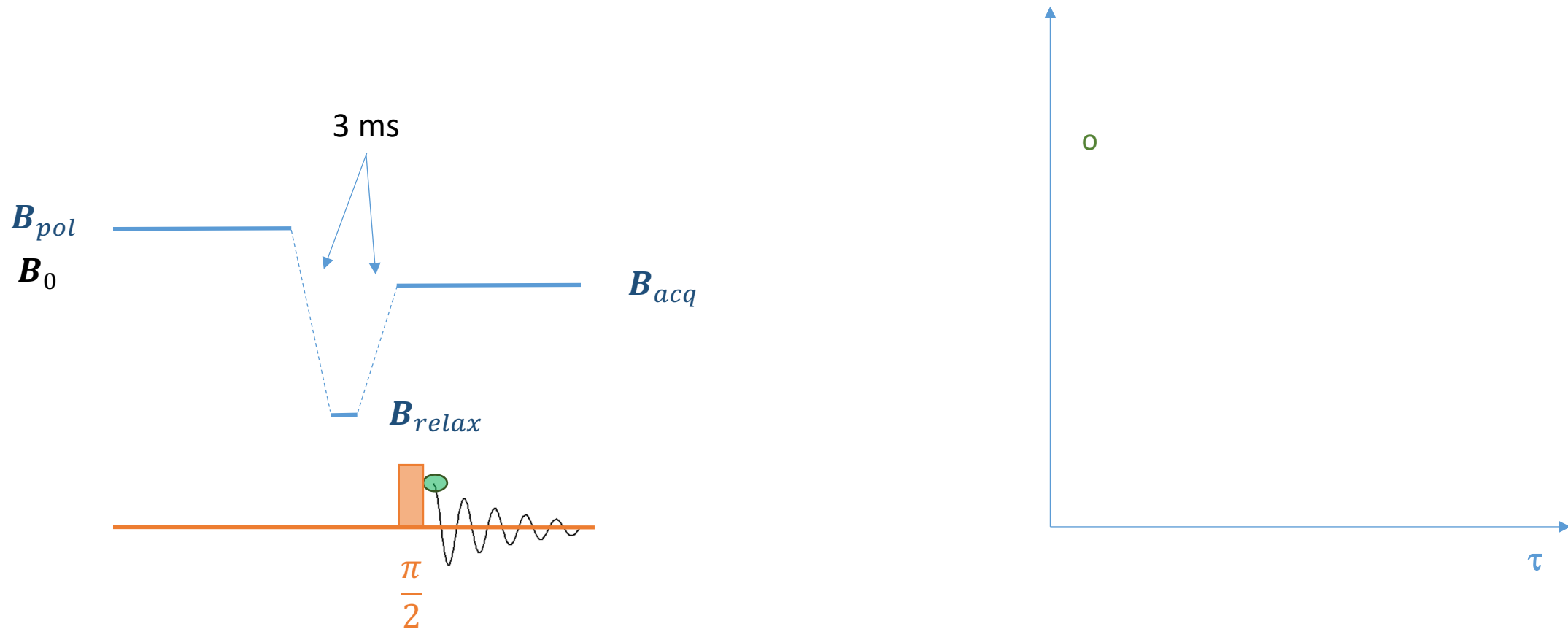
τ_c : correlation time

N. Bloembergen, E.M. Purcell, R.V. Pound, Relaxation effects in nuclear magnetic resonance absorption, Phys. Rev. 73 (1948) 679–712

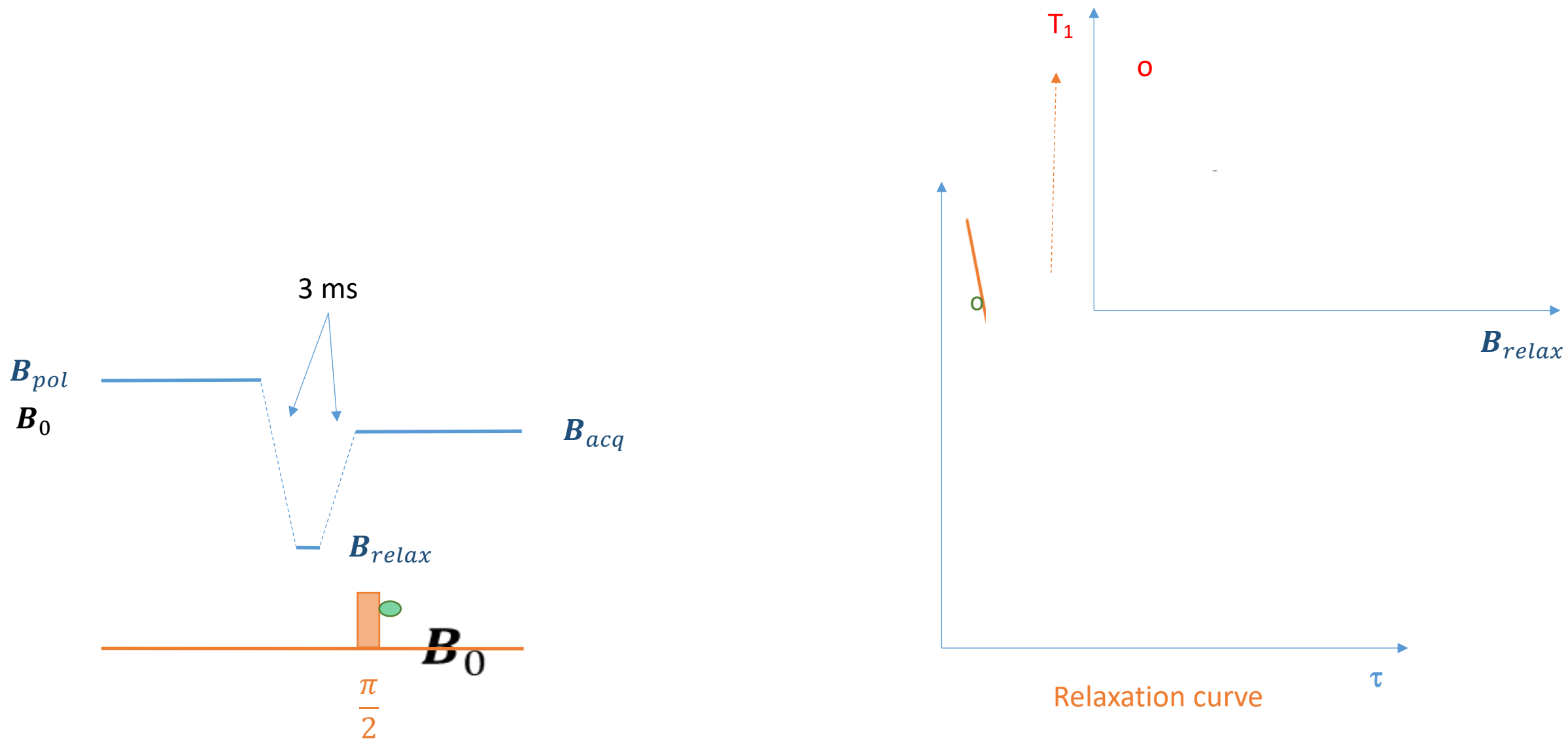


D.C. Look I.J. Lowe J. C hem. Phys. 44 (1966) 2995

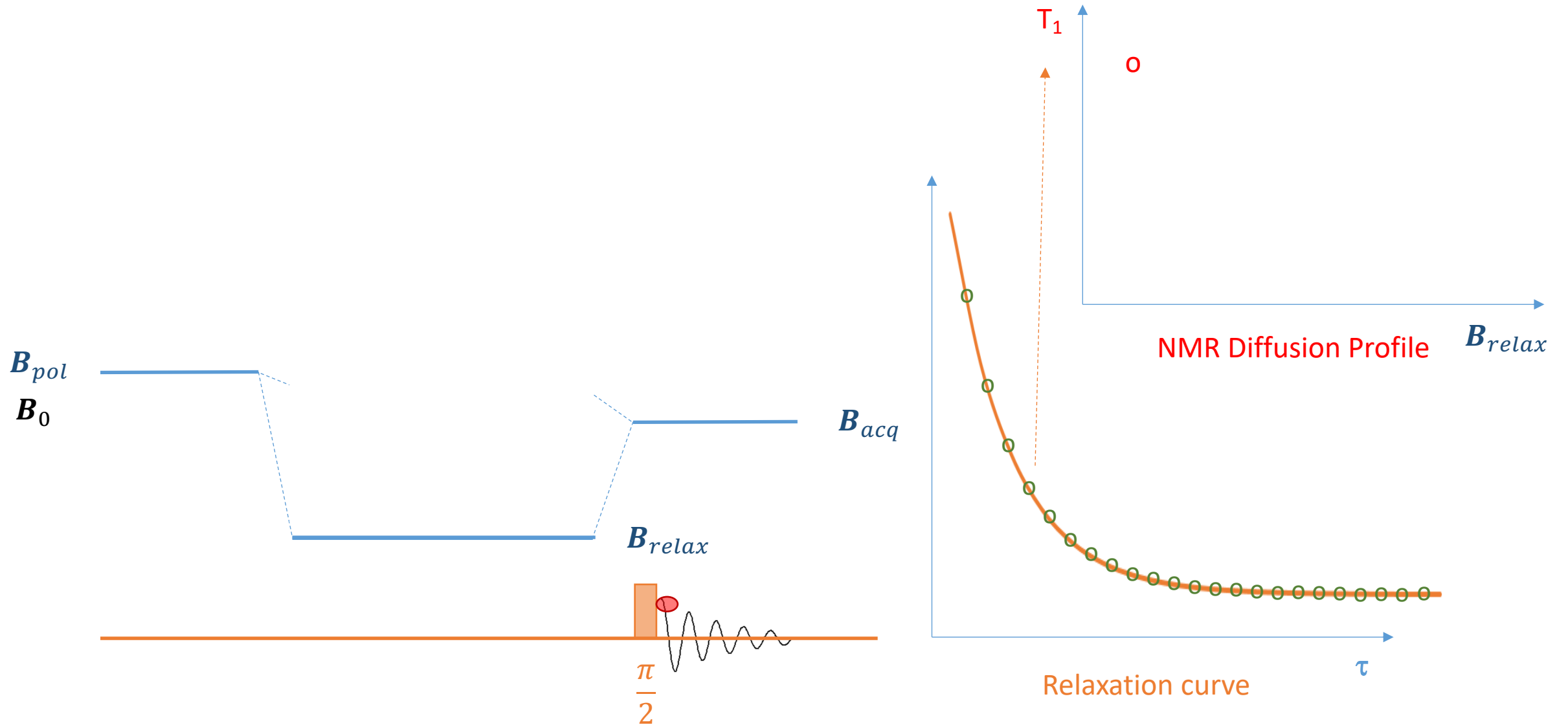
principle of relaxometry experiment



principle of relaxometry experiment

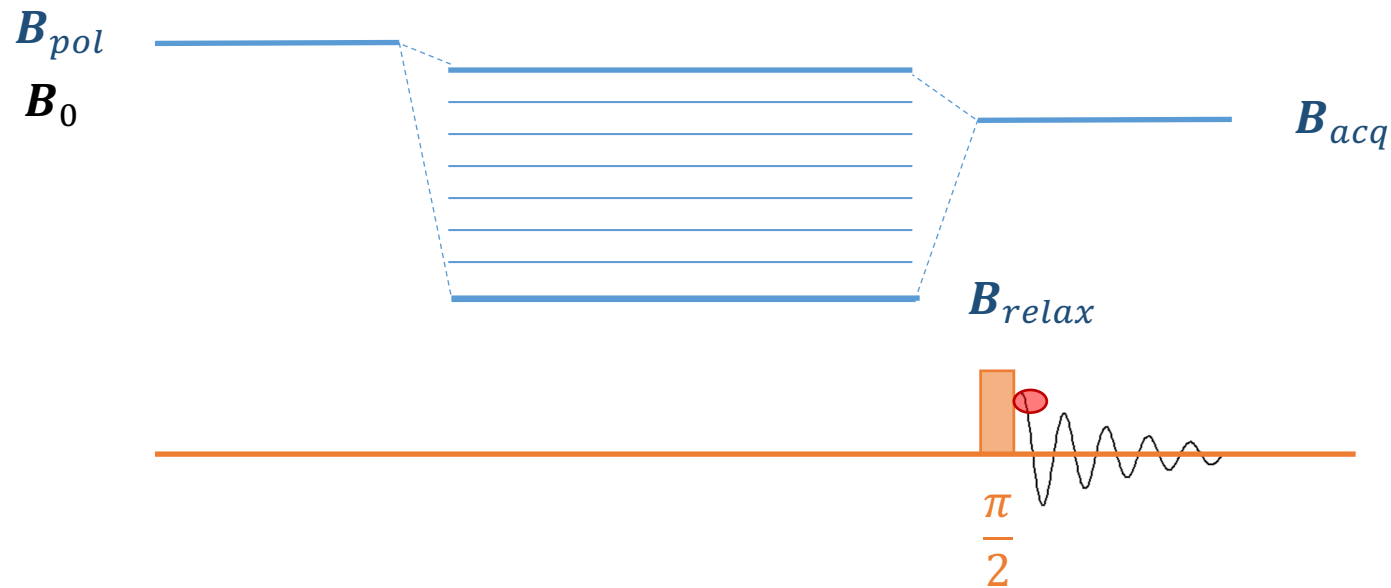


principle of relaxometry experiment



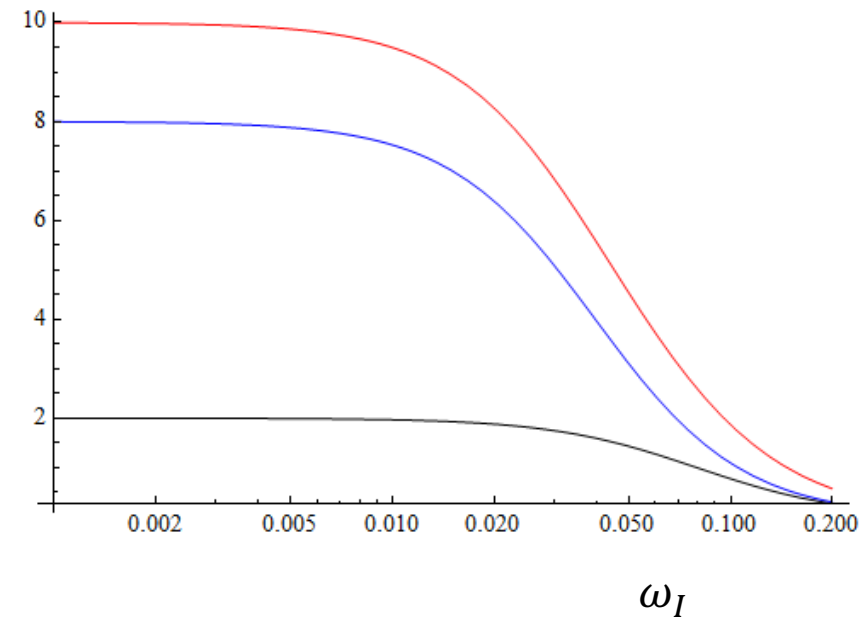
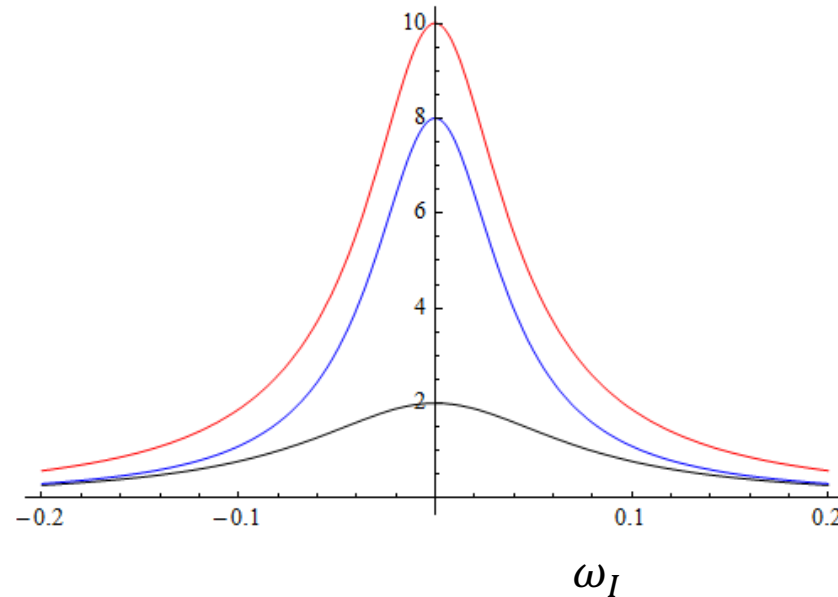
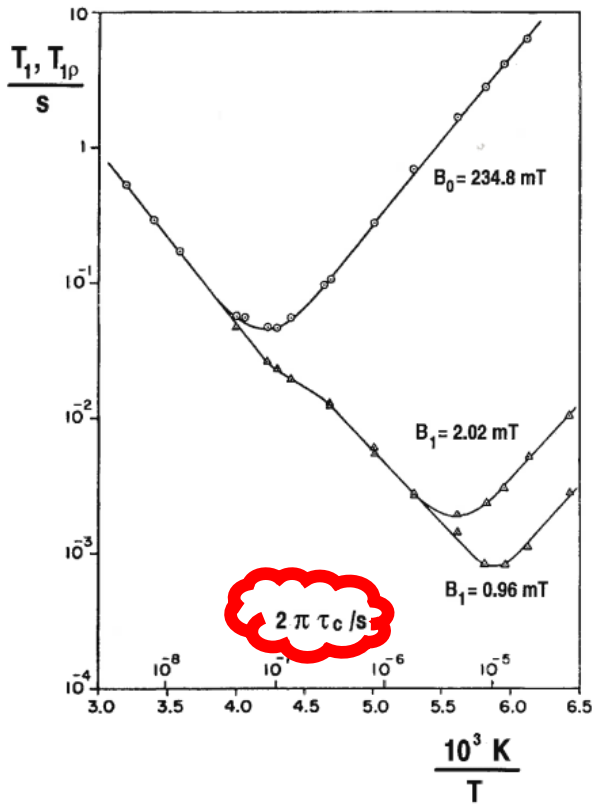
technical aspects

- B_{acq} allows a single tuning for all larmor frequencies
- B_{relax} can varie from 40 MHz to 10 kHz
- Low Relaxation field (\sim kHz)
- Switching time (2-3 ms)

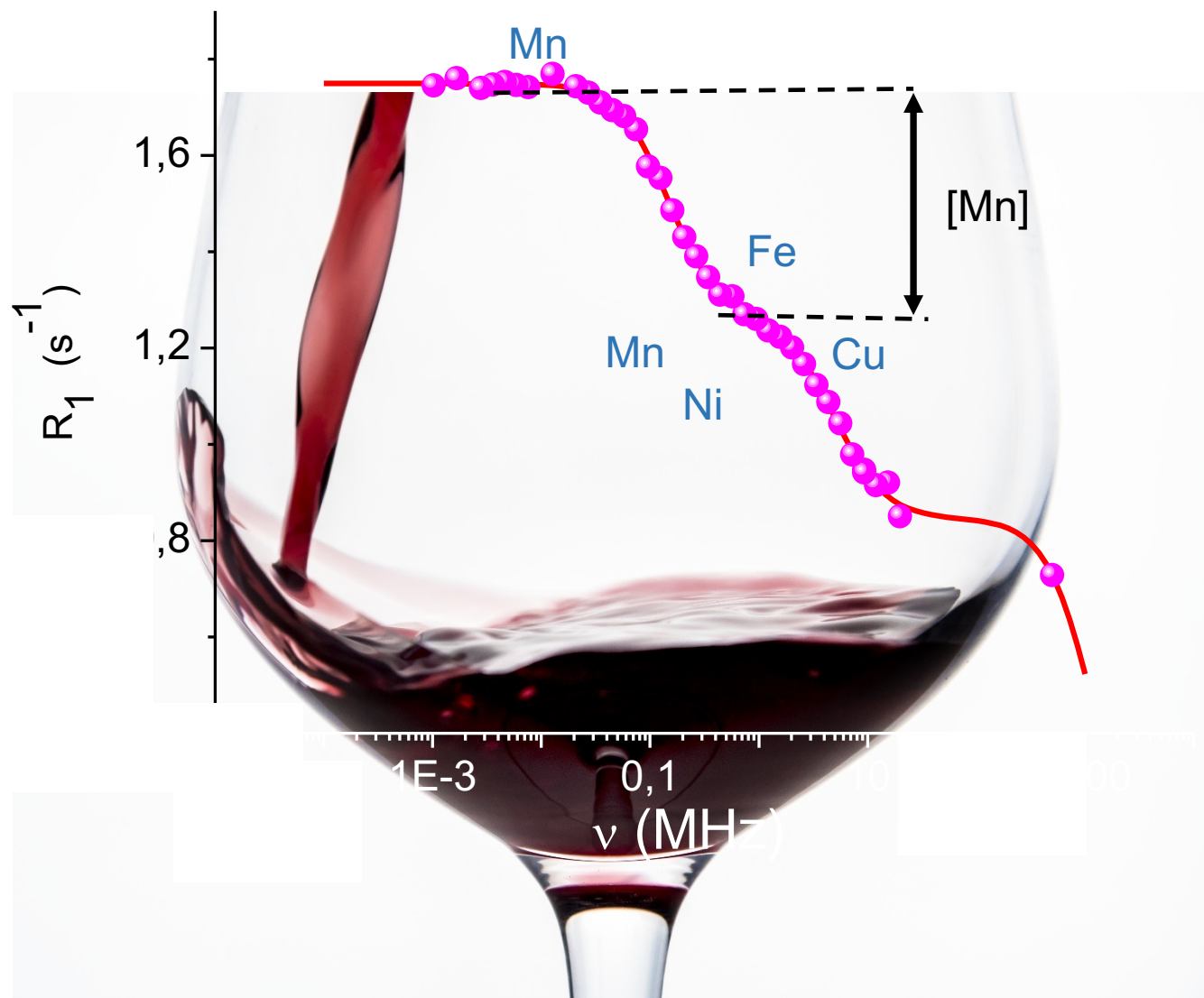


BPP relaxation model

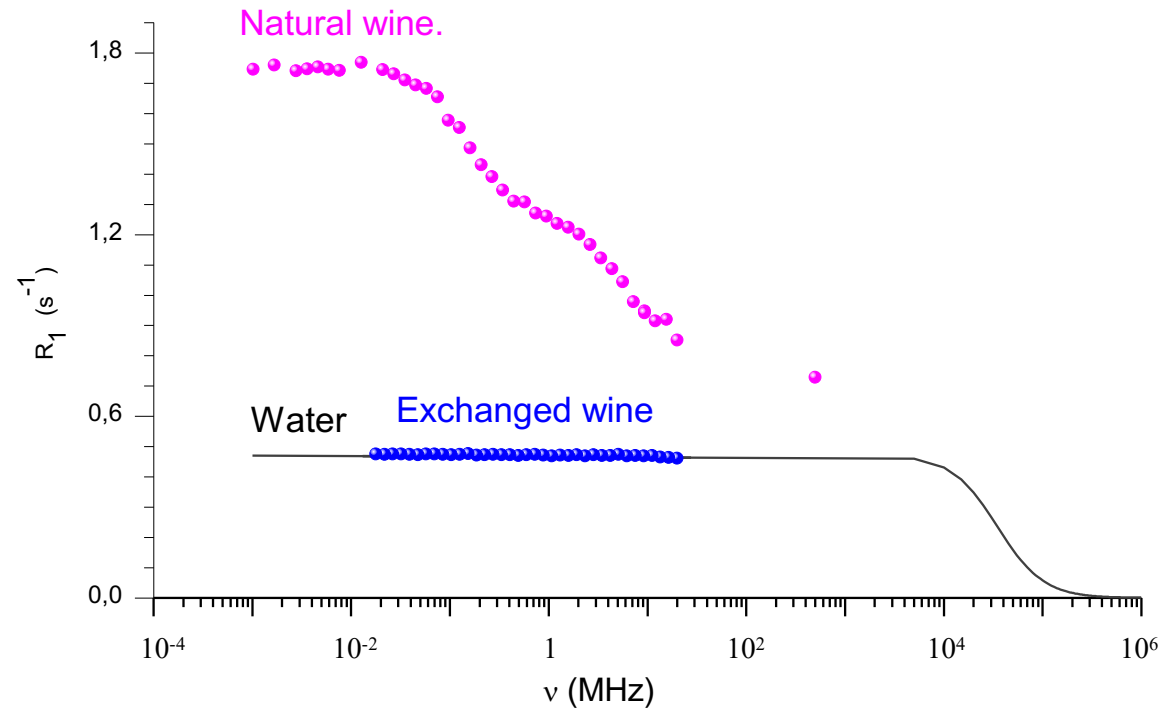
$$\frac{1}{T_1}(\omega_I, \tau_c) = R_1(\omega_I, \tau_c) = \tilde{C}_o \left[\frac{\tau_c}{1 + (\omega_I \tau_c)^2} + \frac{4\tau_c}{1 + 4(\omega_I \tau_c)^2} \right]$$

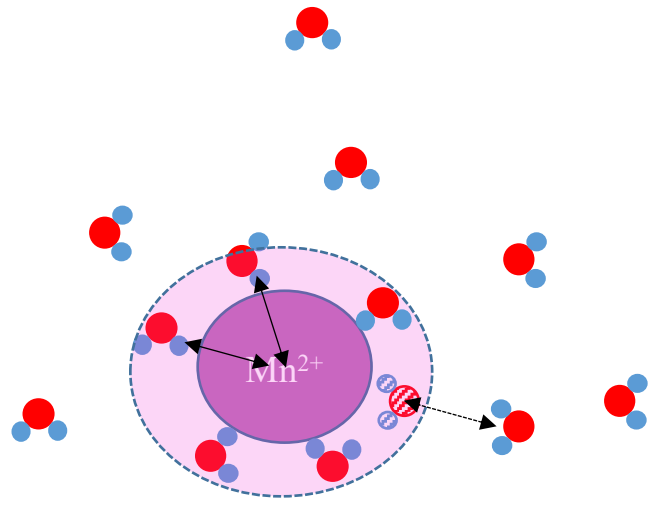


NMR Diffusion Profile



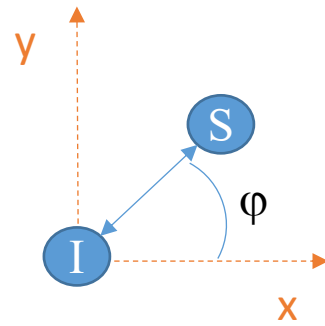
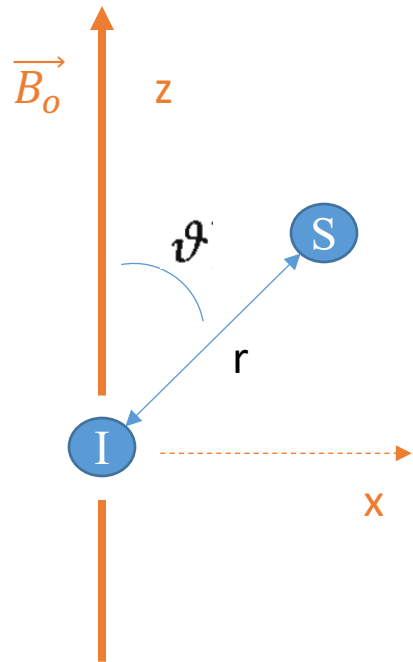
NMRD profile of wine (white Chardonnay)





Dipolar relaxation

$$\mathcal{H}_0 = -\hbar\omega_I I_z - \hbar\omega_S S_z$$



$$\mathcal{H}_d = f_d \sum_{k=-2}^2 F^{(k)} \mathcal{O}^{(k)}$$

$$f_d = \frac{\mu_0}{4\pi} \gamma_I \gamma_S \hbar^2$$

$F^{(0)}$	$=$	$F^{(0)*}$	$=$	$r^{-3} (1 - 3 \cos^2 \vartheta)$
$F^{(1)}$	$=$	$F^{(-1)*}$	$=$	$r^{-3} (\sin \vartheta \cos \vartheta e^{-i\varphi})$
$F^{(2)}$	$=$	$F^{(-2)*}$	$=$	$r^{-3} (\sin^2 \vartheta e^{-2i\varphi})$
$\mathcal{O}^{(0)}$	$=$	$\mathcal{O}^{(0)\dagger}$	$=$	$I_z S_z - \frac{1}{4} (I^+ S^- + I^- S^+)$
$\mathcal{O}^{(1)}$	$=$	$\mathcal{O}^{(-1)\dagger}$	$=$	$-\frac{3}{2} (I^+ S_z + I_z S^+)$
$\mathcal{O}^{(2)}$	$=$	$\mathcal{O}^{(-2)\dagger}$	$=$	$-\frac{3}{4} I^+ S^+$